Student Unmanned Aerial System

Senior Design Final Report April 2012

By

Ryan Jantzen[1] Antwon Blackmon[1] Walker Carr[1]
Brian Roney[2] Eric Prast[2] Alek Hoffman[2]

[1]Department of Mechanical Engineering
[2]Department of Electrical and Computer Engineering

Project Sponsor
Florida Center for Advanced Aero-Propulsion

Department of Mechanical Engineering
FAMU-FSU College of Engineering
2525 Pottsdamer St, Tallahassee, FL 323

Contents

1. Abstract 9
2. Introduction 9
2.1 Project Introduction 9
2.2 AUVSI Competition 10
2.3 Competition requirements 12
2.4 Needs Assessment 13
3. Project Completion Concept 14
3.1 Project Objectives 14
3.2 Functional Description 18
3.3 Team organization 19
3.4 Project Planning 20
4. Concept Generation and Selection 22
4.1 Aircraft Configuration Design and Selection 22
4.2 Materials Selection 33
4.3 Propulsion System Design and Selection 40
4.4 Power Supply System Design and Selection 46
4.5 Avionics System Design and Selection 52
4.6 Imagery System Design and Selection 57
5. Final Concept Design- SUAS 63
5.1 Aircraft Design 64
5.2 Airframe Design 78
5.3 Simple Avionics Design 80
5.4 Propulsion System Design 82
5.5 Autopilot System Design 86
5.6 Video Feed System Design 88
5.7 Camera gimbal design 93
5.8 Power Supply System Design 94
6. Manufacturing Process 98
7. Engineering Economics 103
7.1 Budget 103
7.2 Spending Justifications 104

7.2a Aircraft Subsystem 104
7.2b Autopilot Subsystem 105
7.2c Propulsion System 105
7.2d Power Supply System 106
7.2e Video Feed System 106
8. Project Prototype and Testing 106
8.1 Individual Component testing 106
8.1a Telemaster components 106
8.1b Cameras 107
8.1c Video telemetry 111
8.1d Motor 114
8.1e Batteries 115
8.1f Autopilot board 117
8.1g Autopilot Telemetry 117
8.1h X-Plane Simulator 118
8.1i Autopilot GUI 119
8.2 Sub-system testing 120
8.2a Avionics Testing 120
8.2b Video feed System Testing 120
8.2c Propulsion System Testing 121
8.2d Power Supply system testing 121
9. Performance Results 123
9.1 Telemaster Senior test flight results 123
9.1a Avionics 130
9.1b Propulsion 131
9.1c Power Supply 134
9.1d Video Feed 135
10. Safety, Health and Environmental Issues 138
10.1 Aircraft Safety 138
10.2 Environmental hazards 140
10.3 Health issues 141
11. Project Conclusion 141

11.1 Summary of results 141
11.2 Future developments 142
11.3 Lessons learned 142
12. Acknowledgements 143
13. Student Biographies 144
Ryan Jantzen 144
Alek Hoffman 144
Brian Roney 145
Walker Carr 145
Eric Prast 145
Antwon Blackmon 146
14. Engineering Drawings 147
15. Appendix 150
A.1 Team # 14 Code of Conduct 150
A.2 Team #14 Gannt Chart 152
A.3 SUAS Functional Diagram 153
16. References 154

List of Figures

Figure 2.1: Ground Target Examples 11
Figure 2.2: Example area search (right) and waypoint navigation (left) 13
Figure 3.1: SUAS Functional Diagram 18
Figure 3.2: Team #14 Structure 19
Figure 3.3: Team #14 Gannt Chart 21
Figure 4.1: Conventional Configuration 22
Figure 4.2: Canard Configuration 22
Figure 4.3: Twin Boom Configuration 23
Figure 4.4: Flying Wing Configuration 23
Figure 4.5: Empennage Configurations 25
Figure 4.6: The NACA 4412 airfoil and its operating parameters. 27
Figure 4.7: NACA 0012 airfoil that will be used for the horizontal and vertical tails. 28
Figure 4.8: XFLR5 Output for Cruise Conditions (55 mph) 29
Figure 4.9: Landing Gear Design 30
Figure 4.10: Final Configuration Layout 32
Figure 4.11: Determination of Static Margin 33
Figure 4.12: Strength versus density material chart 34
Figure 4.13: Fracture toughness versus Young's modulus chart 34
Figure 4.14: 16" by 10" Propeller 45
Figure 4.15: Top-level aircraft electronics diagram 52
Figure 4.16: Xbee Pro 900 RF Module and Futaba 7CAP Transmitter 56
Figure 4.17: Imagery Downlink System Configuration 62
Figure 5.1 : Coefficient of lift versus angle of attack for the SD7037 airfoil. 67
Figure 5.2: Moment coefficient versus angle of attack for the SD7037 airfoil 68
Figure 5.3 Coefficient of lift versus coefficient of drag for the SD7037 airfoil 68
Figure 5.4: Schematic of determining the lever arm for an aircraft. 71
Figure 5.5: Coefficient of lift versus angle of attack for the SD7037 wing and NACA0012 horizontal and vertical stabilizer flying at cruise conditions (V = 55mph) 72
Figure 5.6: Coefficient of moment versus angle of attack for the SD7037 wing and NACA0012 horizontal and vertical stabilizer flying at cruise conditions (V = 55mph). 72

Figure 5.7: Coefficient of lift versus coefficient of drag for the SD7037 wing and NACA0012 horizontal and vertical stabilizer flying at cruise conditions (V = 55mph). 73
Figure 5.8: Output from the XFLR5 simulation of a SD7037 wing and NACA0012 tailplane flying at 55 mph and a 3 degree angle of attack. 74
Figure 5.9: Pro Engineer CAD drawing of the final design of our UAS 75
Figure 5.10 Diagram of the fuselage layup 78
Figure 5.11 Aircraft movements 80
Figure 5.12: Control Surface Locations 81
Figure 5.13: Aileron Control Surface Servo 81
Figure 5.14: Elevator CS servo (Top) and Rudder CS servo (Bottom) 82
Figure 5.15 Eflite Power 60 Brushless DC motor 83
Figure 5.16: CC Phoenix HV ESC 84
Figure 5.17: Mission power requirements profile 85
Figure 5.18: Propulsion System Block Diagram 85
Figure 5.19: Basic Layout of the autopilot system. 86
Figure 5.20: Telemetry kit used for autopilot communication. 87
Figure 5.21 Autopilot Block Diagram 88
Figure 5.22: Video Feed System Block Diagram 89
Figure 5.23: Sony Block Camera FCB EX-980S 90
Figure 5.24: FCB-RS Interface Board (left) and Sony Block Camera connection types (right) 91
Figure 5.25: Arduino Mega 2560 - Front side 92
Figure 5.26 Arduino Mega 2560 - Back side 92
Figure 5.27: Spektrum RC transmitter (left) and receiver (right) 93
Figure 5.28 Pro-E design of gimbal system. 93
Figure 5.29: 8-cell 3850 mAh 29.6V Battery 95
Figure 5.30: 3-cell 1300 mAh 11.1V Battery 95
Figure 5.31: Castle creations BEC Pro 96
Figure 5.32: Final Electronics Top Level Diagram 97
Figure 6.1: Foam profile of fuselage prior to sanding 99
Figure 6.2: Boxes for construction of fuselage mold 100
Figure 6.3: Plaster mold after removal from box 101

Figure 8.1 Sony KX-181 Test Camera 107
Figure 8.2: Telemetry Range Test 109
Figure 8.3: APM board 117
Figure 8.4: X-Plane 9 Simulator interface 118
Figure 8.5: USB Simulator controller 119
Figure 8.6: Autopilot Ground station GUI. 119
Figure 8.7: Telemaster Senior Test Aircraft on the Ground 121
Figure 8.8: Power Supply System in Telemaster Senior 122
Figure 9.1: Telemaster being tweaked 123
Figure 9.2: Components installed in Telemaster 124
Figure 9.3: Batteries installed in Telemaster 124
Figure 9.4: Securing wings on Telemaster 125
Figure 9.5: Telemaster Senior Test Aircraft and Mr. Jim Ogorek 125
Figure 9.6: Telemaster Senior Test Aircraft Side View 126
Figure 9.7: Telemaster Senior Test Aircraft Back View 126
Figure 9.8: Telemaster taking off 127
Figure 9.9: Telemaster in flight (Back) 127
Figure 9.10: Telemaster in flight (Side) 128
Figure 9.11 Telemaster taxiing for Takeoff 129
Figure 9.12: Futaba RC Transmitter 130
Figure 9.13: Futaba RC Receiver 130
Figure 9.14: Telemaster 3rd Flight - Above Seminole RC runway 135
Figure 9.15: Pan / Tilt Camera Gimbal Design Concept 136
Figure 9.16: Bluebeam Cloverleaf Antennas 137
Figure 10.1: Lithium Polymer Battery Combustion 138

List of Tables

Table 3.1: Key Performance Objectives 15
Table 3.2: Objective Testing Environments 17
Tables 4.1-4.3: Final Aircraft Design Parameters 31
Table 4.4: Typical properties of fiber reinforced epoxy matrices 38
Table 4.5: Brushless DC motor decision matrix 44
Table 4.6: AXI 4130/20 Specifications 45
Table 4.7: Battery Characteristics 47
Table 4.8: Battery decision matrix 49
Table 4.9: Aircraft electronic components specs and voltage zones 50
Table 4.10: voltage zones and suppliers 51
Table 4.11: Autopilot Decision Matrix of Ardupilot Mega and Paparazzi Tiny v2.11 55
Table 4.12: Camera Selection Parameters 59
Table 4.13: Camera Decision Matrix 60
Table 5.1: Final design parameters for our UAS 75
Table 5.2: Aircraft Control surfaces 80
Table 5.3: Power 60 Characteristics 83
Table 7.1: Team #14 SUAS Budget Breakdown 103

List of Graphs

Graph 4.1: Constraint diagram used for the initial power loading and wing loading..... 26
Graph 4.2: Motor Power output vs. Current Input for the AXI 4130/20 46
Graph 7.1: Budget Pie Chart..... 104
Graph 8.1: Big battery Discharge Curve at 5 A 116
Graph 8.2: Small battery Discharge Curve at 5 A..... 116
Graph 9.1: Battery voltage and Motor consumption over time (Flight #1) 131
Graph 9.2: Battery voltage and Motor consumption over time (Flight #2) 132
Graph 9.3: Battery voltage and Motor consumption over time (Flight #3) 132
Graph 9.4: Battery voltage and Motor consumption over time (Flight #4) 133
Graph 9.5: Power out and Amp Hours for all flights 133

1. Abstract

The Student Unmanned Aerial System (SUAS) Project was completed by FAMU/FSU College of Engineering Senior Design Team #14 during the Fall 2011 – Spring 2012 academic year. The project was headed by the FAMU/FSU COE Mechanical Engineering Department, in order to compete in the 2012 AUVS SUAS Competition. Team #14 was comprised of three mechanical engineering students, two electrical engineering students and one computer engineering student.

By analyzing the 2012 AUVSI competition rules and guidelines, key performance objectives were defined for the SUAS. To accomplish these performance objectives, several subsystems were designed to complete specific objectives and/or to support other subsystems accomplishing these objectives. The construction of the SUAS encompassed electronic communications, electronic component, power supply and aeronautical design.

Team #14 members worked together to design and construct these subsystems, either by a manufacturing or systems engineering approach. The resulting subsystems were tested thoroughly and integrated. The resulting SUAS was the finished product of the ME and ECE senior design capstone course. This paper describes the design, testing and implementation processes of the SUAS project.

2. Introduction

2.1 Project Introduction

The FAMU/FSU Student Unmanned Aerial System (SUAS) was designed and constructed to compete in the Association for Unmanned Vehicle Systems International (AUVSI) 2012 Student UAS competition, and also to satisfy the requirements of the Mechanical Engineering and Electrical Engineering Capstone project. The 2012 AUVSI Student UAS competition is based on a fictional military mission. The broad mission of the UAS is to support a team of Navy Seals with intelligence surveillance and intelligence (ISR). The SUAS will complete a mission made up of several separate operations, all of which must be completed within a forty minute time frame. The first operation is the autonomous navigation of the competition course. This operation includes the takeoff and landing phases of flight, waypoint

navigation and an area search. The second operation is ongoing target identification. The SUAS must be able to identify ground targets with five characteristics: shape, background color, orientation, alphanumeric, and alphanumeric color. The ground targets will be scattered along the competition course, and upon target identification, the image data and target location must be relayed back to the ground station. The third operation is in flight re-tasking, where the flight plan of the UAS is modified by adding additional waypoints or adjusting the search area.

The overall goal of Team #14 is to design a relatively inexpensive SUAS that is capable of competing in this competition by fulfilling these mission requirements while maintaining the safety and integrity of our design and demonstrating the team's proficiency in mechanical, electrical and computer engineering.

2.2 AUVSI Competition

The AUVSI Seafarer Competition is a Systems Engineering approach to building an effective versatile surveillance and reconnaissance aircraft. The aircraft must autonomously navigate through GPS waypoints and remain inside a designated airspace. While traversing through these waypoints the aircraft is required to acquire information about ground based targets throughout the course. Such targets will be painted with alphanumerics, teams will be graded on their ability to find, locate, and determine the targets shape and markings. During the Enroute Search targets will be placed on the direct path or adjacent to the assigned airspace. Once finishing the Enroute Search phase, the aircraft should perform an autonomous Area Search. During this phase the air vehicle must to find and locate multiple targets in a designated airspace. The aircraft can use a custom search pattern to their liking in order to realize as many targets in the allotted timeframe. Each group will receive points for the correct alphanumeric characteristics and GPS coordinates of each target found. Additional points may be awarded for an autonomous takeoff and landing.

Takeoff and Landing

The takeoff and landing must be performed in the designated asphalt surfaces, roughly 100 ft wide. Takeoff from a moving vehicle is prohibited. The use of special launching devices will be inspected for safety before being cleared for competition use. Once airborne the vehicle must remain above 100 ft and under 750 ft MSL. Takeoff under manual control with transition to

autonomous flight is permitted. Extra credit and cash rewards are given to teams with an autonomous takeoff.

GPS Waypoints

Global coordinates will be given the day prior to the flight competition, such that the designed system must be able to quickly input waypoints. The navigation system must be able to adjust waypoints during flight due to the dynamic nature of modern warfare.

Target Search

The aircraft must remain within the altitude specifications (100-750 MSL) during the target search. One target will be directly along the route when the vehicle is at 500 ft MSL, while another target will be up to 250 ft away from the path. The UAS must identify targets without violating the altitude requirements or drifting ± 100 ft from the flight path.

Ground Targets

Ground targets will be constructed of plywood in basic geometric shapes and colors. The target will be marked with an alphanumeric in a different color than the background of the target. The maximum target size (length and width) is 8 ft with a minimum of 2 ft. The alphanumeric will be painted to fit the dimensions of the target, occupying 50-50 % of the target face. The thickness of each alphanumeric will vary from 2-6 inches. There are an unknown number of targets in the Area Search.

Figure 2.1: Ground Target Examples

Area Search

The UAS must search for specific targets while remaining between 100-750 ft MSL. There will be a minimum of 200 ft margin between the search area and the no fly zone boundary. Students should record target location, shape, color, orientation, alpha, and alpha color to receive full credit for acquisition.

Mission Duration

Each team will be given a total of 40 minutes of mission time, this is window begins when transmitters are turned on and ends when mission data sheets are turned in. Teams completing the mission in under 40 minutes will receive bonus points, with a minimum completion time of 20 minutes. If teams do not complete the mission in 40 minutes points will be deduced each minute, with a maximum time limit of 60 minutes. After 60 minutes remaining teams must turn in their flight data sheets or be disqualified. If 40 minutes elapses and the aircraft has not achieved flight the team will not be able to perform a mission.

2.3 Competition requirements

The mission profile for the autopilot system consists of two basic parts. The first part consists of autonomous waypoint navigation. Waypoints will consist of GPS coordinates in the format of ddd.mm.ssss and altitudes that the aerial vehicle will need to be at. The autopilot system will need to direct the aerial vehicle to these waypoints and altitudes in the order that they are given.

The next part is the area search. The area search is when the autopilot will perform an autonomous area search at a height between 100 and 750 ft MSL. The team will be using the camera system to find any targets within the search area. There will also be a new search area given that can be given where the autopilot will need to direct the aerial vehicle to search.

After the aerial vehicle completes these missions it will return to the launch area where the team will land the plane without the autopilot system needed. An optional task of the autopilot system is to direct the aerial vehicle to take off and land without the help of the team. This task can be implemented to the discretion of the team as it is not required for the mission profile.

Figure 2.2: Example area search (right) and waypoint navigation (left)

There is also a safety requirement. This includes both material and personnel safety. The ground control system displays should be readable in bright sunlight conditions. The system should also be capable of operating in fog conditions of 2 miles of visibility or greater with no rain. The system should be capable of completing mission objectives in temperatures up to 100 deg Fahrenheit. The system should be able to forced altitude changes and be able to fly at a higher weight than air flight. The batteries used in the air vehicle shall contain bright colors. This would assist in finding the batteries in the event of a crash. The air vehicle needs to also be able to be manually overridden by the safety pilot at any point in flight. The air vehicle cannot takeoff from moving vehicles but should be able to takeoff and in crosswinds of about 8 knots and gust of about 11 kts. The aircraft should also comply with the 2011 Official Academy of Model Aeronautics (AMA) National Model Aircraft Safety Code.

2.4 Needs Assessment

The implementation of Unmanned Aerial Systems (UAS) has expanded to numerous applications outside of military usage to areas such as civil and commercial applications as well as university research and development. In June 2012, the Association for Unmanned Vehicle Systems International (AUVSI) will be hosting its 9th annual Student Unmanned Aerial Systems (SUAS) Competition which focuses on the design and fabrication of a UAS that is capable of completing specific mission requirements. Entries to this competition must fulfill the safety requirements set forth by AUVSI as well as have the capability to navigate through GPS waypoints, autonomously search a specified area for ground targets and be able to provide information from the targets by taking images of them, all with no human interaction with the

vehicle itself. The purpose of our project is to design a relatively inexpensive UAS that is capable of competing in this year's competition by fulfilling these mission requirements while maintaining the safety and integrity of our design.

3. Project Completion Concept

3.1 Project Objectives

The principle goal of team fourteen is the safe and effective execution of systems engineering to accomplish the required tasks of the 2012 Unmanned Aerial System Competition. After reading through the rules for the 2012 competition, we have identified five major objectives of project performance that must be satisfied for us to be successful. The main component of our principle goal is the completion of the minimum requirements of each objective. Important aspects of our principle goal are also to work together as an efficient team, have fun and successfully complete the requirements of the FAMU/FSU College of Engineering undergraduate senior design project.

Objective 1: Autonomy

Aircraft must autonomously navigate the competition course during waypoint navigation and during an area search. Aircraft must remain autonomous during all phases of flight including takeoff and landing.

Objective 2: Imagery

Aircraft imagery capabilities must be able to identify a minimum of two of the five target characteristics. (Shape, background color, orientation, alphanumeric, alphanumeric color) Upon competition of the minimum requirement of this parameter, identifying all five target characteristics will be attempted.

Objective 3: Target Location

Aircraft's target positioning capabilities must be able to determine target location (ddd.mmm.sss) within 250 ft. Upon competition of the minimum requirement of this parameter, determining target location within 50 ft will be attempted.

Objective 4: Mission Time

Mission time is defined as the time from [aircraft transmitter activation] to [aircraft shutdown and completed mission report]. The total mission time to complete all mission tasks is not known at this time for the 2012 competition. However, assuming a similar mission time as the previous year's competition; total mission time could be forty minutes or less. At the end of the given mission time, a mission report with associated imagery will be turned in to the competition judges.

Objective 5: Operational Success

The aircraft must complete at least 50% of the required mission tasks within the given flight window and mission time. The overall goal of this parameter is to complete 100% of all mission tasks within the given flight window, without using the entire mission time.

Objective	**Threshold**	**Overall Completion**
Autonomy	During way point navigation and area search.	All phases of flight, including takeoff and landing
Ground Target Identification	Identify any two target characteristics (shape, background color, orientation, alphanumeric, and alphanumeric color)	Identify all five target characteristics
Target Location	Determine target location ddd.mm.ssss within 250 ft	Determine target location within 50 ft
Mission time	Less than 40 minutes total Imagery/location/identification provided at mission conclusion	20 minutes Imagery/location/identification provided in real time
Operational Availability	Complete 50% of missions within original tasking window (no more than one time out)	Complete 100% of missions within original tasking window (no time outs used)
In-flight re-tasking	Add a fly to way point	Adjust search area

Table 3.1: Key Performance Objectives

It is our goal to meet all thresholds and at least one of the overall completions as part of the Key Performance Objectives. These milestones include fully autonomous waypoint navigation and area search, imagery search characteristics, target location, waypoint adjustment, and timely completion. The overall completions include an autonomous takeoff and landing, flawlessly identifying target details, accuracy of target location within 50 feet, never violating the allotted time window, and adjusting search requirements mid-flight. The overall goal of our design system is to execute as many Key Performance Objectives as possible with maintaining a safe and reliable UAV system. To complete these objectives, the complete aircraft was divided into several subsystems, and a system engineering approach was used to design the complete SUAS. These subsystems are:

- Aircraft Subsystem: Airframe, structure and control surfaces.
- Avionics Subsystem: Autopilot module, RC module and control surface servos.
- Imagery Subsystem: Camera module, gimbal and camera control servos.
- Propulsion system: Motor module and speed controller.
- Power Supply subsystem: Batteries, voltage regulators and transmission network.

To test these various Key Performance Objectives, individual sub-systems will be tested during multiple test flights. The performance of each subsystem during the test flights will determine the completion level of each of the Key Performance objectives. The testing environment and subsystem responsibility is shown below.

Objective	Sub-System	Environment
Autonomy	Avionics	All phases of flight, including takeoff and landing
Ground Target Identification	Imagery	During waypoint navigation and area search
Target Location	Imagery	During waypoint navigation and area search
Mission time	Power Supply and Propulsion	All phases of flight, including takeoff and landing
Operational Availability	Complete Aircraft	All phases of flight, including takeoff and landing
In-flight re-tasking	Avionics	During waypoint navigation

Table 3.2: Objective Testing Environments

All the subsystems used to complete the key performance objectives are constrained by the important aspects of aircraft design. The major constraints on our design are established by the competitions rules and general principals of flight. The final craft must be less than 55lb, operate in a flight altitude window of 100ft-750ft, have the ability to accept GPS waypoints and determined search areas, communicate with a third party ground sensor, and be able to maintain flight for a minimum of 20 to 40 minutes. Constraints for individual aircraft subsystems include:

- Weight
- Power consumption
- Drag
- Heat
- Component availability for purchase

3.2 Functional Description

To complete the key performance objectives, the various subsystems are integrated with one another to form the complete aircraft. The functional diagram for the SUAS is shown below.

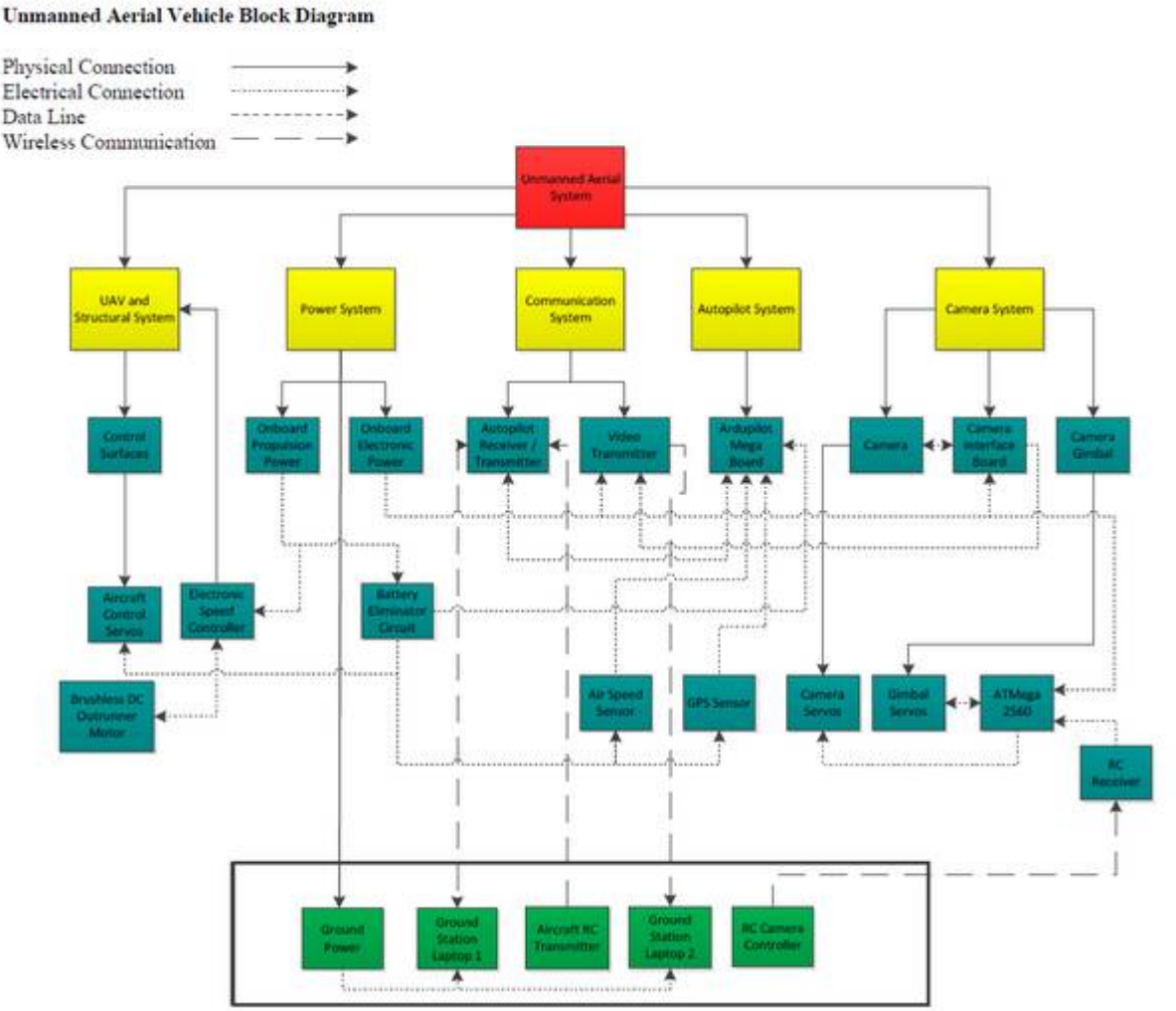

Figure 3.1: SUAS Functional Diagram

3.3 Team organization

Senior Design Team #14 consists of six FAMU/FSU engineering students, three Mechanical Engineering majors, two Electrical Engineering majors and one Computer Engineering major. The team is advised by Dr. Rajan Kumar at the Florida Center for Advanced Aero-Propulsion (FCAAP) and Dr. Mike Frank at the FAMU/FSU College of Engineering Electrical and Computer Engineering Department. Dr. Kumar was the primary sponsor advisor and also advised the ME side of the team. Dr. Frank was the ECE side advisor.

The members of Team #14 were each assigned a team officer position and were further tasked with a particular section of the overall SUAS design. As is seen in figure 3, the aircraft design is broken into 6 sections: Structure, Propulsion, Materials, Power, Controllers and Sensors. Each team member was also responsible for overseeing a specific area of the team organization and performance, determined by their officer position.

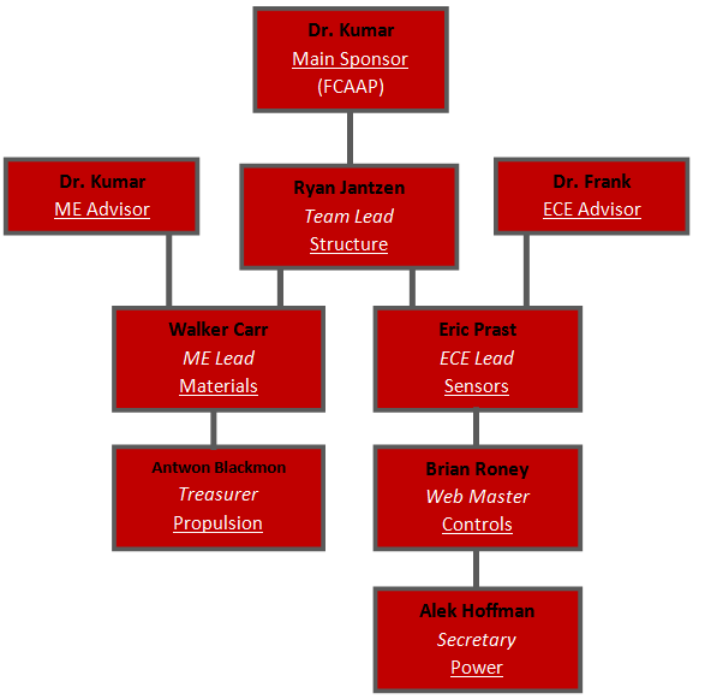

Figure 3.2: Team #14 Structure

The officer descriptions can be found in the Code of Conduct in the Appendix. The SUAS design departments were assigned based on experience, interest and engineering major. The structure department covers the design of the aircraft's flight characteristics including the design of all the external parts that make up the aircraft. The materials department deals with the materials used in the construction of the aircraft and also the internal structures of the airframe. The propulsion department is responsible for researching and designing an appropriate propulsion system for the aircraft, including the motor and motor components. The sensors department is responsible for the target recognition and image processing capabilities of the aircraft, including camera design and video transmission. The controls department covers the aircraft's autopilot navigation, all avionics sensors and transmitters, and the human control override. The power department is responsible for designing a power supply system capable of supplying the entire aircraft electronics system with power throughout the entire flight time. One auxiliary section of the project is the ground station, where the human/aircraft interface takes place. This aux section will be divided among the ECE students, and consists of several laptops, software and receivers. It is important to note that although the structure of Team # 14 is separated across six persons, all members of the team contribute to the completion of team goals, and in no way is a team member constricted to their assigned departments.

3.4 Project Planning

In order to efficiently design the UAS during the 2011-2012 academic year, along with successfully passing all of our engineering courses, time management is of utmost importance. Several tools were utilized by Team # 14 in order to manage our time more effectively. The first tool utilized is the dropbox website. By having an online space accessible by all the members of the team, we are able to collaborate on the completion of team goals, even when we are not physically together. Another tool utilized was Google's calendar program, with which meetings and deadlines were scheduled. By linking the team's individual emails to the calendar, reminders are email out automatically. The final major tool utilized to manage time was the Gannt chart, as shown in figure 3.2.

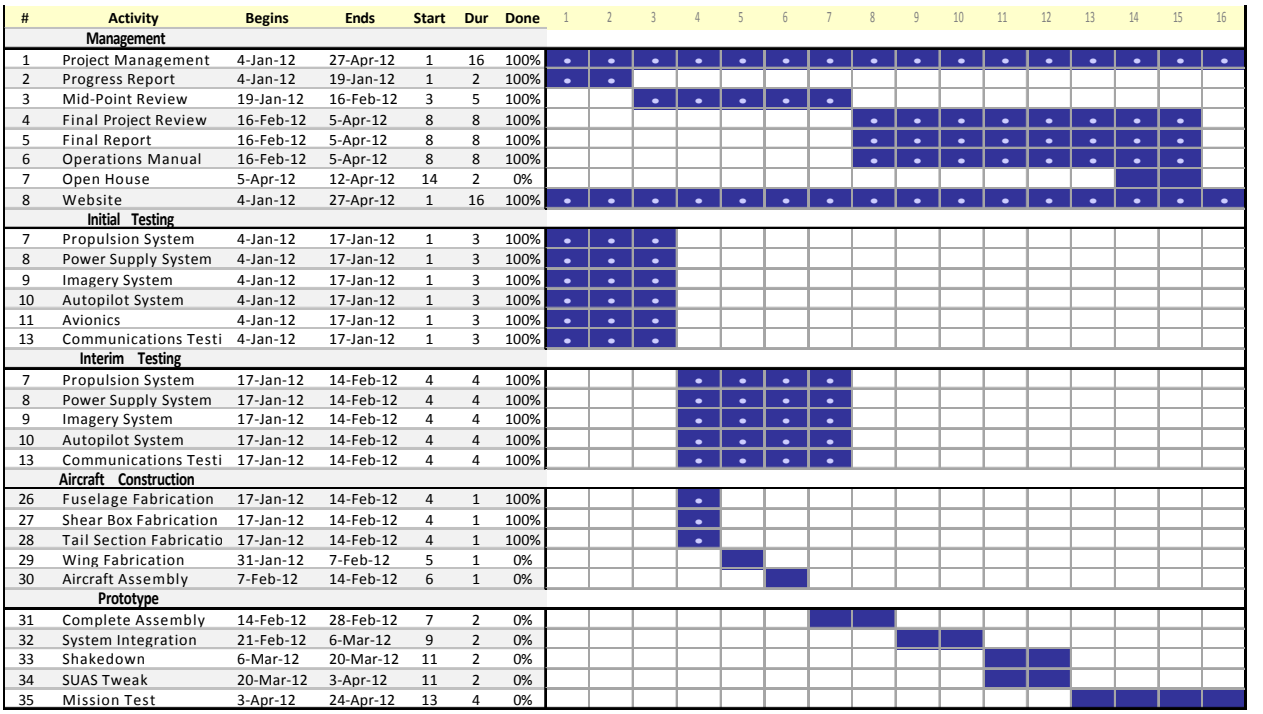

#	Activity	Begins	Ends	Start	Dur	Done
	Management					
1	Project Management	4-Jan-12	27-Apr-12	1	16	100%
2	Progress Report	4-Jan-12	19-Jan-12	1	2	100%
3	Mid-Point Review	19-Jan-12	16-Feb-12	3	5	100%
4	Final Project Review	16-Feb-12	5-Apr-12	8	8	100%
5	Final Report	16-Feb-12	5-Apr-12	8	8	100%
6	Operations Manual	16-Feb-12	5-Apr-12	8	8	100%
7	Open House	5-Apr-12	12-Apr-12	14	2	0%
8	Website	4-Jan-12	27-Apr-12	1	16	100%
	Initial Testing					
7	Propulsion System	4-Jan-12	17-Jan-12	1	3	100%
8	Power Supply System	4-Jan-12	17-Jan-12	1	3	100%
9	Imagery System	4-Jan-12	17-Jan-12	1	3	100%
10	Autopilot System	4-Jan-12	17-Jan-12	1	3	100%
11	Avionics	4-Jan-12	17-Jan-12	1	3	100%
13	Communications Testi	4-Jan-12	17-Jan-12	1	3	100%
	Interim Testing					
7	Propulsion System	17-Jan-12	14-Feb-12	4	4	100%
8	Power Supply System	17-Jan-12	14-Feb-12	4	4	100%
9	Imagery System	17-Jan-12	14-Feb-12	4	4	100%
10	Autopilot System	17-Jan-12	14-Feb-12	4	4	100%
13	Communications Testi	17-Jan-12	14-Feb-12	4	4	100%
	Aircraft Construction					
26	Fuselage Fabrication	17-Jan-12	14-Feb-12	4	1	100%
27	Shear Box Fabrication	17-Jan-12	14-Feb-12	4	1	100%
28	Tail Section Fabricatio	17-Jan-12	14-Feb-12	4	1	100%
29	Wing Fabrication	31-Jan-12	7-Feb-12	5	1	0%
30	Aircraft Assembly	7-Feb-12	14-Feb-12	6	1	0%
	Prototype					
31	Complete Assembly	14-Feb-12	28-Feb-12	7	2	0%
32	System Integration	21-Feb-12	6-Mar-12	9	2	0%
33	Shakedown	6-Mar-12	20-Mar-12	11	2	0%
34	SUAS Tweak	20-Mar-12	3-Apr-12	11	2	0%
35	Mission Test	3-Apr-12	24-Apr-12	13	4	0%

Figure 3.3: Team #14 Gannt Chart

The Gannt chart visually depicts the project plan which can be broken into five different categories, each with their own number of activities. They are project management, research, design, prototype and competition. Project management deals with the day to day management of the project team, as well as the completion of the required deliverables and presentations. Research covers the overall research into the competition rules, past competitors' designs, and research into the separate components of the design project. The design category contains the four steps of the project design process, as well as the individual design of all the specific components. Prototype deals with physically building the aircraft, testing the aircraft and preparing for the competition. The competition category contains the final steps of the design project goal, which are the requirements of entry into the competition, as well as the completion of the actual competition. A full size Gannt chart is included in the Appendix.

4. Concept Generation and Selection

4.1 Aircraft Configuration Design and Selection

Planform Concepts:

The aircraft planform is a crucial part of the design of a successful unmanned aerial vehicle. The planform is the shape and layout of a fixed wing aircraft's fuselage and wings. In order to make an informed decision, we considered four different configuration layouts. These layouts include the conventional, canard, double boom, and flying wing planforms.

Figure 4.1: Conventional Configuration

The first concept considered was the conventional planform, as shown in figure 1. The conventional planform includes a traditional style aircraft with a fuselage, wing and empennage. This concept is both simple and stable but it is difficult to manufacture in an easily transportable fashion and it has a larger wetted surface area which leads to increased drag.

Figure 4.2: Canard Configuration

The second concept considered was the canard planform, as shown in figure 2. The canard planform is configured with control surfaces towards the front of the aircraft. It is easier to construct than the conventional planform and has adequate maneuverability but has poor stability and requires a complex control surface analysis.

Figure 4.3: Twin Boom Configuration

The third concept considered was the double boom planform, as shown in figure 3. The double boom planform is similar to the conventional configuration but its main difference is that it has twin booms extending from the wing into the empennage. The benefits of this configuration are that it integrates well with the payload, is relatively easy to manufacture, and it is very transportable, meaning it can be designed to be broken down into several pieces for transporting to the airfield. The drawbacks from this configuration are that its heavy, the center of gravity is difficult to balance, and there are a limited number of different tail configurations that can be used when working with a twin boom.

Figure 4.4: Flying Wing Configuration

The last concept considered is the flying wing planform, as shown in figure 4. The flying wing planform has no rear empennage and has a swept back wing that acts as both the wing and fuselage for this configuration. This allows the fuselage to act as a lifting body during flight. The drawbacks of this design are its poor stability and maneuverability, difficulty in transport, and a complex analysis is required for the configuration's flight dynamics.

The fuselage influences the performance of the aircraft as well as the lateral and longitudinal stability. The primary function of the fuselage is to accommodate the payload such as the avionics and imagery subsystems. The fuselage must be designed so that the payloads are easy to access for maintenance while out in the field.

Wing Design:

The next decision that must be made is the configuration of the wing for our aerial vehicle. When designing the wings performance, stability, manufacturability, operational requirements and flight safety must all be taken into account. The wings must provide sufficient lift to the aircraft during all phases of flight while minimizing the drag and pitching moment. When designing the wings for our UAS, the first decision to be made is the vertical location of the wing with respect to the fuselage. The airfoil geometry will then be selected for the wing that best fits the mission profile. From there, it can be determined if the wing will need any high lift devices, such as flaps, to provide more lift than what the airfoil generates. Other parameters that must be decided during the wing design process include the aspect ratio, taper ratio, chord, span, twist angle, dihedral angle, sweep angle and incidence. Once all of these wing parameters are determined, it is possible to calculate the lift, drag and pitching moment of the design and determine if the configuration is adequate.

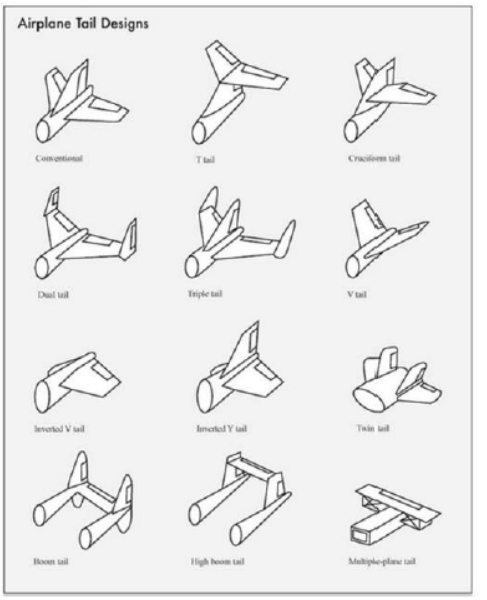

Figure 4.5: Empennage Configurations

Empennage Design:

Once the wings have been designed for our aircraft, we will then begin designing the empennage. The empennage includes the horizontal and vertical tail surfaces. These not only provide lift to the aircraft but also longitudinal and lateral control. The design of both the horizontal and vertical tail sections will be designed to have longitudinal and directional stability. There are many different empennage configurations, which are seen in Figure 5, that need to be considered once we select the planform layout. The parameters that must be decided during the empennage design process include the horizontal location with respect to the fuselage, planform area, tail arm, airfoil selection, aspect ratio, taper ratio, chord, span, sweep angle, dihedral angle and incidence.

Final Concept:

We started the sizing process of our aircraft by doing a constraint analysis for the power loading (P/W) and wing loading (W/S) that would be required to meet all of the design requirements of our aircraft. Power loading is the power required for our aircraft normalized by the weight of the aircraft while wing loading is the weight of the aircraft normalized by the wing area. The constraint analysis takes into consideration all the flight design requirements, such as stall, cruise, takeoff and landing requirements, and helps determine a “design” point where all

these requirements are met. Equations for each of these flight design requirements were given by Raymer (2006) that were derived using equations of motion as well as relationships for the specific flight requirement to get it in terms of power loading and wing loading.

From this constraint diagram, we determined an initial power loading of 14.25 Watts/lb and an initial wing loading of 2.71 lb/in^2.

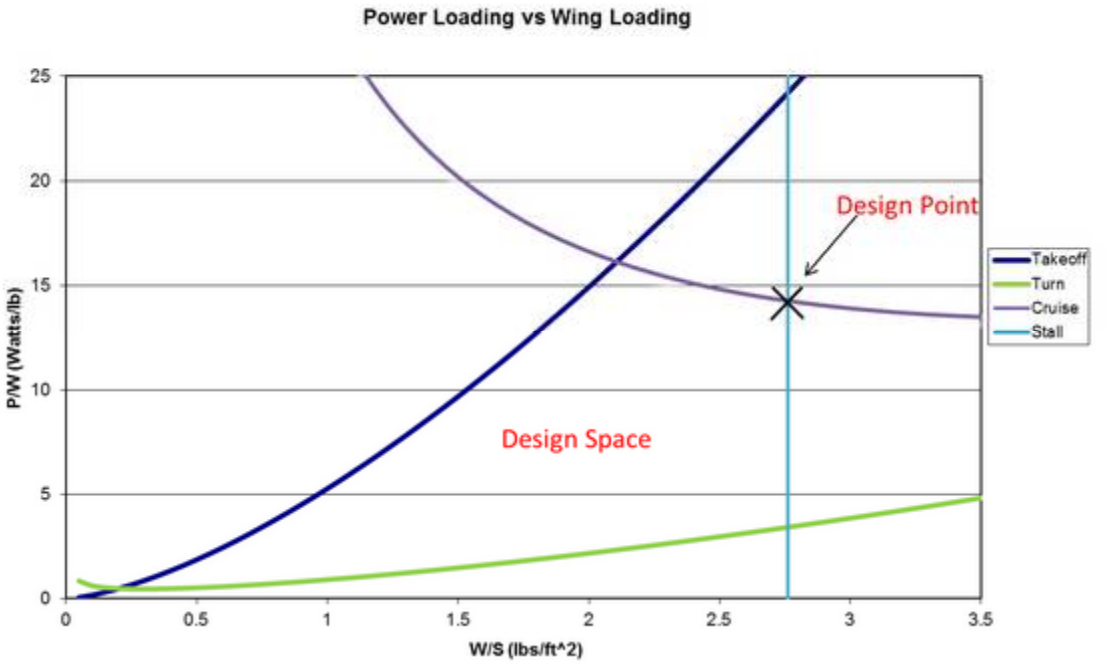

Graph 4.1: Constraint diagram used for the initial power loading and wing loading.

The next decision that was made was the configuration of the wing for our aerial vehicle. When designing the wings, performance, stability, manufacturability, operational requirements and flight safety must all be taken into account. The wings must provide sufficient lift to the aircraft during all phases of flight while minimizing the drag.

For the selection of the airfoil for our design, we decided to look for an airfoil that possesses a high coefficient of lift while keeping the drag to a minimum. Due to the design requirements of having to loiter and take aerial photography, we foresee having to fly at lower speeds while imaging targets on the ground. This requires that the airfoil that is selected must have a gradual stall at lower speeds and higher angle of attack. The following figures compare

the lift curves, drag curves, and drag polars produced from a wing design program called Profili, which uses the well-known X-FOIL program to solve for the airfoil polars

By comparing the following lift and drag curves and drag polars, it seems that the SD 7032 is the clear winner for having the highest and lowest drag. Unfortunately, we decided that this airfoil would not be adequate for our design because of how thin it is. This would not only be hard to manufacture but also it would be structurally weaker than the thicker designs due to its relatively small thickness. The airfoil we found to best fit our mission profile was the NACA 4412. We chose this airfoil mainly due to the gradual stall that it occurs when operating at higher angles of attack. As mentioned previously, we foresee ourselves operating at lower stalling speeds while loitering and taking aerial photography so having a gradual stall that is easily recoverable was a major decision factor. The NACA 4412 airfoil and its major operating parameters are shown in figure 5.

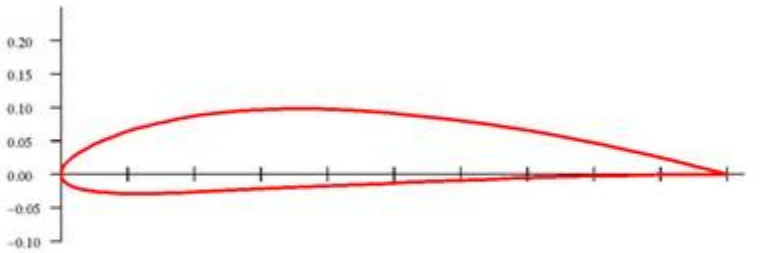

NACA 4412	
Max CL	1.51
Max CL angle	11.00
Max L/D	57.20
Max L/D angle	5.50
Max L/D CL	1.19
Stall angle	6.00
Zero-lift angle	-4.00

Figure 4.6: The NACA 4412 airfoil and its operating parameters.

The two main geometric features that we were concerned with in the initial design of our wing planform were the aspect and taper ratios. The aspect ratio is the ratio of the span of the wing to the chord of the wing. We have decided on using an aspect ratio of 10 for the design of our UAV because higher aspect ratios tend to lead to high aerodynamic efficiency (L/D).

The taper ratio is the ratio of the tip chord length to the root chord length. Wings that are tapered effect the lift distribution along the span of the wing, making it more elliptical which is

the most efficient wing planform for the design of an aircraft. Since elliptic wings are expensive and difficult to manufacture, we plan on implementing a tapered wing into the design of our wing. We have chosen to use a taper ratio of 0.45 based on the recommendation given by Raymer (2006) who says it produces a lift distribution that is very close to the ideal elliptical distribution.

When designing an empennage of an aircraft, stability, trim and control characteristics must be kept in mind. One of the main objectives for the tail of an aircraft is to keep the aircraft stable in all phases of flight. We used the same methodologies of the previous wing design section for the design of the empennage of our aircraft. The first decision we made when designing the tail of our aircraft was the airfoil it would use. We selected the NACA 0012 symmetric airfoil for both the vertical and horizontal tail geometries. We selected a symmetric airfoil for our tail because they are known to provide stability against pitching moments when used for the horizontal tail and they provide stability against yawing moments when used for the vertical tail. Figure 6 shows the NACA 0012 geometry and lists it main flight parameters.

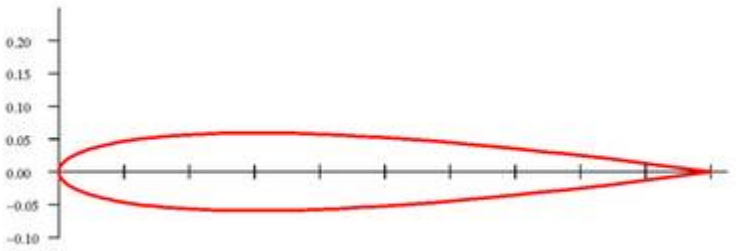

NACA 0012	
Max CL	1.51
Max CL angle	11
Max L/D	57.2
Max L/D angle	5.5
Max L/D CL	1.19
Stall angle	6
Zero-lift angle	-4

Figure 4.7: NACA 0012 airfoil that will be used for the horizontal and vertical tails.

After determining the main geometric and aerodynamic features of our wing and tail, we used an analysis program called XFLR5 to determine the performance of our initial layout. This program lets you design the wings and tails of aircraft operating at low Reynolds numbers. The first analysis we performed was the aircraft operating at cruise conditions to determine the lift, drag and pitching moment coefficients in a stable flight regime. The output of the analysis is

shown in figure 7. This figure shows the span-wise distribution of lift over the wing of the aircraft, the induced drag profile and the downwash produced by the wing and tail. This also shows the streamlines over the wing along with the tip vorticies produced as a result of the difference of pressure at the tips of the wings.

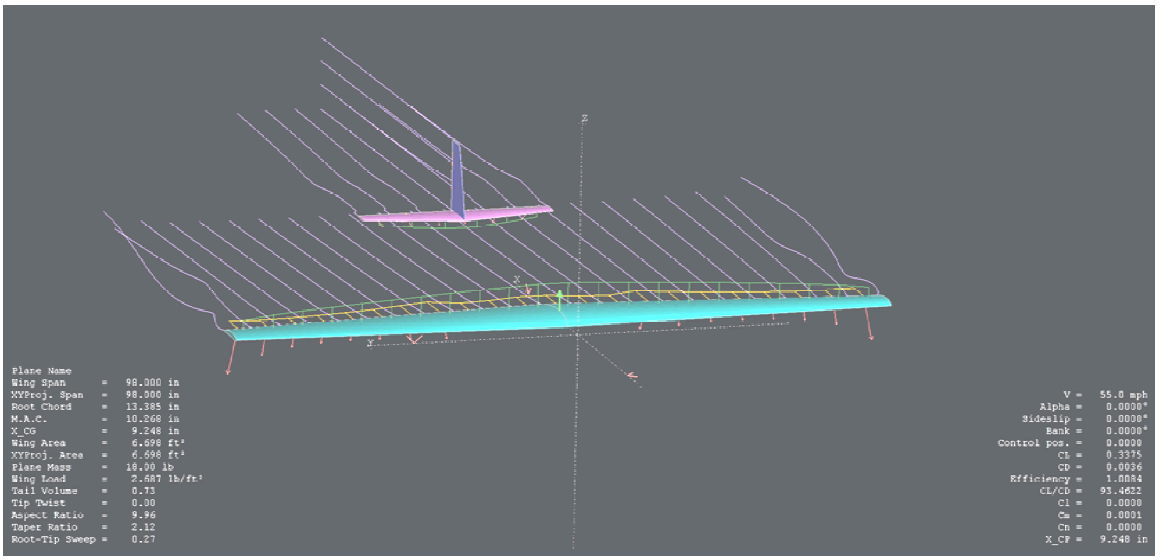

Figure 4.8: XFLR5 Output for Cruise Conditions (55 mph)

The landing was constructed based on a previous plane's landing gear. We decided to go with a triangular formation of the wheels. The front wheel is angled at a 15 degree angle and the two rear wheels are angled at 30 degree angles. This formation was proven to be stable based on the levelness of the plane. The landing will be made out of aluminum or carbon fiber based on which is more resistant to the stress of the plane landing and being in contact with the ground.

Figure 4.9: Landing Gear Design

After numerous iterations and configuration changes in the XFLR5 program, we came to a point where the conceptual design started showing stabilizing effects and we used this configuration as the final design. Although this is our final design, there are still numerous iterations that must be done to learn how stable our aircraft is during all phases of flight. The aircraft will continue to be tweaked through its test flights.

Wing	
Span	98 in
Area	6.7 ft-2
Root Chord	13.4 in
Tip Chord	6.3 in
Aspect Ratio	10
Taper Ratio	0.47
Sweep	0.27o
MAC	10.3 in
MAC Location Span-wise	2.5o
Wing Loading	2.7 lb/ft2
Cruise CL	0.34
Airfoil	NACA 4412
Ailerons	
Span	55-95% Half Span
Chord Percentage	20%
Max Deflection	±30o

Horizontal Tail	
Span	28.3 in
Area	0.93 ft2
Root Chord	6.3 in
Tip Chord	3.15 in
Aspect Ratio	6
Sweep	9.4o
Taper Ratio	0.5
Airfoil	NACA 0012
Elevator	
Span	Full Span
Chord Percentage	0.2
Max Deflection	±30o

Vertical Tail	
Span	20.7 in
Area	0.37 ft2
Root Chord	6.9 in
Tip Chord	3.45 in
Aspect Ratio	4
Sweep	14.04o
Taper Ratio	0.5
Airfoil	NACA 0012
Rudder	
Span	Full Span
Chord Percentage	20%
Max Deflection	±30o

Tables 4.1-4.3: Final Aircraft Design Parameters

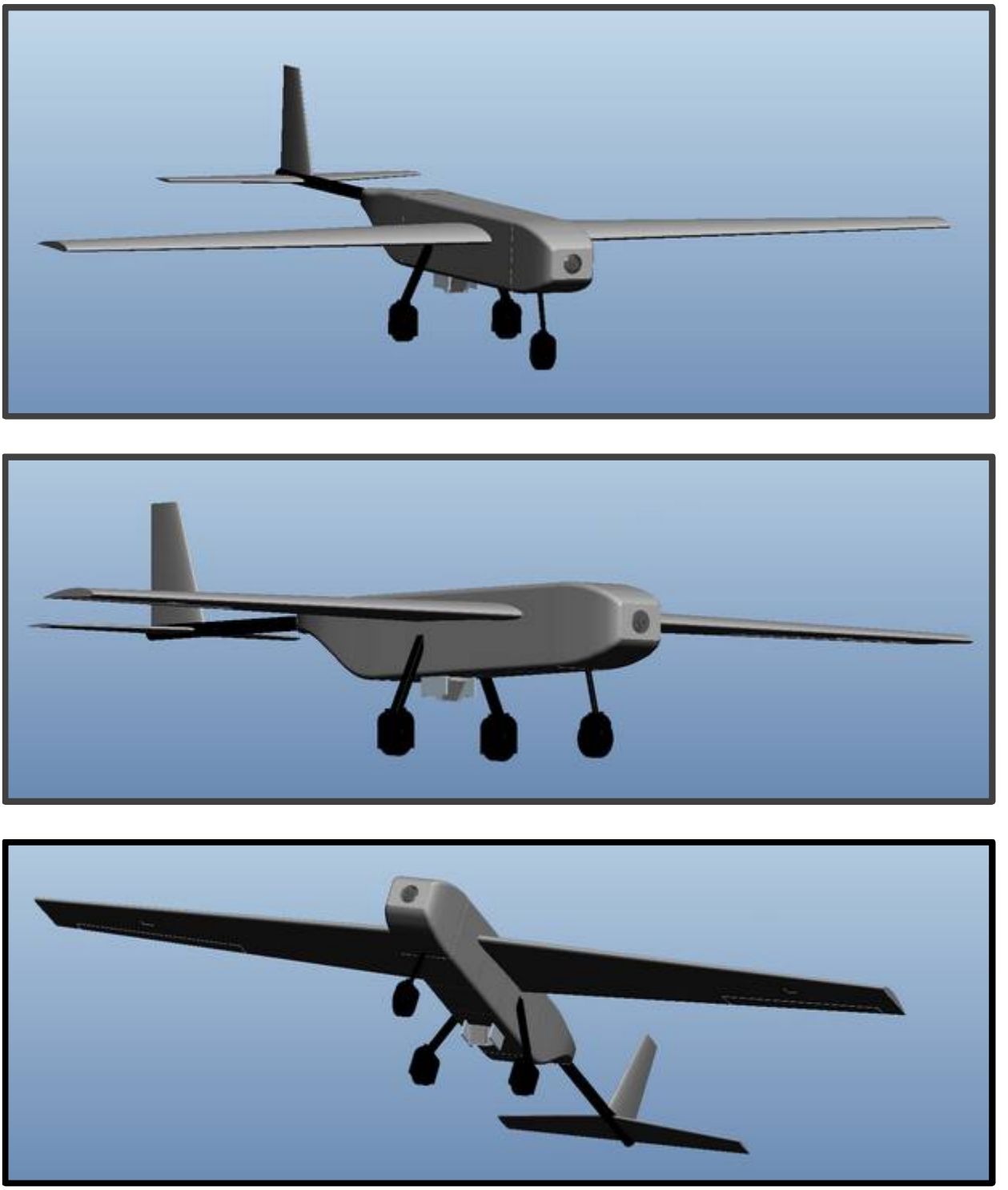

Figure 4.10: Final Configuration Layout

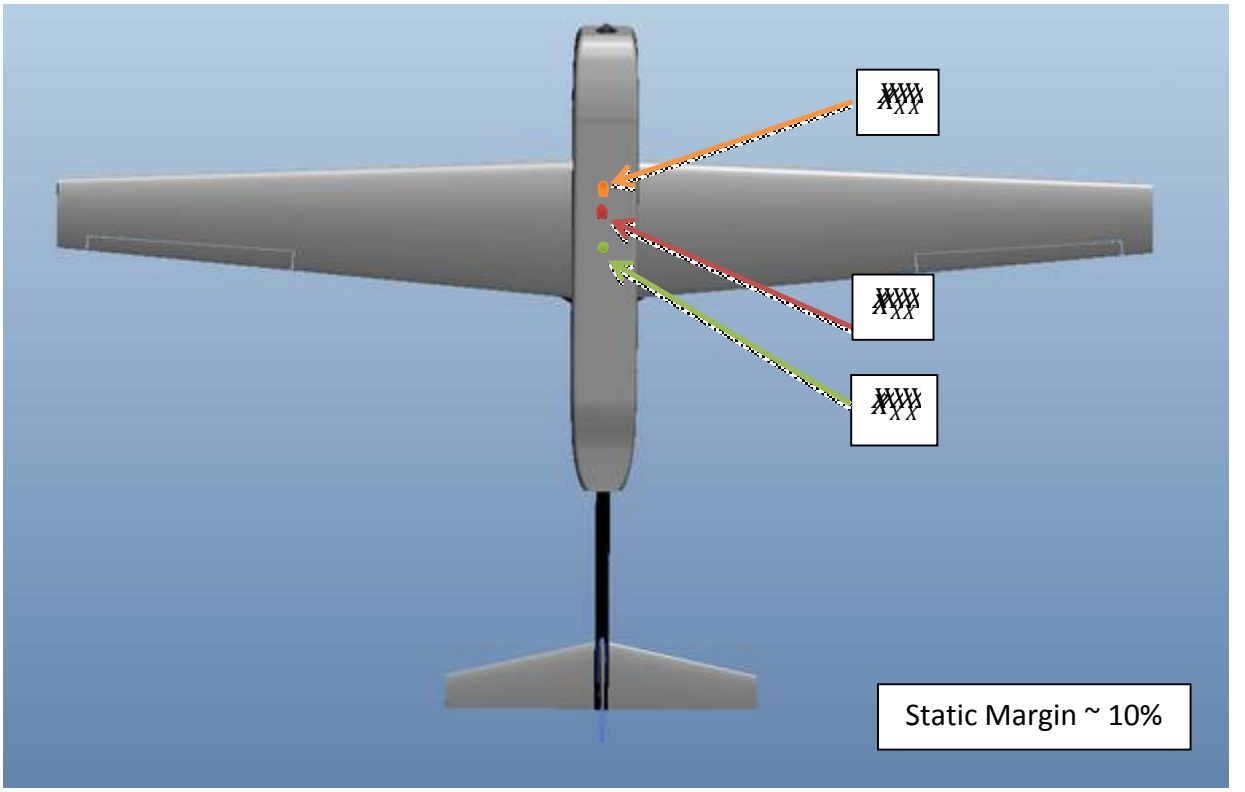

Figure 4.11: Determination of Static Margin

4.2 Materials Selection

With our current design specifications we seek an airframe that is highly durable, light weight, and easy to manufacture with equipment available to us. With this in mind the most important material properties to consider are density, strength and toughness. Materials that possess a combination of low density and high strength and toughness will be the most useful for our applications. Having low density will decrease the overall mass of our system, allowing for less motor power and more air time. Because the wings experience both tension and compression, tension from the lift forces on the bottom of the wing and compression from the weight of the fuselage bearing down on the top, and that all control surfaces create bending moments on their fuselage connection points, materials that feature good strength properties are required. Toughness is necessary in all control and lift surfaces as failure in these areas will ruin the stability of the craft and cause it to crash. On the off chance that the plane is hit by something

high impact resistance is also required. Below are charts displaying strength and toughness properties in relation to density and modulus of elasticity.

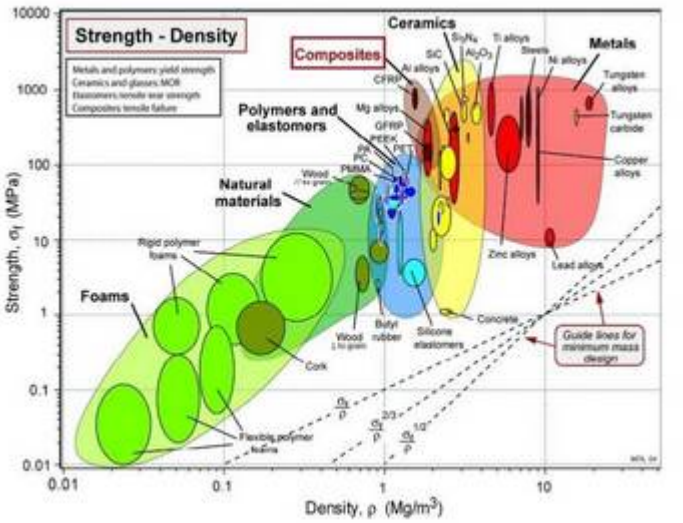

Figure 4.12: Strength versus density material chart

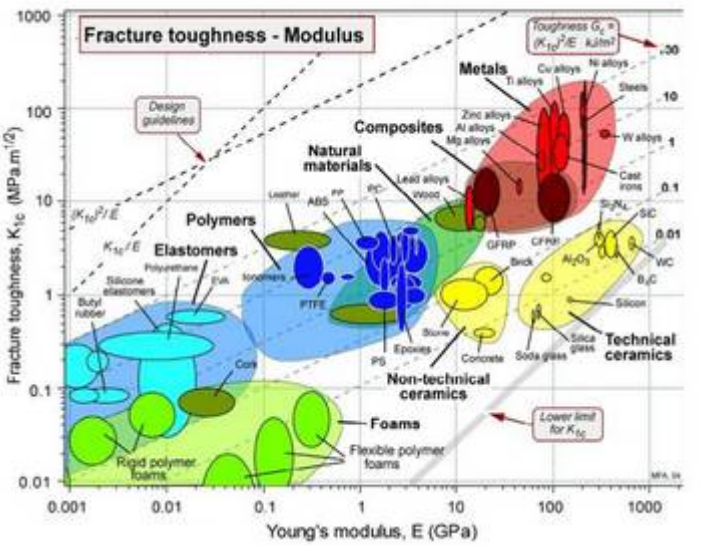

Figure 4.13: Fracture toughness versus Young's modulus chart

It can be seen that, for their density, composites have exceptionally high strength, while different types of wood also have relatively high strength with very low density. Different types of foam are also of interest for their incredibly low density, where their lower strength can be

offset by reinforcement with small amounts of reinforced plastics. All of these materials, foams, wood, and composites, can be easily procured by us or produced at facilities on campus. For these reasons we will attempt to utilize all three materials in our design.

The wing sections, tail, and fuselage will all follow similar fabrication methods. The fuselage will be constructed by forming the composite cloth skin layers onto a mold. This mold can either be a male plug mold or a female shape mold and will be covered with PVA release film so that the skin doesn't stick to its surface. The first layer of composite sheet will be tightly wrapped to the mold and then be evenly painted with the proper amount of resin designated by the cloth's manufacturer. Each following layer is applied with a 90 degree turn in respect to fiber direction and the appropriate amount of resin. This will provide greater strength in all directions of deformation. Once all layers are placed a piece of peel ply sheeting, or a combination of perforated release film and breather cloth, will be applied and the entire mold and sheeting will be placed into a vacuum bag. The mold will be left in place for at least 6-9 hours, depending on the resin used, to dry.

The wing sections and tails will be formed by cutting a foam section of appropriate length, either by heated wire or a CNC machine, and then forming the outer skin layers to the foam core with the same process used on the fuselage. In this case a peel ply sheet is only needed on the outside of the entire wing section, including the skin, because the composite layer must bond to the foam with the resin. Only an epoxy resin can be used because a polyester resin will dissolve the bonds of the internal foam structure.

The internal structure of the plane, including supports for the fuselage and mounting positions for the payload, will be constructed of sandwiched balsa wood and carbon fiber sheet. The balsa wood will consist of multiple layers placed so that their grain direction alternates by 90o and then wrapped in carbon fiber and infused with resin.

Concept 1: Resin Impregnated Fiberglass and Blue Foam

This concept utilizes fiberglass reinforced plastics (FRP), consisting of woven fiberglass cloth sheets impregnated with an epoxy resin, and blue extruded polystyrene (EP) foam. The blue foam in use will feature a compressive strength of 25 psi and a density of 1.9 lb/ft3. Blue EP

foam is a standard in wing core construction and is relatively cheap and easy to procure. A drawback of using the blue EP foam is that when cut by heated wire droplets of the removed foam can create protrusions on the surface, rendering the core unusable.

Concept 2: Resin Impregnated Fiberglass and Spyder Foam

This concept will use the same fiberglass sheets and resin as Concept 1 but will use Spyder foam for the wing core material. Spyder foam features a cell structure aligned perpendicular to the wing surface creating a compressive strength of 60 psi while maintaining a density of only 2.2 lb/ft3.(2) This foam costs more than the standard blue EP foam but is more than twice the strength, allowing for a smaller and shorter spar cross-section, less layers of fiberglass skin, and a much lower chance of failure. The cell structure of Spyder foam also allows for more resin movement into the foam, creating a better bond with the outer skin layers. When cut by heated wire Spyder foam also has none of the drawbacks featured by blue foam.

Concept 3: Resin Impregnated Carbon Fiber and Blue Foam

In this concept carbon fiber sheets will be used to create the skin of the craft in place of fiberglass sheets. The same blue foam used in Concept 1 will be used and the same type of epoxy resin can be used. A carbon fiber sheet that shares a similar weight to a fiber glass sheet features much higher toughness and higher tensile strength. This means that lift forces and impact energies on the fuselage can be supported with a smaller overall number of skin layers. Carbon fiber sheeting has a higher price than fiberglass sheets but less material is needed. The same sheets used in creating the fuselage support ribs can also be used for the skin which will reduce shipping costs and overall wasted material.

Concept 4: Resin Impregnated Carbon Fiber and Spyder Foam

This concept will be like that of Concept 3 but use Spyder foam for the wing core material instead of blue foam. This concept will be similar in weight to that of Concept 2 but will offer a much higher strength with an overall smaller amount of material. Of all designs this will be the most expensive but offer the highest durability and lowest possible chance of failure.

Concept 5: Hybrid Composite Skin

This concept will utilize both carbon fiber and fiberglass sheets in the construction of the planes outer layer. Fiberglass will be used as the primary material for the skin while carbon fiber will be used to reinforce critical sections of the plane, including the wings, tail, and nose cone. In any area where both materials are used carbon fiber will form the outer most layer so that its high toughness will be fully utilized.

Based upon the hybrid composite structure concept chosen earlier in the concept generation phase of the design, multiple fiber reinforced plastic (FRP) matrix systems and core materials were selected for different components of the design. FRPs will be the main materials of choice throughout the aircraft because of their high strength to density ratios and ability to be molded into almost any shape. Where needed core materials of a lower strength and density will be sandwiched between layers of FRPs to provide greater structural stability without a large increase in weight.

Two types of fiber reinforcement, carbon fiber and fiberglass, were chosen while a single type of epoxy resin system was chosen to create the plastic matrix. Different fiber reinforcements were chosen so that specific properties could be tailored for each segment of the aircraft. The 635 Thin Epoxy Resin system from US Composites was chosen for its high cure strength, moisture resistance, structural and chemical stability, and ability to bond well with both wood and foam. The epoxy resin system comes in two parts as the resin itself and a hardening agent. These two parts need to be mixed exactly in a two to one ratio, two parts resin to one part hardener, to ensure a proper cure.

The carbon fiber of choice was a 3k 2x2 twill weave, meaning that three thousand filaments make up each fiber and every fiber runs over two then under two other fibers in the weave. Carbon fiber has a higher strength and stiffness while also possessing a lower density than fiberglass. It is however not as flexible as and greater in thickness than fiberglass, meaning that it is harder to form on curved surfaces and has a higher tendency to develop inclusions of air in the matrix. These factors, and the fact that it is four times more expensive than fiberglass per yard, limit the use of carbon fiber to structural members that require the higher strength and

stiffness properties. The fiberglass of choice is 120 E-glass, or 4hs satin weave fiberglass. This fiberglass is of an extremely tight weave with low thickness and high flexibility.

The core materials used for the sandwich structures and wings will be standard aircraft balsa wood, utilized in almost all RC aircraft applications, and expanded polystyrene foam. The balsawood will be used inside of the fuselage because of its ease in shaping through the use of laser cutters, and foam will make up the core of the wing. Using these core materials in conjunction with the FRP outer skins will drastically reduce the weight of the plane without compromising structural strength.

Material	T. Strength 0o/90o (KSI)	T. Modulus 0o/90o (MSI)	In-Plane Shear (KSI)	Poisson's Ratio
Carbon Fiber	87	10.1	13	0.11
Fiberglass	23	2.18	3.95	0.1

Table 4.4: Typical properties of fiber reinforced epoxy matrices

Final Concept:

The outer skin of the fuselage will consist of four layers of fiberglass impregnated with epoxy resin, layed down with the second layer at $+45^{o}$, the third at $+90^{o}$, and the fourth at -45^{o} where all angles are relative to the first layer of fabric. This skin will be bonded to an internal support structure, pictured below, with quick hardening epoxy. The support structure was modeled after traditional RC aircraft internals and other aircraft created previously in the AUVSI SUAS competition while keeping in mind the increased structural stiffness from the multi-layer outer skin.

The center plate of this structure will be constructed of 3/8" plywood as discussed earlier while each rib will be constructed of balsa wood and a layer of carbon fiber in the sandwich core style. The rib at the front of the structure, where the nose cone connects to the fuselage, is termed the firewall. The firewall is a solid piece that acts as both a mounting point for the motor and

nose cone, and a shield from heat and electrical interference generated by the motor. The two center ribs act as support for the wing structure and connection points.

The wings will consist of a fiberglass outer skin of four layers, layed up in the same style as the fuselage, with an EPS foam core. There will be two spars running through the wing from the tip chord to 6" before the root chord where they will be fitted to the shear box with epoxy. The spars act as the main support for the load felt by the wetted area of the wing, where the load is transferred from the fiberglass skin to the foam core and then into the spars, but the fiberglass skin will absorb some of the tension forces and the foam core will do the same with compressive forces.

With the requirements of high mobility and ease of assembly in our design it was decided that an easy way of attaching and removing the wings for storage was necessary. This system all needed to be strong enough to safely handle the highest loads felt by the wings. Our solution to this was to have two solid rectangular bars of carbon fiber running through the fuselage and into each wing. These connectors will be rigidly attached to the frame by epoxying them to the two central ribs. Inside of the wing is a shear box made of carbon fiber that matches the profile of each connector and the aligning wing spar. The connectors will be press fitted 6" into these shear boxes until they meet the spar that has been fitted into the other end of the box. The front connector has dimensions of 0.654"H x 3/8"W while the rear connector has dimensions of 1/8"H x 0.40"W. Identified in the picture below are the two wing connectors.

The shear box is constructed of four layers of carbon fiber, mimicking the alternating layers of the wings and fuselage in a 0^o, $+45^o$, $+90^o$, -45^o pattern, with the front and rear being sized to fit the wing connectors. The front shear box has outer dimensions of 0.75"H x .471"W and the rear shear box has outer dimensions of .2"H x .471"W. There will be a section cut out of each wing core that will fit the outer dimensions of the box so that it can be secured into place by epoxy.

The wing spars are made of multiple layers of carbon fiber to better support the combined compressive, tensile, and shear forces that they encounter. They are placed at 25% and 70% of

the chord length from the leading edge to fit with the taper of the wings and the area removed from the wings by the aileron. The spars are rigidly attached 1" into the shear box with epoxy. After the shear box the front spar takes on the outer dimensions of the shear box for another 8" and then tapers to 50% of the outer dimensions at the wing tip chord. The rear spar begins to taper immediately after the shear box to 50% of its dimensions at the wing tip chord. The front spar, which takes the majority of the load, runs orthogonal to the root chord surface while the rear spar follows the angle of the wing from the end of the shear box to the tip chord. The spars will fit inside of cavities cut into the wings by the foam core manufacturers and will be joined to the foam with epoxy.

The tail boom will be a unidirectional pultruded carbon fiber tube with an outer diameter of 1". The boom will run from inside of the fuselage, attached to the frame at the rear rib, and have the tail section attached to the opposite end.

Because the spar structure and the wing connectors with shear box are carrying the weight of the plane, and lift forces generated by the wings, they are the most important structural members of the plane. A stress analysis was performed on each part to make sure that they will not fail under operating conditions.

4.3 Propulsion System Design and Selection

Propulsion means to push forward or drive an object forward. A propulsion system is a machine that produces thrust to push an object forward. The thrust from the propulsion system must balance the drag of the plane when the plane is cruising. The thrust from the propulsion system must exceed the drag of the plane for plane to accelerate. The battery power will need to be last at least an hour. In choosing a motor we are looking at a few options. There are two main options an electric powered and a gas/glow motor.

Electric Motors:

Electric powered model aircrafts have gained popularity, mainly because the electric motors are more quiet, clean and often easier to start and operate than the combustion motors. People who use these types of motors tend to try and make their planes as light as possible to

obtain a reasonable flight time or wing loading. The coreless motor has the rotor coils not wrapped around an iron core but just fastened into shape with glue, which makes the rotor much lighter and faster to accelerate and thus suitable for servos. Since the coreless motors don't have iron cores they have much less iron losses, which make them more efficient than cored motors. However, the coreless motors will not stand continuous high RPM and/or loads without falling apart. That's why they are generally rather small, with low speed and low power. A DC motor converts the electric current into Torque and the voltage into rotations per minute (RPM). There are two main types of electric motors; brushed and brushless.

Brushed motors need some maintenance, since both the brushes and the commutator will wear after a while due to the friction. Most quality motors allow brush replacement. The commutator itself also needs cleaning as it gathers deposits of carbon and gunk due to the graphite powder from the brushes. It may be cleaned by a very light polishing action with scotch rite or with a so-called commutator stick. Brushes are usually made of three different compounds: Graphite, Copper and Silver. Brushes made of silver are normally used in competitive racing as they have low resistance, but they produce the highest commutator wear and also have medium brush wear and lubrication. Silver brushes produce sludge that only can be removed by lathing the commutator. Copper brushes don't produce sludge and work best at high rpm. These brushes produce medium commutator wear and have high brush wear and low lubrication. Graphite brushes produce low commutator wear, have low brush wear and high lubrication but have high resistance, which means that they are not suitable for racing. Sparks that occur between the brushes and the commutator can cause radio interference. In order to prevent radio interference it is recommended the use of ceramic capacitors soldered between each motor terminal and the motor case. For extra security against interference, a third capacitor should also be fitted between the motor terminals.

Brushless motors are little more expensive but they have higher efficiency typically between 80 to 90%. Since they have no brushes, there is less friction and virtually no parts to wear, apart from the bearings. Unlike the DC brushed motor, the stator of the brushless motor has coils while the rotor consists normally of permanent magnets. The stator of a conventional (in runner) brushless motor is part of its outer case, while the rotor rotates inside it. The metal

case acts as a heat-sink, radiating the heat generated by the stator coils, thereby keeping the permanent magnets at lower temperature.

Brushless motors are 3-phase AC synchronous motors. Three alternated voltages are applied to the stator's coils sequentially (by phase shift) creating a rotating magnetic field which is followed by the rotor. It's required an electronic speed controller specially designed for the brushless motors, which converts the battery's DC voltage into three pulsed voltage lines that are 120o out of phase. The brushless motor's max rpm is dependent on the 3-phase's frequency and on the number of poles. Increasing the number of poles will decrease the max rpm but increase the torque. A recent type of brushless motor is the so-called "out runner". These motors have the rotor "outside" as part of a rotating outer case while the stator is located inside the rotor. This arrangement gives much higher torque than the conventional brushless motors, which means that the "out runners" are able to drive larger and more efficient propellers without the need of gearboxes.

Glow Engines:

Glow engines are actually internal combustion engines that form the heart of any gas or nitro powered RC plane. Most nitro R/C models use a 2- or 4-stroke glow engine, sized specifically for that model. Typically, they range in displacement from .049 cu. in. to 1.2 cu. in. (80cc to 20cc) — a variety that satisfies virtually any model's power requirements. Glow engines cannot be operated with the same gasoline you'd get at a filling station pump. They require a special fuel, called "glow fuel." It contains methanol as the base, with varying amounts of nitro methane to increase the energy that the fuel can provide. Oil, pre-mixed into the fuel, lubricates and protects your tiny engine as it pounds out amazing power.

There are two primary kinds of glow engines; two-stroke and four-stroke. Two-Stroke simply means that the engine "fires" (ignites the fuel in its combustion chamber) with every revolution of the piston. Generally, they're a good place for new nitro modelers to start. Two-strokes are easier to operate, less vulnerable to problems if misused, and deliver more power for their size and weight. Four-Stroke engines fire once with every two revolutions of the piston. They consume less fuel, sound more realistic, and provide more torque but cost more, are harder to adjust and require more maintenance. Most glow engines have a simple ignition system that

uses a glow plug rather than a spark plug so there's no coil. The glow plug is heated by a battery-operated glow starter; meanwhile, the modeler uses a recoil starter, Electric 12V Starter or Starter Box to turn over the engine. When fuel enters the combustion chamber, it's ignited by the heated glow plug and the engine starts. At this instance the engine begins gaining the momentum to continue running after all the starter accessories are removed. The engine's carburetor supplies the fuel and air needed for combustion. A rotating throttle arm controls the amount of fuel and air that enters the combustion chamber. The high-speed needle valve controls the mix or proportions of fuel vs. air at mid- to high-speeds. The idle mixture screw is similar to the high-speed needle valve, except that it controls the mix of fuel and air when the engine is only idling. When you've adjusted the high-speed and idle mixtures properly, your engine should operate smooth and steady throughout its range of speeds. True gas engines have a lower power to weight ratio than glow engines.

Propeller:

The propeller is the part of an RC vessel that pushes air (or water) behind it by spinning quickly, causing the craft to move forward. The propeller gets the energy to do this from the engine to which it is connected. Engines come in two basic forms: electric or internal-combustion, which is also known as a glow engine in the RC world. Because they are less expensive and easier to maintain, beginners are advised to choose an electric RC craft. They are also much less noisy than glow engines, so you can use them in a wider variety of areas, rather than just private fields and RC air fields.

Most simple RC airplanes use a single two-blade propeller attached to the nose of the craft. Most RC boats use one propeller as well, but a special type that is suitable for use underwater. RC blimps typically use two small propellers, one on each side of the bottom portion of the blimp (gondola). These propellers can vary speed and direction to precisely control movement, or even hover. Hydrofoams also use two propellers, but they have three blades instead of two, and have a ring connecting the blades going around the circumference of the tips. The fastest and most expensive form of RC craft is jets. They use a multi-bladed propeller, called an impeller, that spins at very high revolutions per minute (RPM) and generate significant thrust.

Final Concept:

Based on the power requirements of the mission profile, a maximum output power of 550 W is used to select an appropriate brushless DC motor. The AXI 4130/20 Gold line brushless DC outrunner motor was selected based on several parameters. The output power, weight, battery cell requirement, cost and efficiency were used to select this specific motor. The decision matrix for the available brushless DC motors are shown in table 10.1. A grade of 1-5, was used in the decision matrix signifying a grade of poor (1), satisfactory (2), good (3), excellent (4) or outstanding (5). More weight was given to the required battery cells, as this increases battery weight dramatically. The power and efficiency of the motors are similar, so less weight was given to those score, while the cost of the motor was deemed of medium importance.

Motor			AXI 5320/28		Elite Power 60		AXI 4130/20	
Criteria	weight		Grade	Weighted G	Grade	Weighted G	Grade	Weighted G
Weight	0.2		2	0.4	4	0.8	3	0.6
Cell # (LiPo)	0.25		3	0.75	4	1	4	1
KV (RPM/V)	0.15		3	0.45	4	0.6	4	0.6
Max Power	0.1		4	0.4	3	0.3	4	0.4
Efficiency	0.1		5	0.5	4	0.4	4	0.4
Cost	0.2		3	0.6	3	0.6	4	0.8
Total	**1**		**20**	**3.1**	**22**	**3.7**	**23**	**3.8**

Table 4.5: Brushless DC motor decision matrix

As can be seen from table 10.1, the AXI 4130/20 was the better choice based on these parameters by only a slight margin. The selection of this motor was also based on the availability of this motor from vendors that could also supply other components of the aircraft, and better reviews from previous testing in RC aircraft. The specific characteristics of the AXI 4130/20 motor are shown below in table 10.2, and are used to analyze the power supply requirements of the propulsion system.

AXI 4130/20 Specifications	
Cell # (Lipo)	8
RPM/V	305
Max Efficiency	88%
No Load Current	1.2 A
Internal Resistance	99 mohm

Table 4.6: AXI 4130/20 Specifications

Propeller Considerations:

The propeller size for this particular motor is recommended by the manufacturer as 16" by 10". Because overloading the motor using an unsuitable propeller can damage the motor severely, a 16" diameter by 10" pitch propeller is selected and will be further tested in the lab when procured. An example propeller is shown in figure 10.3.

Figure 4.14: 16" by 10" Propeller

Power Consumption Considerations

With these motor parameters, a graph can be draw showing the output power of the motor versus the input current from the power supply system. The supplied voltage is dependent on the

type of battery and the number of cells used. For this graph, a LiPo battery is assumed, with the manufacturer recommended 8 cells. LiPo cells supply 3.7 V individually, so the recommended supply voltage to this motor is 29.6 volts. On graph 10.1, the two mission profile points are plotted. The first point (p1) is the required power for takeoff which will last approximately 3 minutes. The second point (p2) is the required power for cruise, which includes the search area maneuvers and will last approximately 57 minutes.

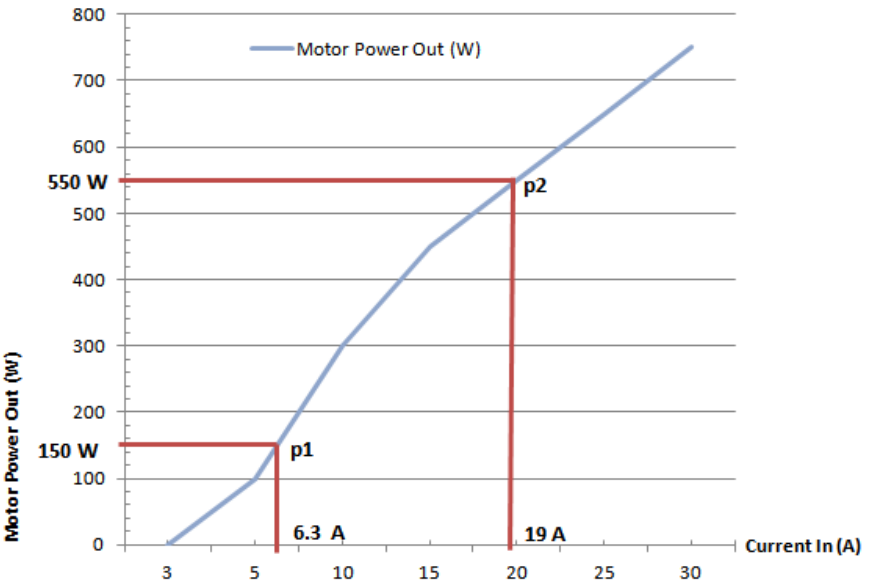

Graph 4.2: Motor Power output vs. Current Input for the AXI 4130/20

4.4 Power Supply System Design and Selection

The power supply system of the aircraft is the system that will supply the electrical energy to all the electrical loads present in the aircraft. This system will consist of an electrical storage device (batteries), a voltage regulation system, the conductors carrying the current to the loads, and a device for recharging the electrical storage device. The requirements for these basic components are drawn from attributes that are universally beneficial for an aircrafts' composition. These requirements are low weight, small size, low heat emission, and the ability to store and deliver the required electrical energy necessary for flight. The target flight time for mission completion is forty minutes. This required flight time provides a foothold for generating a power supply conceptual design. However, due to the fact that the various aircraft components

that will be powered through this system have not yet been picked, the battery specifics and voltage regulator specifics cannot be determined at this stage in the design process.

Another important aspect of the power supply system design process is its' close relationship with the propulsion system of the aircraft. The propulsion plant of the aircraft could be powered either by gasoline or by electricity. If the propulsion is handled by a gasoline engine, the power supply system will not have to supply the amount of power required for an electrical propulsion plant. The design of the propulsion plant will affect the power system in the selection of the batteries and the voltage regulation components. Without knowing the aircrafts' definite propulsion plant, the design of the power supply system can only be cursory and based on the comparison of the available battery types.

Batteries:

The electrical storage device is the most important part of the power supply system. There are a wide variety of batteries on the market specifically designed for applications such as Remote Control airplanes and cars. The different batteries are distinguished by their chemical composition and three major types have achieved popularity in the RC community. The three popular types of batteries and their traits are shown below in figure 8.

Battery Composition	Abbrev.	Specific Energy (Wh/kg)	Energy Density (Wh/L)	(Dis)Charge Eff.	Specific Power (W/kg)
Nickel-Cadmium	NiCad	40-60	50-150	80%	150
Nickel-Metal Hydride	NiMH	60-120	140-300	66%	250-1000
Lithium-Ion Polymer	LiPo	130-200	300	99.80%	7100

Table 4.7: Battery Characteristics

Based on these battery characteristics, three different designs can be generated based on the three types of batteries. By analyzing the requirements of the power supply system and applying the requirements to these three battery types, a decision can be made on which battery type is best suited for the aircraft.

Power Supply System Design Concepts:

Nickel Cadmium (NiCad) batteries are referred to as old technology, and are not as common in the RC world as they once were. As can be seen from figure 1, the charge/discharge

efficiency of the NiCad battery is much higher than the NiMH batteries, but there are many reasons the NiCad batteries are used less frequently than the other types. NiCad batteries must be fully discharged after each use; otherwise they will develop what is called “memory” or an inability to discharge fully during use. The capacity per weight, which can be seen from the specific power, is lower than the two other batteries, which makes it a poor contender for use in an aircraft. The Cadmium that is used in the manufacture of the battery is also harmful to the environment, and was the purpose behind the development of the nickel metal hydride battery. The benefits of using the NiCad battery are the inexpensive cost of the battery, the absence of safety issues dealing with an aircraft crash, and the NiCad’s ability to discharge high current with no damage to the battery.

Nickel metal hydride (NiMH) batteries were developed to replace the NiCad batteries, and have several benefits over NiCad. NiMH batteries are not required to be fully discharged each use, and do not develop a memory over time. The capacity per weight is much higher than the NiCad battery, and it is available at a price not much higher than the NiCad. This battery is also easy to charge and discharge as compared to the LiPo battery and like the NiCad, does not have any inherent safety issues.

Lithium ion polymer batteries are the newest battery to be developed and brought to market. This battery’s capacity per weight is many times the capacity of the NiMH and NiCad batteries. The composition of the battery cells also results in the LiPo battery being around half the weight of a NiCad or NiMH battery. Because LiPo batteries can achieve twice the capacity of the other batteries with half the weight, they are ideal for using in an aircraft. However, there are issues that have prevented the LiPo battery from dominating the RC market. The biggest negative factor in using LiPo batteries is the fire hazard inherent in using these batteries. If a LiPo cell is incorrectly charged or physically damaged, it may burst into flame, and severely damage the aircraft and its components.

From the analysis of the three types of batteries, it is clear that the design of the aircraft power supply system could be completed using either the NiMH battery or the LiPo battery.

Final Concept:

By taking the calculated power consumption values for the avionics, propulsion and image processing systems, a power supply system can be designed to supply the systems in the most efficient manner possible. The power supply system components are the batteries, the voltage regulators required in the aircraft, and all the conductors carrying the required current to the loads. Other auxiliary components of the power supply system are the battery recharging and balancing devices, the ground station power supply system and any required electromagnetic Interference (EMI) shielding.

Battery Decision Matrix Criteria	weight		NiMH Battery Grade	Weighted G		LiPO Battery Grade	Weighted G
Performance	0.2		4	0.8		5	1
Weight	0.25		3	0.75		4	1
Size	0.25		1	0.25		5	1.25
Cost	0.1		5	0.5		1	0.1
Safety	0.2		5	1		3	0.6
Total	**1**		**18**	**3.3**		**18**	**3.95**

Table 4.8: Battery decision matrix

The LiPo battery was the choice battery mostly due to its low weight per capacity, small size, and high performance. The LiPo battery type was analyzed to insure that it was the best choice for this particular aircraft application. A unique feature of the LiPo battery is its discharge curve. As shown in graph 10.2, the voltage of the LiPo battery remains fairly linear until the individual cell voltage falls under the “critical voltage”. For most LiPo cells, this is approximately 3 volts. Over discharging of the LiPo cells damages the battery, and will decrease the lifespan of the battery pack. The ESC that will be connected to the motor and motor batteries will prevent this from happening, as it has a low voltage cut-off around 3 V. However, if any additional batteries are added to the power supply system, a low voltage cut-off device must be added to insure the batteries are not over discharged.

Another consideration when using LiPo batteries is the volatility of the chemicals used to manufacture the batteries. LiPo batteries can burst into flame or explode when the cells are damaged or punctured. Damage can also be caused to the battery from over charging or over

discharging the cells, either of which may ruin the battery pack. Good practices that decrease the probability of LiPo battery damage include a pre-usage inspection, using a LiPo battery charger and never discharging a LiPo battery below a cell voltage of 3 volts.

Adding together all the required current capacities for the various aircraft, the total cuurent capacity required from the batteries can be calculated as:

$$X_{XXX} = (X_{XXXXXXX} + X_{XXXXXXXXX} + X_{XX\ XXXXX})$$

Plugging in all the values:

$$X_{XXX} = (431\ X\ Xh + 6935.7X\ Xh + 750\ X\ Xh) = 8.12\ Xh$$

The total current capacity for the aircraft is calculated as 8.171 Ah.

With the required battery capacity of at least 8.5 Ah, the entire aircraft electronics system can be analyzed and the total power supply system designed. The aircraft electronic components with their required supply voltages and currents are shown in table 10.9. The components can be grouped according to supply voltage into four different voltage zones.

Component	Required Voltage (V)	Supplied Voltage (V)	Voltage Zone
BEC	29.6	29.6	1
Motor ESC	29.6	29.6	1
AXI 4130/20 Motor	29.6	29.6	1
CS Servos	3-6	5	2
Gimbal Servos	3-6	5	2
Paparazzi Board (Complete)	6-18	11.1	3
CCD Block Camera	6-12	11.1	3
Lawmate Video Tx	10.5-13	11.1	3
Xbee Tx	3-3.6	3.3	4

Table 4.9: Aircraft electronic components specs and voltage zones

With the voltage zones being so far apart it is necessary to either use multiple voltage regulators, or separate batteries for the two main voltage zones. By using an 8-cell LiPo battery, the required voltage of 29.6 volts can be supplied to the components in zone 1. The 11.1 volt supply voltage of zone 3 could be supplied by using a 3-cell LiPo battery. The integrated BEC in

the Phoenix ICE 100 Brushless ESC is capable of regulating the 29.6 volts from the zone 1 battery to the 5 volts required for voltage zone 3. The final zone, zone 3, can be supplied by the zone 3 battery and regulated to 3.3 volts through the Paparazzi onboard regulator. The voltage zones and their suppliers are shown in table 10.10. The total current capacity for each zone supplier was calculated using the values of current consumption from table 10.9.

Zone	Supplier	Voltage (V)	Total Required Capacity (mAh)
1	[2] 8-Cell LiPos (7700mAh)	29.6	7145.7
2	ESC Integrated BEC	29.6	N/A
3	[1] 3-Cell LiPo (1300 mAh)	29.6	971
4	Paparazzi Board	5	N/A
			8116.7

Table 4.10: voltage zones and suppliers

The appropriate 8-cell LiPo battery should have a capacity of at least 7145.7 mAh and the 3-cell battery should have a capacity of at least 950 mAh. The two selected battery designs are to use two 8-cell 3850 mAh LiPo batteries in parallel to supply voltage zone 1. With these two batteries in parallel, the supplied voltage will be 29.7 V and the total capacity will be 7700 mAh. Voltage zone 3 will be supplied with a single 3-cell 1300 mAh LiPo battery. The single battery will supply zone 3 with 11.1 volts and will supply up to 1300 mAh. The two battery types selected are both manufactured by Thunder Power and are specifically designed for RC airplane applications. Selecting batteries with capacities higher than what is required allows for more a larger operating window time wise and decreases the possibility that the batteries will be overly discharged. The total top-level electronics design for this aircraft is shown in figure 6.

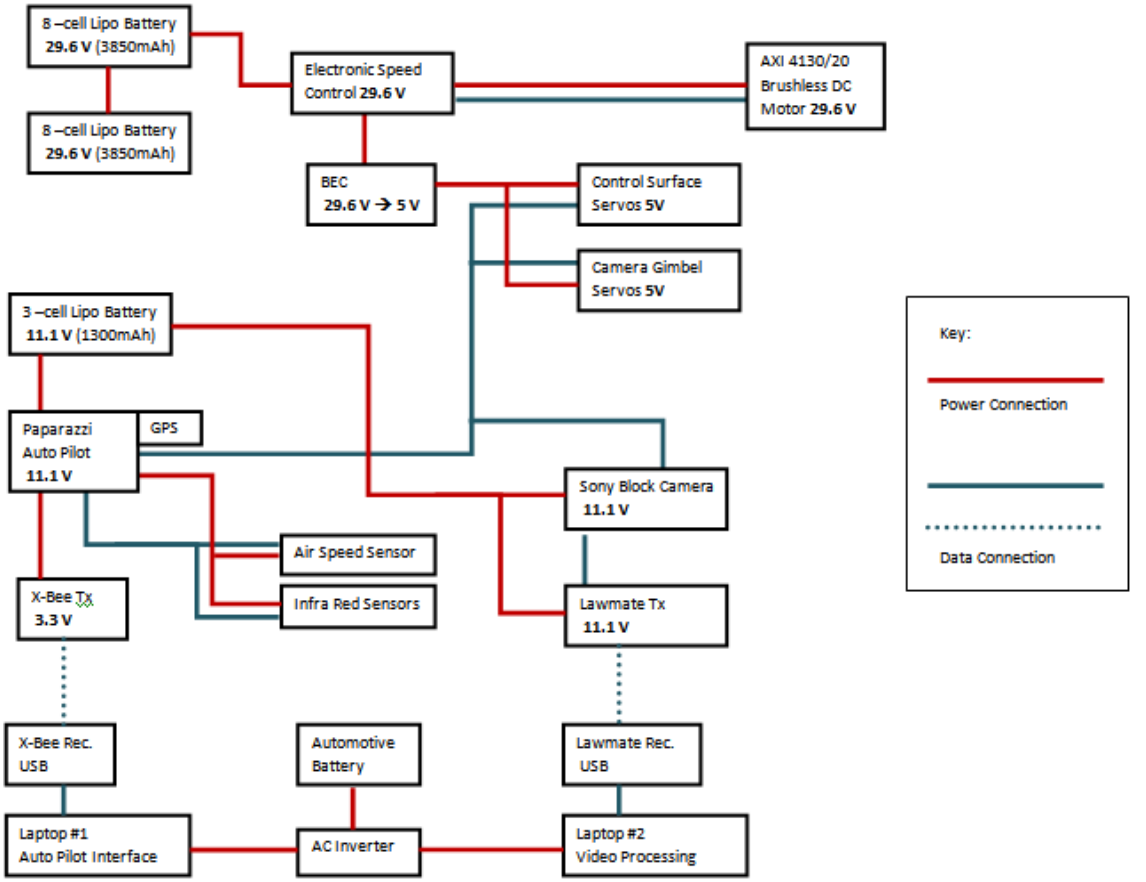

Figure 4.16: Top-level aircraft electronics diagram

4.5 Avionics System Design and Selection

Autopilot Requirements:

The UAS must complete waypoint navigation and search an area for given targets and then return back to base. The UAS must complete these objectives without being controlled by any person. The autopilot system will allow the UAS to complete these objectives with this requirement.

The ideal autopilot for this project will have a few system elements that will be vital in selecting the one best suited for the mission. Since most autopilots are not designed to search a given area, the source code of the autopilot must be easily modifiable so that this capability can be added to the system. The ideal autopilot will also use a small amount of power throughout the entire flight. It would be very helpful if the autopilot could also interface with most sensors,

allowing the team to mix and match sensors for the mission. Lastly, the autopilot board needs to have some way to be able to control the camera system gimbal.

Autopilot System Concepts:

The first system considered is the Ardupilot Mega autopilot system. The ideal batter for this system is a 7.4V 2s pack with a peak amperage of 1A. This board has a built in switching power supply to accommodate the 5V bus used for outputs. The weight is approximately 45g and the dimensions are 40mm x 69mm. The positives for this system are that it has a built in kill switch that is needed for if the autopilot malfunctions and the UAS needs to be flown manually. Also, the software for the autopilot interface runs in windows, making it very portable. The negatives to this board are that it lacks the extra ports for the camera system gimbal, meaning the gimbal would have to be controlled using some other system. Also, there is no source code directly given with the software, so modifying it to be able to handle the search area will be difficult.

The second system is the Piccolo SL autopilot system. The input voltage ranges between 5-30V, and has an average power usage of 4W. The weight of the system is 100g, and the dimensions are130 x 59 x 19 mm. A positive to this board is that it has been tested at running over 100 degrees Fahrenheit, which is one requirement for the system to complete the mission. Another positive is that it has over ten I/O ports, allowing for many other parts of the system to be controlled besides the servos. This would be helpful for the camera system gimbal. Some negatives to this board is that the developer kit is sold separate from the actual autopilot board, so the cost to integrate the search area could would be more expensive, and the source code included in the developer kit is not made to easily be modified. This is a major disadvantage for trying to implement the search area.

The third system considered is the Paparazzi Tiny v2.11 autopilot system. The input voltage ranges from 5-18V with a maximum amperage of 2.5A. This system also has a built in switching power supply for supporting the 5V bus on the board. The weight is 24g and the dimensions are 70.8 mm x 40 mm. Some positives for the Paparazzi board is that it has a built in kill switch, it has two extra ports to control the camera system gimbal, the entire source code is downloadable of their website, and it interfaces with most sensors. Although the website does have a list of preferred sensors. Some negatives is that the board is not pre-built, the website just

lists the parts used to build the board, and the interface software only runs on Linux platforms, making it less portable than most other autopilots.

Majors Sensors: GPS and IMU

The GPS is the Global Positioning System sensor used to track the location of the sensor. This is vital in navigating the waypoints and completing the search area task. The GPS uses satellites to track its position on the earth. The IMU is the Inertial Measurement Unit, which uses three orthogonal accelerometers and a gyroscope to measure the linear acceleration and orientation of the system. This is important to keep the UAS upright and to tell the autopilot the speed at which it is traveling.

The first GPS sensor is the u-Blox LEA series sensor. This GPS is recommended for most UAV projects due to its simplicity and easy interface. The sensor has a 4Hz update rate and the average power consumption is 47mA at 3.0 V. The second GPS sensor is the NAVILOCK NL-507ETTL. This GPS sensor has 16 channels for transmission, making it very reliable in always getting a reading from it. It has a 1Hz default update rate, but it can be pushed up to 4Hz and the average power is 47mA at 3.3V. The third GPS sensor is the SPK GS406. This sensor has a power usage of 75mA at 3.3V. This device only has a 2Hz update rate.

The first IMU sensor to be considered is the Booz IMU v1.2. It has a 16 bit ADC and does 200,000 samples per second. This IMU was built primarily for the Paparazzi autopilot but has been recently modified to interface with most autopilots now. The second IMU is the YAI v1.0. This is very similar to the Booz IMU because it has a 16 bit ADC and does 200,000 samples per second but this IMU was built to better interface with the lower cost sensors. The third IMU sensor to be considered is the Aspirin IMU. This is a next generation flat IMU, where most IMUs are built up from the board. It uses a three-axis accelerometer, gyroscope, and magnetometer. The magnetometer helps with the GPS calculation by measuring the magnetic fields of the Earth to find where the sensor is on the planet.

When selecting an autopilot board, there a few important factors to consider. The power usage, size, board layout, ground control system, and flight simulator need to be looked at for

each board being considered as these are all important factors. The power usage and size are obvious factors because the aerial vehicle will be running on a limited amount of power, so the less power used the better. Also, since the aerial vehicle should be as light as possible the autopilot board should be as small and light as possible. The board layout has to do with the way the input and output ports are set up. For example, an autopilot board with no servo controls would be a very poor choice because there would be no way to control the flaps on the aerial vehicle. The ground control system is the interface between the aerial vehicle and user. The flight simulator is used to see how the user's aerial vehicle will handle flying. This is a good way to test new designs.

Final Concept:

After searching through various autopilots, there are two main autopilots that are going to be looked at: the Paparazzi Tiny v2.11 and the Ardupilot Mega. Both of these autopilots are made for small UAV's similar to the objectives of this project. They also meet our budget requirements because their board design is free to download along with their autopilot software. They both have websites with forums for support as well. Here is how both boards scored in a decision matrix designed around the five factors previously mentioned:

Autopilot Decision Matrix		Ardupilot Mega		Paparazzi Tiny	
Criteria	weight	Grade	Weighted G	Grade	Weighted G
Power Usage	0.2	3	0.6	3	0.6
Size and Weight	0.15	2	0.3	4	0.6
Board Layout	0.25	1	0.25	4	1
GCS	0.3	4	1.2	4	1.2
Flight Simulation	0.1	4	0.4	5	0.5
Total	**1**	**14**	**2.75**	**20**	**3.9**

Table 4.11: Autopilot Decision Matrix of Ardupilot Mega and Paparazzi Tiny v2.11

Based on table 4.11, it is clear to see that the Paparazzi Tiny v2.11 is the best selection to complete the mission objectives. The Tiny board is 70.8 x 40mm (about the size of a credit card) and weighs around 24 grams. The board has a variety of ports, including 8 PWM outputs, one USB, 8 analog input channels, and many others (Figure 3). The ground control station is will get

the job done and is very customizable, allowing a user to add a variety of widgets to the display screen. The flight simulator is similar to many others, allowing a user to put in the specifications of their aerial vehicle and run the simulator.

The autopilot data communication can be handled by several different types of modules. The 900MHz and 2.4GHz bands are public bands that anyone can use so the module being used would need to be in one of these bands. These bands would also be good for a fast data transfer. The modules would need to be small and power efficient and handle the range. Since the mission objectives do not state a maximum range handled, we predict that a range of 5 miles would be sufficient to complete the objectives. The modules would also need to interface with the autopilot board.

The R/C receiver that interfaces to the autopilot board is the main controls of the autopilot. The R/C receiver needs to be capable of complete manual control of the plane due to the mission requirements. The R/C interface also needs to have a switch that can tell the autopilot board to switch between manual mode and autonomy mode. Along with these important requirements the receiver needs to interface with the autopilot board and be efficient with space. The unit must also operate at a frequency that does not interfere with the camera system (2.4GHz) and autopilot data communication (900MHz).

With the Paparazzi Tiny v2.11 autopilot board being selected previously the best data communication modules will be the Xbee Pro 900 module. This module has a line of sight range up to 6 miles with a high gain antenna, data rate of 156 Kbps, and operates at 900MHz. The module also has the interfacing software built into the autopilot board, making it easy to interface with the autopilot board

Figure 4.17: Xbee Pro 900 RF Module and Futaba 7CAP Transmitter.

The R/C unit being used is Futaba 7CAP transmitter and receiver. This combination is in the possession of the team and therefore the best option to use. The unit uses 7 channels and operates at 72MHz. The transmitter has all the necessary controls to be able to completely control the aerial vehicle and also has a three position switch that can be used to control the autonomy and manual modes for the autopilot. The autopilot program used uses an .xml file to configure the channel settings on the R/C receiver and therefore is very configurable for the Paparazzi Tiny v2.11.

4.6 Imagery System Design and Selection

Our goal is to design an intelligent imagery system capable of accurately determining the target location from an aerial position. The system will need to locate the targets background color, shape, orientation, alphanumeric, and alphanumeric color. Some of the function requirements for this task are the following:

- Accurately determine target characteristics from 500-750 ft
- Lightweight design to be mounted on the airframe
- Low power consumption
- Transmit images or video back to the ground-station
- 120 degree or greater Field of View

Imagery:

The two main possibilities to capture, send, and process images are to either use still-image camera pictures or implement a real-time video display. Both choices have immediate advantages as well as disadvantages to the unmanned aerial system.

A still picture camera requires far less transmission data than a constant data feed. Pictures with a still camera are usually captured at a much higher resolution than a video camera. Also the camera will require far less transmission power to send less data. In contrast, a still-picture camera is required to take many pictures to capture the target. The user will need to implement multiple cameras or apply a gimbal system to change the cameras viewing angle. Still images will not be updated as quickly as a live video feed and could possible cause a delay in

changing the camera position. In this case, the target could easily be missed. Target acquisition will most likely take longer than normal opposed to a constant data feed. Camera systems such as a DSLR provide a higher resolution than most video cameras but are heavy to mount to the airframe and expensive.

Implementing a live video stream allows the user to constantly update their position for an immediate target acquisition. This technique shortens the amount of time required to find a target as well as makes shorting images much easier. These video systems are similar to security cameras or machine vision cameras. They provide a lightweight design that is easily mounted to a gimbal. Unfortunately, constant data feeds require much more power than a still image system, and must be transmitted at a higher frequency, most likely in the gigahertz range to maintain a 6-8 Mbit/sec bit rate. Live camera video requires a clean signal for operation as well as real time image stabilization.

Data Link Transmission:

In order to transmit the captured images or video feed a specific data link must be created between the ground-station and the aerial vehicle. The UAS will fly along GPS waypoints during its mission and need to wirelessly transmit data back down to the ground-station at a maximum distance of up to 2-3 miles. Achieving this goal will require a carefully designed system to broadcast at VHF to UHF range depending on whether the data sent will be through a video feed or as digital stills.

There will also be two other separate data links from the UAS to the ground-station. The first being the Autopilot data sent to ground-station such as position, angle of attack, airspeed, altitude, etc. This communication link will need to be operated at a different frequency far away from the Imagery system. For safety reasons, the UAS must also have a data link that provides a manual engine override of the Autopilot during any time. It could be advantageous to use an Autopilot with additional servos can broadcast the manual control on the same frequency.

As specified in the competition description, the targets on the ground will be geometrically shaped and display alphanumerics. Each target will be a different colored shape

with dissimilar alphanumerics. The minimum dimension of the target (length or width) will be 2 ft. with a maximum of 8 ft. The sizing of the alphanumerics will be sized to occupy 50-90 % of the length/width and between 2-6 inches in thickness, and will vary in color and contrast.

The camera design should primarily be able to distinguish the target characteristics from the specified flight altitude, while remaining lightweight as possible. The camera system must have at least ± 60 degrees horizontal and vertical FOV. The camera resolution will be limited if a downlink system is used. The camera will need a gimbal system to adjust the FOV during the flight as well as a control system on the ground to operate the gimbal. There is an abundance of commercially available camera systems, but few that meet the requirements of the mission profile. The two main possibilities to capture, send and process images are to either use still-image camera pictures or implement a real-time video display. Both choices have immediate advantages as well as disadvantages to the unmanned aerial system.

Final Concept:

In this section many different types of commercially available off the shelf cameras were compared and graded based on the following parameters. The cameras were graded on a scale from (1) poor to (5) outstanding in each category.

Camera Selection Parameters Criteria	weight
Weight	20%
Mounting	8%
Resolution	15%
Zoom	10%
TX Ability	8%
Price	15%
Toughness	5%
Power Req.	10%
Dimensions	9%
Total	**100%**

Table 4.12: Camera Selection Parameters

Camera Decision Matrix		Nikon D300 DSLR		Sony KX-181 HQ		Sony FCB Block		Axis 212 PTZ	
Criteria	weight	Grade	Weighted G	Grade	Weighted G	Grade	Weighted G	Grade	Weighted G
Weight	0.2	2	0.4	5	1	4	0.8	3	0.6
Mounting	0.08	3	0.24	3	0.24	4	0.32	5	0.4
Resolution	0.15	5	0.75	3	0.45	3	0.45	3	0.45
Zoom	0.1	5	0.5	0	0	5	0.5	3	0.3
TX Ability	0.08	3	0.24	3	0.24	5	0.4	4	0.32
Price	0.15	1	0.15	5	0.75	3	0.45	2	0.3
Toughness	0.05	4	0.2	1	0.05	2	0.1	5	0.25
Power Req.	0.1	5	0.5	4	0.4	3	0.3	3	0.3
Dimensions	0.09	1	0.09	5	0.45	3	0.27	1	0.09
Total		**29**	**3.07**	**29**	**3.58**	**32**	**3.59**	**29**	**3.01**

Table 4.13: Camera Decision Matrix

After analyzing several different camera configurations it was determined that a live video feed would be a better alternative than retrieving images from an SD card. Cameras such as the Nikon DSLR would be unacceptable for this mission because its heavy design and inability to send images without the addition of a wireless USB module. The Sony KX-181 camera is a very inexpensive analog camera that is lightweight and is commonly used on RC aircrafts.

It was determined that the Sony FCB Block Camera was the best choice for the mission requirements. The IX11A Block Camera has the capability of sending the images as analog Video Blanking Syncs (VBS) and a high-speed serial interface with TTL signal-level control (VISCA protocol). This camera has 18x optical zoom capability and an analog resolution of 520 TV lines. The FCB Block Camera also gives the user the ability to customize an On-Screen Display (OSD) which would be used for information such as heading, airspeed, altitude, and GPS coordinates. If permitted by budget constraints, a second test camera would be purchased to test communications equipment as well as be available for use if the main camera failed.

Downlink:

Sending images or video streams wirelessly to the ground station is a very challenging prospect, but equally advantageous in order to determine target characteristics in real time. The communications equipment must provide enough bandwidth to support the camera downlink. The bandwidth requirements become a very challenging problem when capturing high resolution

images. Using this method the video signal would be converted to analog signal which contains luminance, brightness, and chrominance. These combined channels create a composite video connection known as NTSC standard. Analog video signals require less bandwidth that that of a digital signal, but are also more susceptible to transmission noise. This can particularly be problematic if implementing autonomous detection software. These static losses in the video feed would create several false positives.

One of the most important features about implementing a video transmission system is its ability to see targets in real time. Based on the chosen camera, Sony FCB IX11A, and its maximum resolution it is possible to determine the average file size produced. Since targets will be colored grayscale images are not possible. Therefore, images will be based on the 24-bit color scheme in which each pixel contains 9 bits. Multiplying the maximum resolution by the number of bits each pixel contains gives the average file size of 3.3 Mb. Directly sending this data to the ground station is possible using a very high speed modem.

As a benchmark the SRM6100 Wireless Serial Modem was used from Data-Linc Technologies, this modem has an average RF transmission rate of 166 Kbit/s. By dividing the image size by baud rate one can determine the transmission time. In this case a 3.3 Mb file would require 2 minutes and a half minutes to be transferred.

$$(XXXXXXXXX\ XXXXXXXXXX) * (24 - XXXXXXXX\ XX\ XXX) = X\ XX\ XXXX\ XXXX$$

$$\frac{XXXX\ XXXX\ (X\ X)}{XXXX\ XXXX\ (XXX)} = XXXXXXXX\ XXX\ X\ (X)$$

During the Enroute search the aircraft will be travelling at approximately 45 miles per hour, which means it will be covering 66 feet per second. Using these transmission parameters the ground station would receive an image every 1.875 miles. Clearly, the transmission of data to the ground station is too slow to accurately find and locate targets. This means that that the images would need to be compressed before being sent, which requires an on-board microprocessor to compress the images before being transmitted. Although there are many

advantages to using digital transmissions it was decided that analog video transmission would be a better option.

The Imagery system will be mounted on the underbelly of the aircraft between the landing gear. The Sony FCB IX11A Block Camera will be used for specific purpose of target recognition during flight. The camera will need a gimbal mount with dual servos to pan and tilt in two directions. By changing the FOV the camera can effectively see 180 degrees horizontally and over 60 degrees vertically.

Since frequent remote testing will be necessary the camera will be powered by a dedicated Lithium Polymer battery. The voltage requirements for the battery change depending on the zoom servos, but at maximum the FCB block camera requires 12 V. The video will be captured by the ¼ Exview HAD CCD sensor and be sent as an analog signal to the ground station. This camera is equipped with 40x optical zoom making it extremely capable of determining the targets from an altitude of 500 ft.

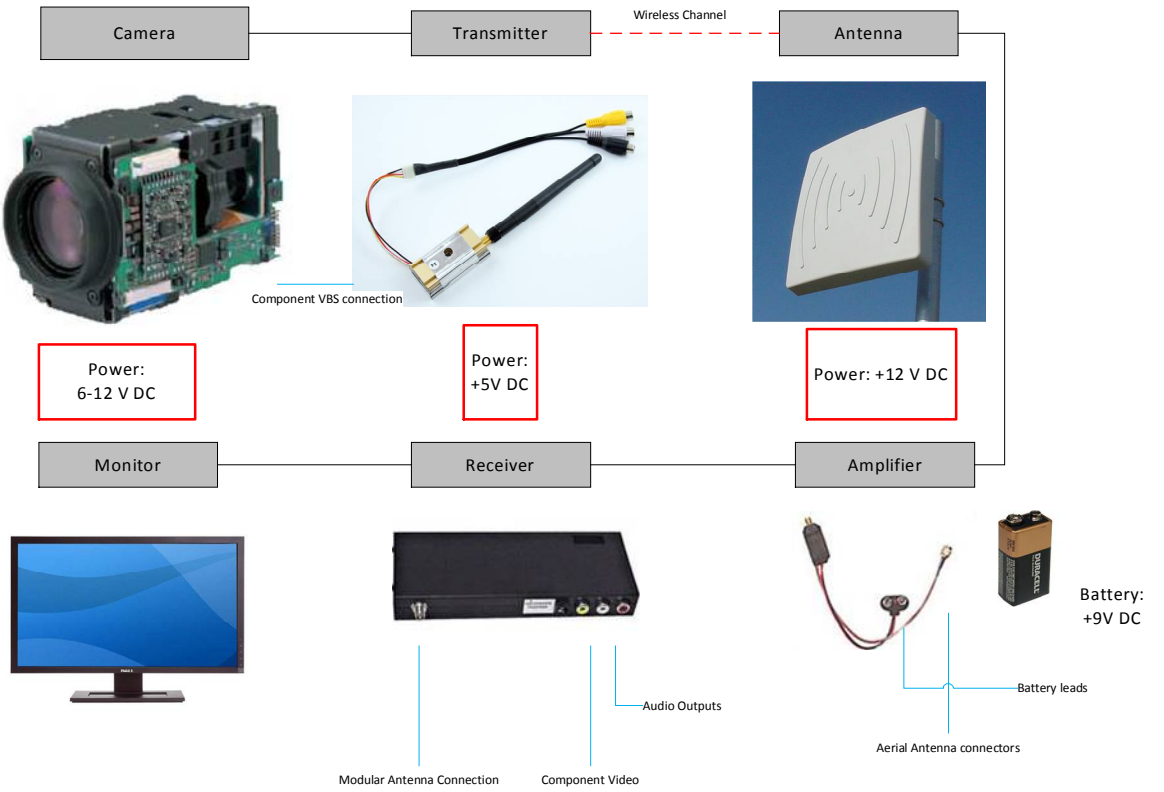

Figure 4.18: Imagery Downlink System Configuration

5. Final Concept Design- SUAS

Because of the advent of Lithium Polymer batteries, as well as advanced open source code and cheap electronics, the popularity of RC planes and hobby unmanned aerial systems has increased enormously in the last several years. Due to this popularity, many components required for the design and construction of the SUAS are hot sale items, and sell quickly. As we began to purchase components in the beginning of the Spring 2012 semester, we found that many of the parts we had planned on acquiring were out of stock, or on backorder. This affected the design of the SUAS in several ways. The following subsystem designs had to be adjusted because of this difficulty in acquiring components:

Propulsion System Changes:

The motor planned for in the design selection was the AXI 4130/20 brushless DC motor, however, after the motor was received we found that mounting the motor and attaching a propeller was extremely difficult. Because the motor manufacturer is based in Europe, all attempts to get a motor mount and propeller adaptor were met with backorders and extremely long shipping times. In the final design, we decided to use an Eflite Power 60 brushless DC motor, which we had on hand and was capable of meeting the propulsion requirements. A propeller adaptor and motor mount were purchased through a local vendor.

Avionics System Changes:

For the Avionics System, the autopilot selected was the Paparazzi Tiny V2. However, the components of the autopilot were out of stock from several vendors. After struggling to purchase all the parts for the autopilot, including a already assembled autopilot, the decision was made to change autopilots completely. The Ardupilot Mega was instead chosen as the final design autopilot, as the parts were readily available. The telemetry for the autopilot ended up being on backorder, which slowed down the testing of the autopilot considerably.

Power Supply System Changes:

As the autopilot system changed, the power supply system had to adapt to the new autopilot board and components. As all the autopilot components are powered form the board itself, the decision was made to power the autopilot board from a battery eliminator circuit

(BEC) which draws power form the motor batteries. This was decided due to the fact that the battery initially picked to power the autopilot has an output voltage not in the nominal range for the Arduopilot Mega.

5.1 Aircraft Design

For the design of our UAS aircraft platform, we went through a multiple stage iterative process to come up with an adequate design to meet all the functional requirements needed for a successful mission. This process included using multiple software packages such as X-Foil, XFLR5, Pro-Engineer, Athena Vortex Lattice (AVL), and MATLAB along with using reference literature for the design of aircrafts, such as Daniel Raymer's *Aircraft Design: A Conceptual Approach* and Andy Lennon's *Basics of R/C Model Aircraft Design: Practical Techniques for Building Better Models*. Once we determined the planform concept in the concept generation and selection process of our design project, we began to research how we could successful meet all design requirements with the planform we selected. This involved going through the previous mentioned books as well as many others to determine the physical requirements our design must implement to be not only stable but also safe. One of the main drawbacks we ran into was the lack of literature available for the design of an aircraft in the size range to fit our mission profile. Although Raymer's book gave us an idea of where to start in the design process, it is primarily written for the design of full scale aircraft, so many of the suggestions given would not suffice due to the nonlinear scaling issues between full-scale and aircraft and the aircraft we designed. This was also the case for Lennon's book as well, except it gives suggestions on how to design small-scale RC aircraft.

Once we compiled a list of recommendations to consider in the design of our UAS, we used X-Foil to find airfoil profiles that were adequate for the Reyonlds number we would encounter during all stages of flight. X-Foil has thousands of airfoil profiles for all different flight regimes, so we filtered the program to find relatively low Reynolds Number (on the order of 500,000) to come up with a list of possible airfoils that we could use for our design. X-Foil is a very user friendly program that allows you to select multiple airfoils to be evaluated to compute force and moment data of the 2D profiles. The 2D data obtained is only an approximation of the forces and moments for wing profiles because it doesn't consider the 3 dimensional effects of the entire wing span, such as the tip effects and downwash. Once we

determined possible selections for the airfoil we would use for our design, we took the force and moment data that was computed and used it to evaluate the approximate 3D forces and moments for our entire wing using XFLR5.

We then used XFLR5 to calculate the force coefficients at different Reynolds numbers we would encounter in our flight profile. This program calculates these coefficients for the wing and horizontal/vertical tail geometries using the vortex lattice method (VLM) based on the thin airfoil theory, which discretizes the surfaces of the wing and tail into panels (infinitely thin vortex sheets) and solves the potential equations for irrotational and incompressible flow fields using discrete vortices.

One of the drawbacks for this software is the fact that the VLM is only valid for solving the potential equations of the flow field around an infinitely thin airfoil profile, meaning that it neglects not only the effects to the thickness (camber) of our airfoil profile but also the viscous effects of the fluid around a body (wing). This results in only an approximation of the forces and moments our aircraft would actually encounter in flight. More accurate data could only be obtained by performing either wind tunnel experiments or numerical simulations (CFD) using a viscous flow solver, both which take more time and resources than were available for the duration of this project. Although using XFLR5 could only give us an approximation of the forces and moments we would be subject to during flight, we were able to approximate the pressure distribution across the wing which we used to begin designing the structural components of the wing, tailplane and other lifting surfaces.

Once the initial force coefficients were obtained using XFLR5 and the pressure distribution and therefore load requirements were determined, we began the actual design of our aircraft in the CAD software Pro Engineer (Pro/E). Using the data obtained from the two previous mentioned programs and the suggestions from aircraft design manuals, we were able to come up with initial designs of the actual model of our plane. Using Pro/E allowed us to define the geometry of our plane to determine its physical size, which we then used to calculate the approximate drag force our aircraft would have to overcome during flight. We were also able to

input the weight of all of the materials we would be using for the construction of our plane so we could estimate the mass and inertia tensor. This allowed us to determine where our center of gravity of the entire plane with all components needed for flight, which is an essential design parameter needed when designing a stable aircraft.

We then used a program written by MIT Professor Mark Drella called the Athena Vortex Lattice (AVL) method to begin the stability analysis of our aircraft. The AVL program allowed us to input the location and mass of all of the main components along with the inertia tensor so we could estimate the aerodynamic coefficients and their derivatives to be used in the stability analysis of our aircraft. Due to the complexity of the program and the lack of reference material, we could not take full advantage of the entire program, which could essentially compute not only static but dynamic stability of the aircraft. We were however able to obtain enough data to compute the static longitudinal stability and determine the static margin of our aircraft, which is essentially the measure of how maneuverable or stable our aircraft would be in flight. Although we were not able to compute the dynamic stability (longitudinal, directional and lateral) in AVL, we were able to program the equations for dynamic stability into a MATLAB function to solve and estimate how our aircraft would react to dynamic conditions given the aerodynamic coefficients and their derivatives provided by AVL.

This entire design procedure was countlessly iterated over the past two semesters to come up with a design that we hope will provide us with a safe and stable aircraft to accomplish our mission profile and functional requirements. Aircraft design is an extremely time consuming process that sometimes takes years for seasoned design engineers to complete in order to meet all functional requirements in a safe manner. Due to the simplicity of our design, we believe that the process we went through in the design of our UAS should provide us with an aircraft that can safely meet all the requirements set forth by our customer as well as the competition.

Airfoil Selection:

The airfoil for the design of our UAS was selected based on the requirements we needed to accomplish to have a successful flight. These requirements include, but are not limited to, a relatively high maximum coefficient of lift, $X_{XX\,XX}$, a high lift to drag ratio, X/X, the ability to

operate efficiently and effectively at relatively low Reynolds numbers ($XX = O\{10^X\}$), and the ease of manufacturability. To comment on the last requirement, when selecting the airfoil to use for our design, there were

definitely other airfoils out there that performed better than the one we chose. The reason we did not select these airfoils were not based on performance, but on the difficulty due to manufacturability. It would have been bad engineering judgment on our part to select an airfoil because of the high X_{XX} it possesses without considering if the complex geometry of some of the high lift airfoils could be manufactured.

For the selection of our airfoil, we first researched airfoils that are effective for aircraft flying in the regime of relatively low Reynolds number, $XX = O\{10^X\}$. Although this seems like this might be a high value, the order of Reynolds number full size aircraft, such as the Boeing 747, operate in are of the order of 100 million. After a literature review of effective low Reynolds number airfoils, we used X-Foil to calculate the coefficient of lift and moment versus angle of attack as well as the coefficient of lift versus the coefficient of drag to find the drag polar over a various range of operating Reynolds Numbers, shown in Figures 5.1 – 5.3 for the Selieg-Donovan SD7037 airfoil, respectively.

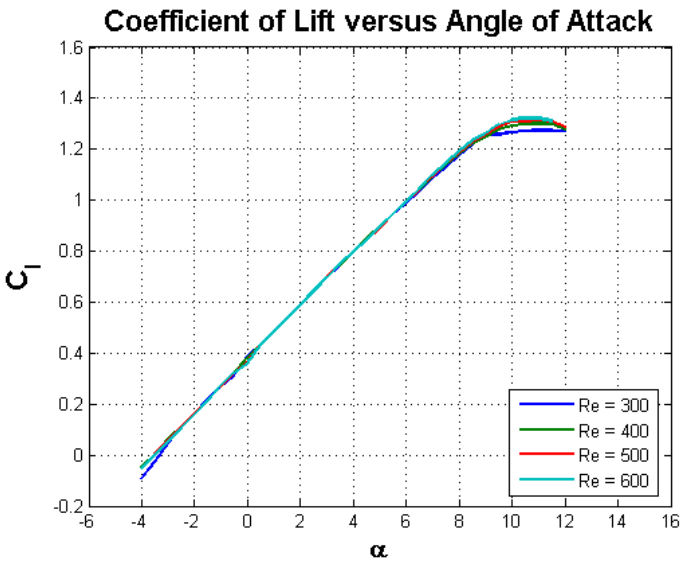

Figure 5.1 : Coefficient of lift versus angle of attack for the SD7037 airfoil.

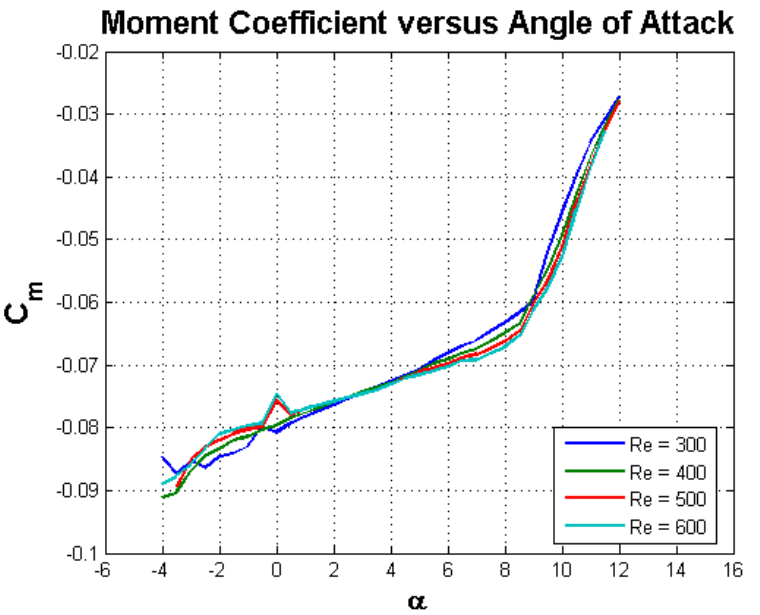

Figure 5.2: Moment coefficient versus angle of attack for the SD7037 airfoil.

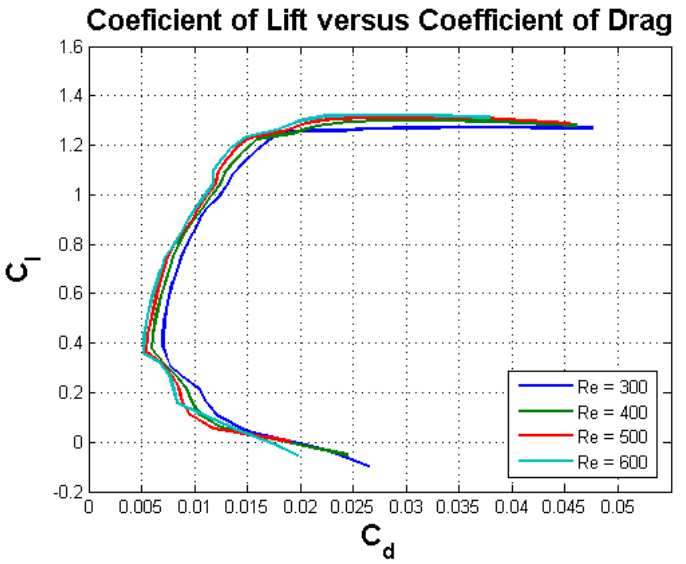

Figure 5.3 Coefficient of lift versus coefficient of drag for the SD7037 airfoil.

Figure 5.1 shows that the change in lift over the change in angle of attack, $^{XX_{XX}}X_{XX}$, is nearly constant over each of the Reynolds numbers that were considered for this study. It can also be seen that the maximum coefficient of lift occurs at roughly an angle of attack of 11 degrees, which also corresponds to the point where the onset of stall occurs. At this point, we would like to point out to the reader that the values plotted in the previous figure correspond to an infinitely long airfoil section where no spanwise effects, including those at the end, or tip effects, are included in this data. These plots correspond to 2D airfoil data, and when spanwise effects are accounted for in the calculations, as well as tip effects, the values of the coefficient of lift will be decrease. Figure 5.3 shows that at low Reynolds numbers, the SD7037 has good performance over the full coefficient of lift ranges as well as the coefficient of drag ranges too.

Wing Design:

There are a number of different design requirements that need to be considered when designing a wing. Some of these requirements include wing geometry, aspect ratio, sweep angle, taper ratio, and dihedral angle. When designing our wing, the first and foremost important requirement was the ease of manufacturability. It would have been extremely easy for us to design something that shows optimum characteristics on paper, but when we do to actually build it, it would be impossible for students with limited manufacturing availability to be able to actually implement that optimum design. With that being said, the first decision we decided on for the design of our wing was to have the wing planform be of rectangular geometry. This also meant that the wing would have and taper ratio of 1 and a sweep angle of zero degrees.

Another main requirement for the design of our wings was the aspect ratio, which is defined as the wing span divided by the mean wing chord. By doing a literature review for other UAV's with similar mission profiles and sizes, we noticed that many UAV's had relatively higher aspect ratios, from AR = 8 to AR = 10. We believe the reason for this is for the aircraft to be able to operate at lower speeds for surveillance and reconnaissance missions. Since these two missions are essentially what we are designing to be able to do, we decided on choosing a relatively high aspect ratio as well, between AR = 9 to AR = 10.

Tail Plane Design:

The sizing of the tail plane was done using recommendations presented by Daniel Raymer's *Aircraft Design: A Conceptual Approach*. He presents a method of using what is known as the tail volume coefficient for both the horizontal and vertical tails. He gives equations for both the horizontal (X_X) and vertical (X_X) tail volume coefficients, which are given by Equations (1) and (2), respectively:

$$X_X = \frac{X_X * X_X}{X * X} \quad (1)$$

$$X_X = \frac{X_X * X_X}{X * X} \quad (2)$$

where X_X and X_X are the areas of the horizontal and vertical tails and X_X and X_X are moment arms for the horizontal and vertical tails, respectively. Also, X is the wing area, X is the wing chord, and X is the wing span. Raymer gives typical values for the tail volume coefficient for both the horizontal and vertical tails based on statistical values from aircraft that are operational. Having a value for the tail volume coefficient allows for the calculation of the required area of the tail given that the designer knows the moment arm. This could also be used to calculate the tail moment arm given that the areas of the horizontal and vertical tail were known.

Determination of Lever Arms:

The lever arms for the horizontal and vertical stabilizers are defined as the distance between the quarter chord of the wing to the quarter cord location on the horizontal and vertical stabilizer, respectively. A schematic of how the lever arm is determined can be seen in Figure 5.4. The lever arms are measured in percent of the Mean Aerodynamic Chord (MAC) of the main wing. Raymer suggest using a lever arm for both the horizontal and vertical tail that is roughly 400% times that of the mean aerodynamic chord of the wing.

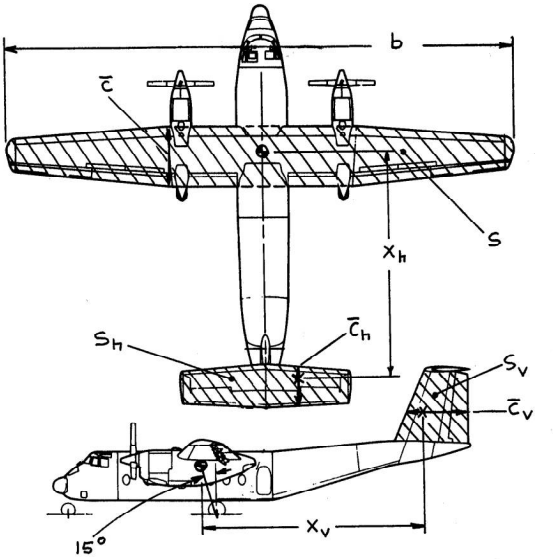

Figure 5.4: Schematic of determining the lever arm for an aircraft.

Final Design:

By using the above requirements for the initial configuration of our aircraft, we were able to iterate through the process previously mentioned to come up with an optimum design that would not only be able to complete all given customer requirements but complete them in a safe and efficient manner. Figures 5.5 through 5.7 show the coefficient of lift and coefficient of moment versus alpha and the coefficient of lift versus the coefficient of drag, respectively, after a number of iterations for developing a stable aircraft given the recommendations we took from Raymer's design book. One thing that must be mentioned is that the plots in Figures 5.5 through 5.7 include the vertical and tail geometry, as well as the spanwise effects, unlike the plots from Figures 5.1 through 5.3.

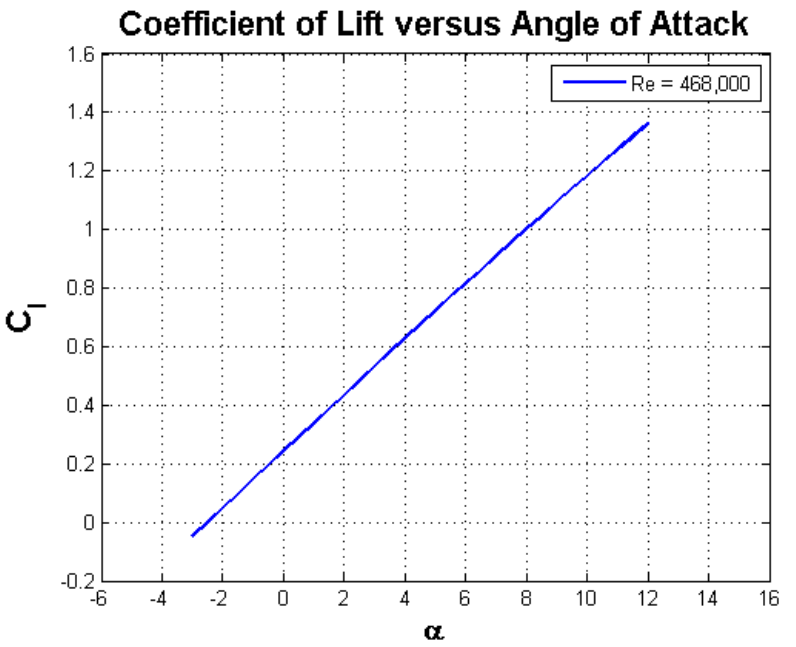

Figure 5.5: Coefficient of lift versus angle of attack for the SD7037 wing and NACA0012 horizontal and vertical stabilizer flying at cruise conditions (V = 55mph).

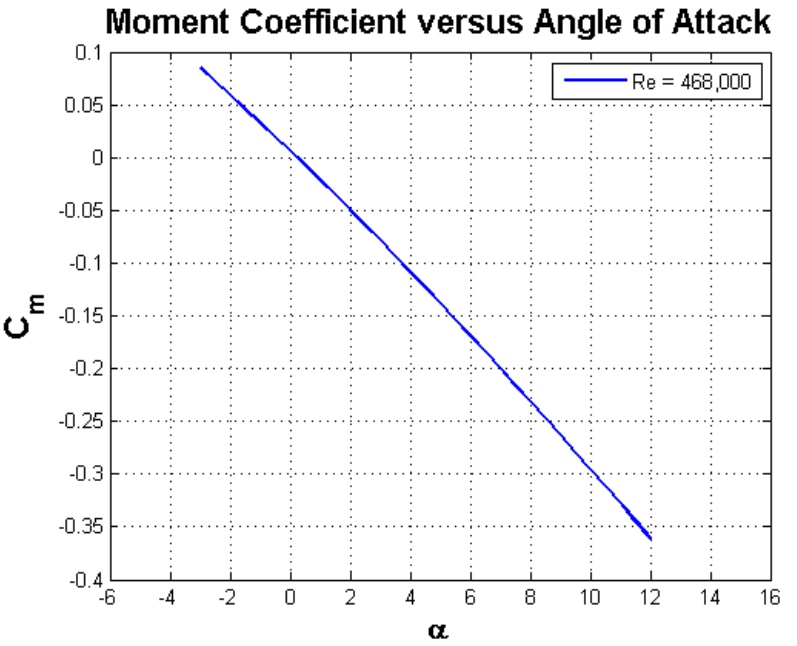

Figure 5.6: Coefficient of moment versus angle of attack for the SD7037 wing and NACA0012 horizontal and vertical stabilizer flying at cruise conditions (V = 55mph).

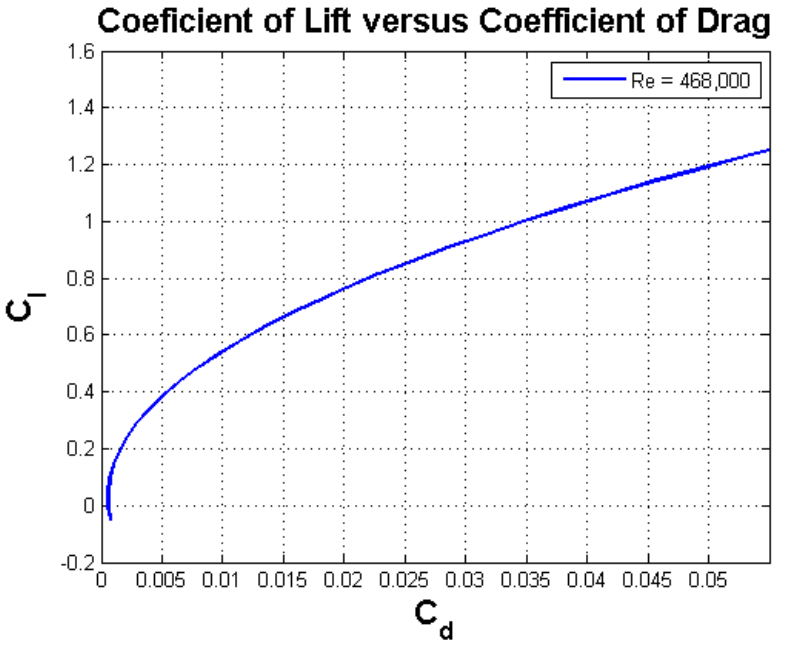

Figure 5.7: Coefficient of lift versus coefficient of drag for the SD7037 wing and NACA0012 horizontal and vertical stabilizer flying at cruise conditions (V = 55mph).

Figure 5.7 shows the output from the XFLR5 software for the combined wing and tail configuration flying at 55 mph and an angle of attack of 3 degrees, which corresponds to a Reynolds number of 468,000 based on the wing chord. In this figure, the green lines correspond to the lift force acting across the wing, the yellow lines represent the induced drag, the pink lines represent the viscous drag, the orange vector represents the moment acting about the planes center of gravity, and the blue lines represent the spreamlines. Once we were able to run this several times with different configurations, we were start to see a trend that certain configurations seemed to show more stable aspect than others. After we were satisfied with the results we were getting from XFLR5, we were able to take the data given at the bottom of the figure and use it to create a CAD model using Pro/E to estimate the weight and inertial effects for further stability analysis.

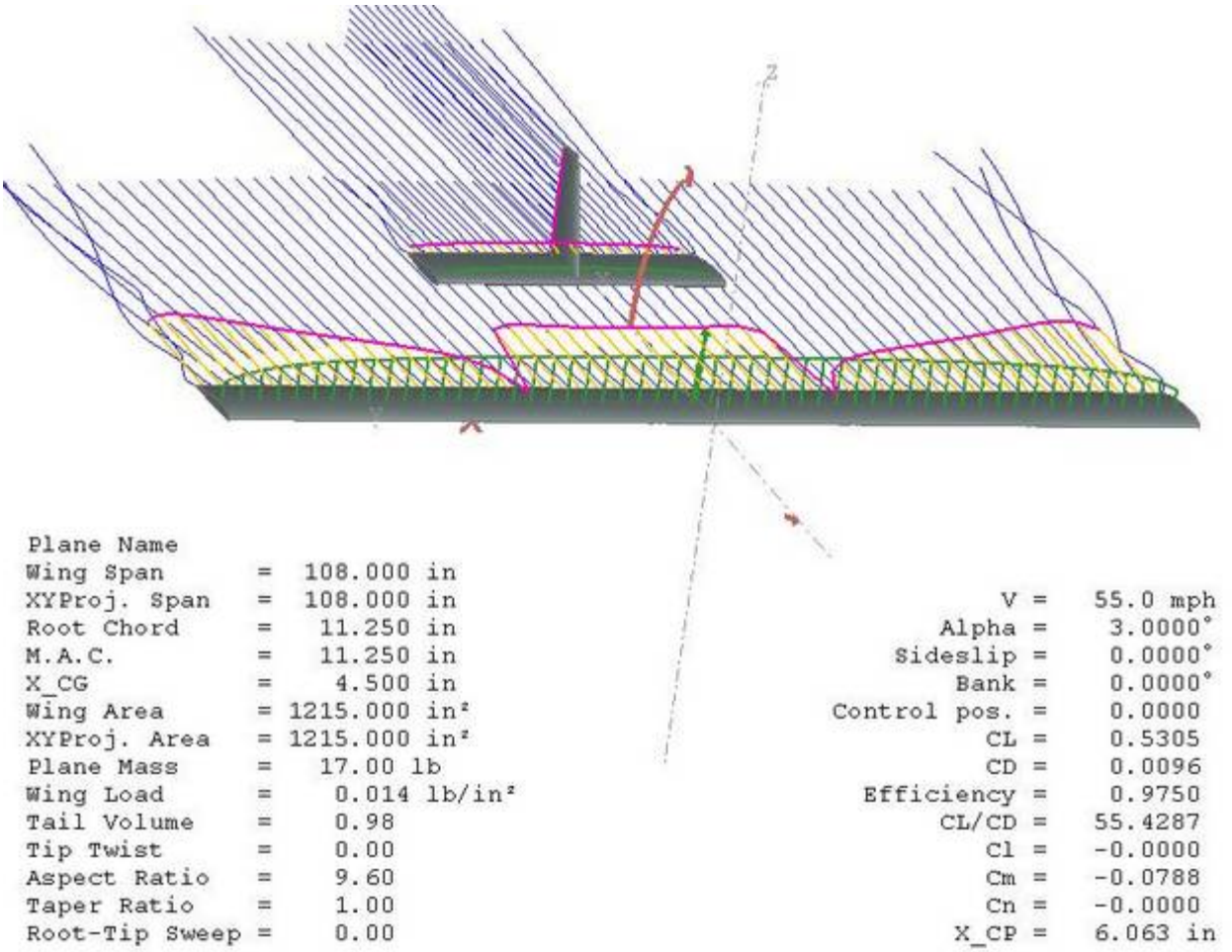

Figure 5.8: Output from the XFLR5 simulation of a SD7037 wing and NACA0012 tailplane flying at 55 mph and a 3 degree angle of attack.

Figure 5.8 shows the 3 view images as well as the isometric view of the CAD models of our final design. While we designed these models, we made sure to keep track of what materials we were going to be using for construction so we could get a better estimate from Pro/E for the mass and inertial effects of the plane. As the plane sits now in Pro/E, its estimated weight is roughly 16lbs. We can use this estimation to compare it to the finished product to see if we used too little or too much material when building our plane. Table 5.1 gives some of the design parameters from our final design.

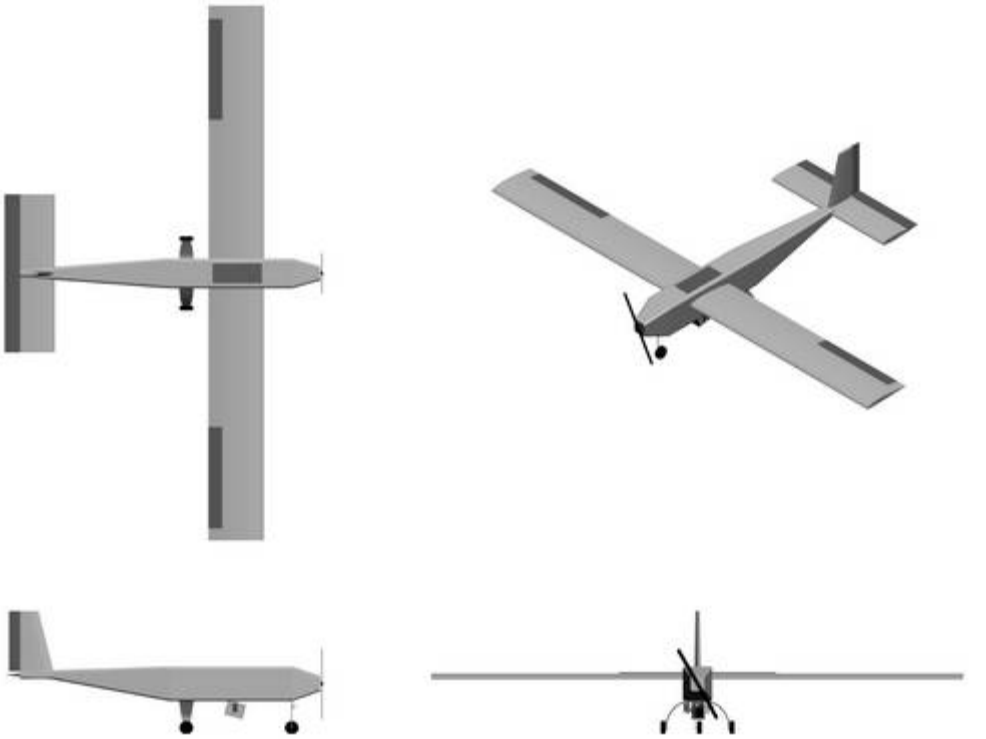

Figure 5.9: Pro Engineer CAD drawing of the final design of our UAS

Weight	16.00 lbs.	H. Tail Span	32.00 in.
Length	63.25 in.	V. Tail Span	12.00 in.
Aspect Ratio	9.60	Aileron Area	57.38 sq. in.
Wing Span	108.00 in.	Rudder Area	22.50 sq. in.
Wing Chord	11.25 in.	Elevator Area	80.00 sq. in.
Wing Area	1215.00 sq. in.	Static Margin	10 %
H. Tail Chord	10.00 in.	Motor Power	900 Watts
V. Tail Chord	7.50 in.	Flight Time	>40 minutes

Table 5.1: Final design parameters for our UAS

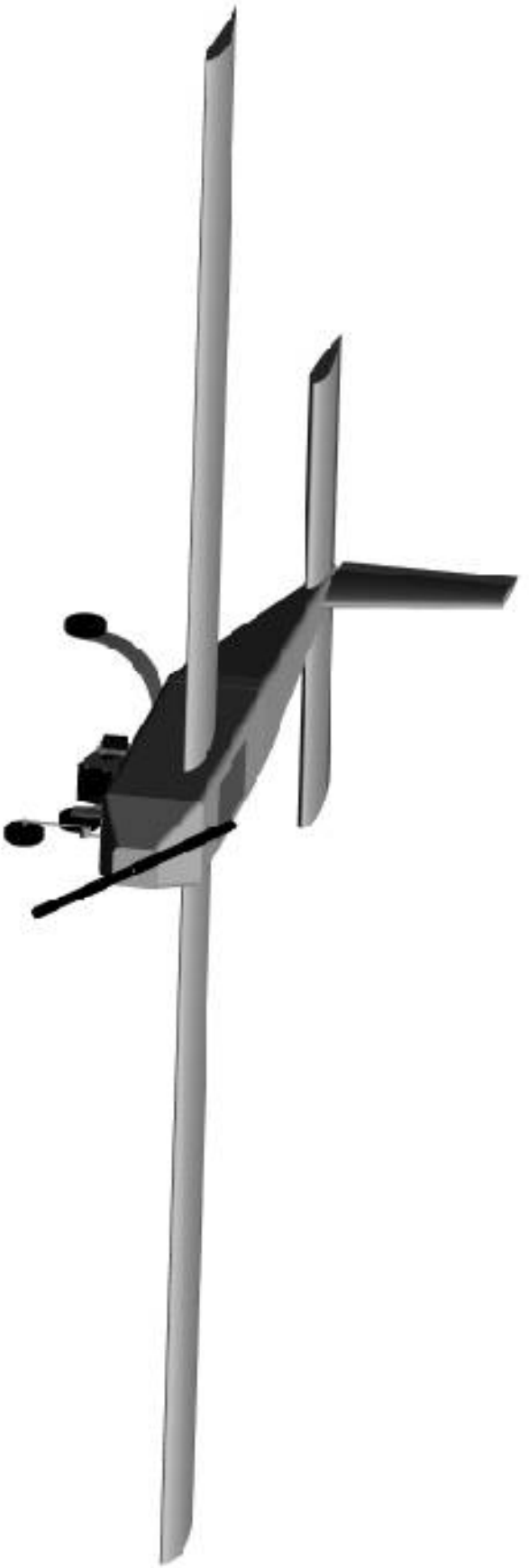

5.2 Airframe Design

The outer skin of the fuselage will consist of two layers of fiberglass impregnated with epoxy resin, layed down with the second layer at +45^{o} relative to the first, providing greater strength in all directions with the 90^{o} angle weaves of the fabric. This outer layer will be bonded to an internal core of 1/8" balsa wood which will provide stiffness to the airframe. An internal section of fiberglass will then be layed up on the inside of the balsa. This internal layer will mimic the structure of the outer layer. Pictured below is a cross section of the fuselage detailing the design.

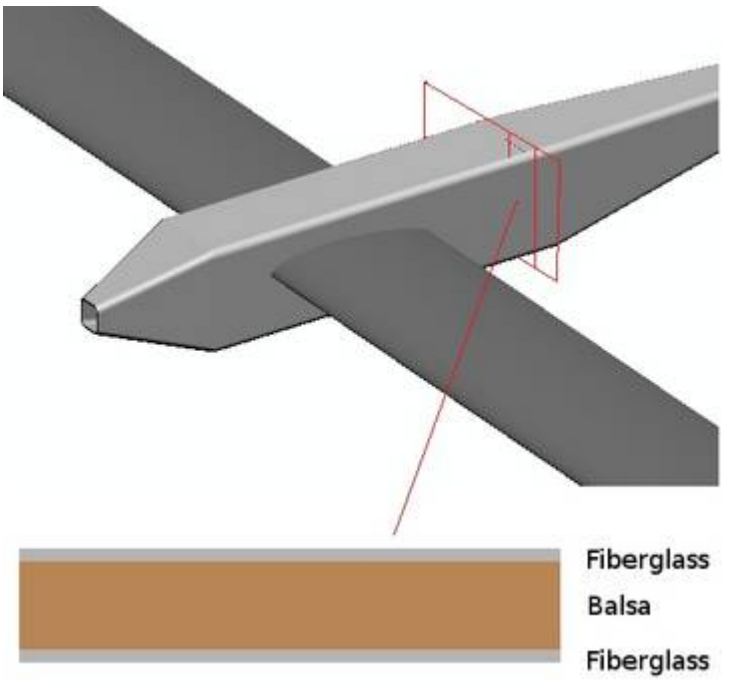

Figure 5.10 Diagram of the fuselage layup

The payload and other subsystems of the plane will be attachable to the inside of the fuselage via plates and screws fitting the dimensions of the various subsystems. Industrial grade Velcro will be used for components that will need to be replaced and moved frequently. There will also be a sandwich structure board of balsa wood and carbon fiber between the nose section of the plane and the head of the fuselage. This will act as the attachment point for both the front landing gear and the motor mounts.

The wings will consist of a carbon fiber outer skin of two layers with an EPS foam core. There will be two spars running 48” through the wing from the root chord. The spars act as the main support for the load felt by the wetted area of the wing, where the load is transferred from the carbon fiber skin to the foam core and then into the spars, but the carbon fiber skin will absorb some of the tension forces and the foam core will do the same with compressive forces. The ends of each wing tip and the root chords will be reinforced with a section of balsa to ensure the profile of the wing.

The vertical and horizontal stabilizers will consist of a carbon fiber outer skin and EPS foam core similar to the main wings, but will consist of only one layer of fiber. This will keep the total weight of the plane down without sacrificing any structural stability, as the tail section will not be seeing similar loads to the wings. As with the wings, the root and tip profiles of the wing will be reinforced with a balsa wood profile and carbon fiber.

With the requirements of high mobility and ease of assembly in our design it was decided that an easy way of attaching and removing the wings for storage was necessary. A section of the foam core of the wing beginning at the root chord and ending 12” into the wing will be reinforced by 1/8” balsa cut outs of the wing profile. A hole in each of these cut outs will guide a ½” internal diameter carbon fiber tube which will be glued to the foam core. This tube will then be friction fit to a solid unidirectional carbon fiber rod running through the fuselage. This connection point will be placed at 55% of the chord length from the leading edge, allowing some load to be carried by the carbon fiber tube and rod combination, while the majority is carried by the spar.

The spars of the wings will be constructed of 1/2” square cross section balsa wood rods, 48” in length, capped with two layers of carbon fiber on the top and bottom surfaces of the rod using CA glue. Each combined section of carbon fiber is 0.2” thick. This structure will then be wrapped in a woven carbon fiber wrapping that will be impregnated with resin and smoothed to the surface of the spar. The entire spar with the wrap will then be vacuum bagged to ensure a proper bond and impregnation. The spars will be placed in the wing at the 25% chord location from the leading edge, the peak point of aerodynamic loading on the wings.

5.3 Simple Avionics Design

The basic components of the avionics design are the control surface servos, which control the plane in flight, and a controller which provides the control signals to the servos. The three different movements of an aircraft are shown in figure 5.11.

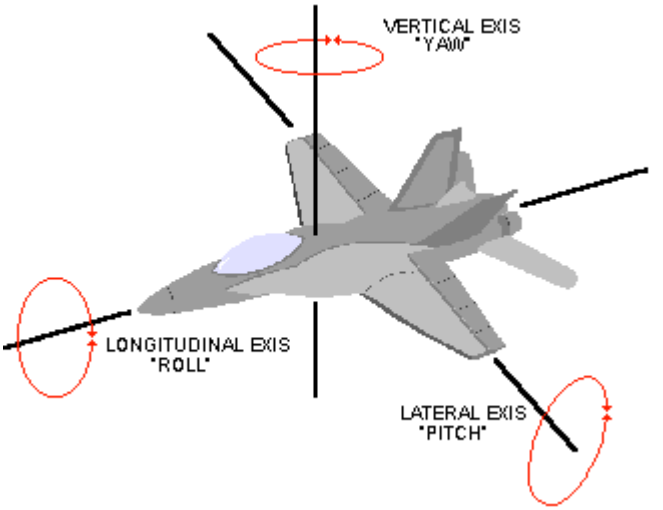

Figure 5.11 Aircraft movements

To achieve flight, servos must control the specific control surface that maintains the particular aircrafts movement. These are as follows:

Aircraft Control Surfaces	
Surface	Movement
Ailerons	Roll
Rudder	Yaw
Elevator	Pitch

Table 5.2: Aircraft Control surfaces

The locations of these control surfaces on the aircraft are shown in figure 5.12.

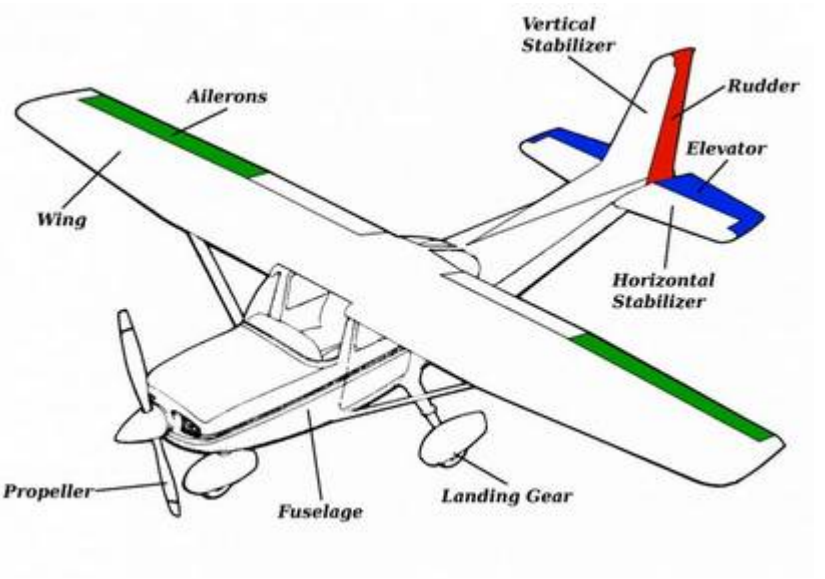

Figure 5.12: Control Surface Locations

At a minimum, four servos are required to control these surfaces, and achieve flight. There is one servo per aileron, one for the rudder and one servo for the elevator. The servos used in the Telemaster Senior aircraft are shown below.

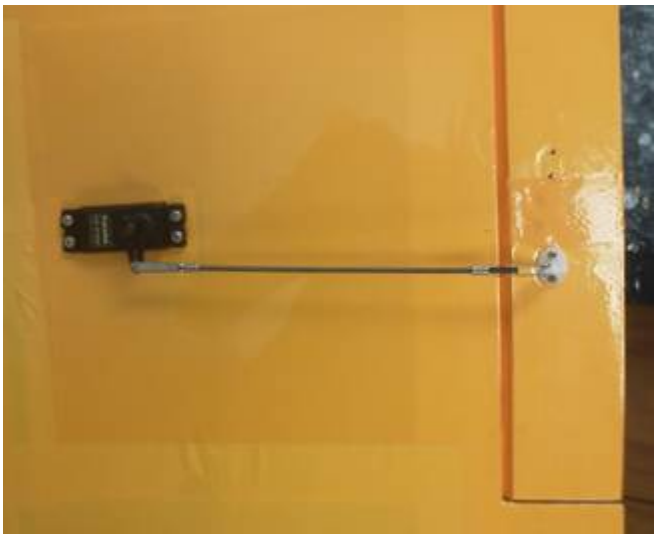

Figure 5.13: Aileron Control Surface Servo

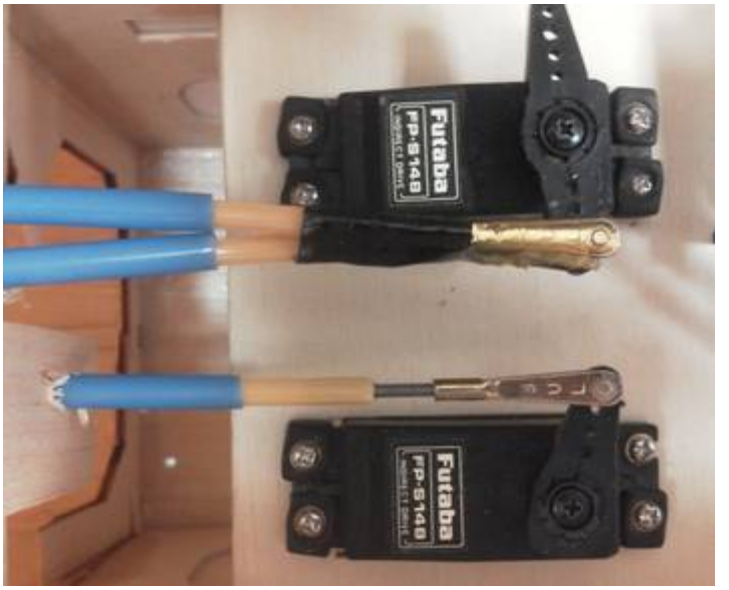

Figure 5.14: Elevator CS servo (Top) and Rudder CS servo (Bottom)

The servos in this design are powered through either the BEC, or the Autopilot board. Control signal inputs to the servos are fed from either the Futaba RC module, or the Autopilot module. The input to these servos is a voltage pulse in the form of a square wave, which cause the control surfaces to be moved appropriately to control the aircraft's flight.

5.4 Propulsion System Design

For the propulsion system of the SUAS, we selected the AXI 4130/20 brushless DC motor. However, the parts required to mount and operate this motor were virtually unavailable in our time frame. The decision was made early in the Spring 2012 semester to use a Power 60 brushless DC motor that we had on hand in the propulsion system final design. The characteristics of this motor are shown below. This motor is extremely similar to the AXI 4130/20 motor, and is capable of flying the SUAS.

Eflite Power 60	
Parameter	Value
Max Continuous Current	51 A
Max Power	1900 W
Max Burst Current	65 A (15 sec)
Weight	380 g
Recomm. Prop Size	16X10, 14X8
Voltage range	18.5-30 V
Safety	0.2

Table 5.3: Power 60 Characteristics

Figure 5.15 Eflite Power 60 Brushless DC motor

In order to use a brushless DC motor, it is necessary to use an electronic speed controller (ESC) to control the throttle of the motor. Because 8-cell Lipo batteries were being used in the power supply system, with an output voltage of 29.6 V, a high voltage ESC was chosen and ordered. This ESC was the Castle Creations Phoeinex ICE HV 60. It is shown in figure 5.16.

Figure 5.16: CC Phoenix HV ESC

A 16X10 propeller was selected for the Power 60 motor, and was attached with the propeller mount. To operate the Power 60, the ESC is connected to the Power 60 motor through three multicolored wires. The ESC throttle cable is then attached to the RC controller receiver, or the Autopilot throttle output. When the large battery pack (29.6 V) is plugged into the ESC, the voltage from the batteries is scaled down and controlled to drive the Power 60 based on the throttle input from the RC handset or the Autopilot.

The flight of the SUAS is comprised of several steps, each with a required power and throttle. With estimations based on the weight and configure of the aircraft, power requirements for each phase of flight were calculated previously. With a long, slow takeoff, cruise with minimum aerobatics and a coasting landing, the mission power profile can be described as shown in figure 5.17.

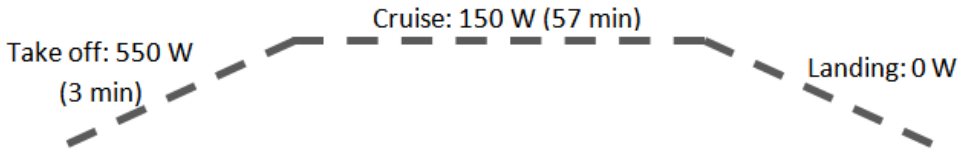

Figure 5.17: Mission power requirements profile

These power requirements are well within the abilities of the Power 60 motor and the ESC. The block design of the final propulsion system design is shown below. The thick red and black wires are attached to the big battery pack during operation. The throttle cable is plugged into the #3 port on the Futaba RC receiver we used, or the #3 plug on the Ardupilot Mega. The Castle Creations HV ESC also includes a data logging feature that is useful for logging motor and battery data for entire flights. This data is downloaded through software and a USB driver.

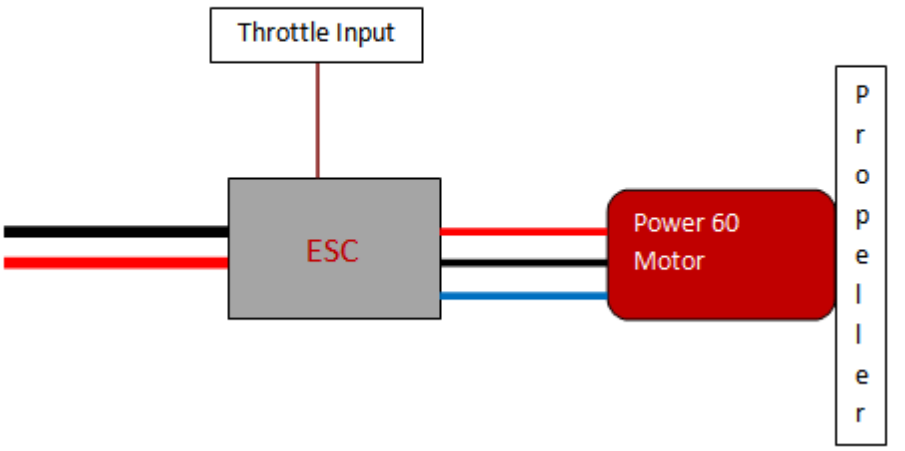

Figure 5.18: Propulsion System Block Diagram

5.5 Autopilot System Design

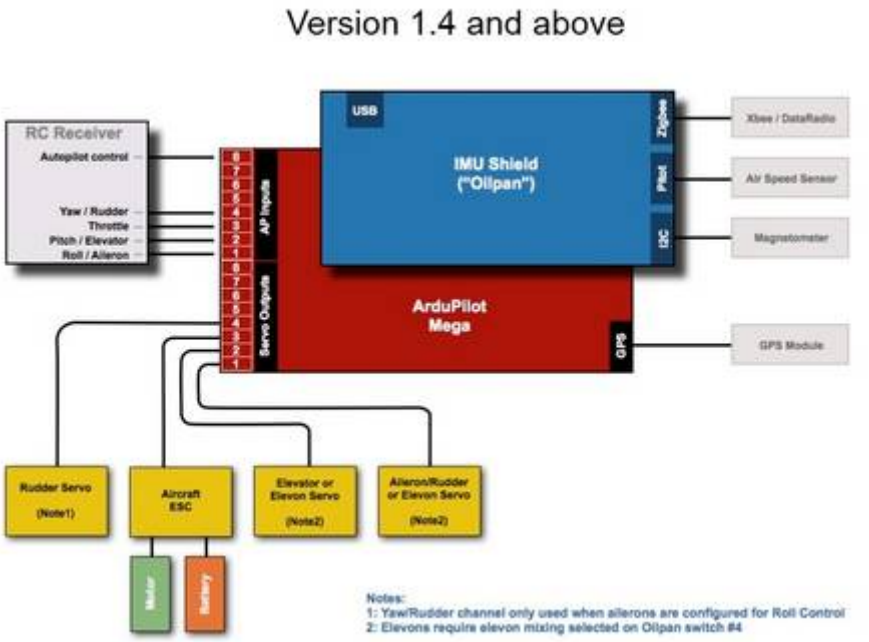

Figure 5.19: Basic Layout of the autopilot system.

The autopilot system used for this project is the ArduPilot Mega (APM) kit ($250) found on www.diydrones.com. Figure 1 shows the basic layout of the APM and all the parts that connect to it. The APM board is highlighted with the 16MHz Atmega2560 processor while the Inertial Measurement Unit (IMU) board has a 3-axis gyroscope and 3-axis accelerometers. There are ports for a GPS module, magnetometer, airspeed sensor, etc. The APM kit comes with a MediaTek MT3329 GPS 10Hz GPS Module.

The airspeed sensor does not come with the kit so the team purchased the Airspeed Kit ($25) from www.diydrones.com. As this is not essential for the autopilot to work, we felt that it was necessary to have it as it gives a much more accurate airspeed. If this is not used, the autopilot calculates the airspeed based on groundspeed and other factors. This will not account for wind gusts which could throw the autopilot off.

Figure 5.20: Telemetry kit used for autopilot communication.

The telemetry kit shown in Figure 5.20 used for this project is the one supplied by www.diydrones.com ($150). The kit uses two Xbee-Pro 900 extended range modules for communication. The kit also comes with two interface boards and an RP-SMA antenna.

The autopilot system is comprised of a few different systems working together. The autopilot is the APM board and the inputs are the RC receiver, the telemetry (Xbee), and the sensors. The outputs are the servos and the aircraft Electronic Speed Controller (ESC). Depending on the mode that the user has put the autopilot in, the autopilot either takes in the commands straight from the RC receiver, or uses the mission loaded to the APM board and directs the outputs as necessary.

When commands are taken from the RC receiver, it is almost exactly like controlling an aerial vehicle without any sort of autopilot connected. There are several modes of the autopilot, like Stabilize, where input is actually taken in from both sources and then output to the servos and ESC. In these types of modes, the autopilot will take the input from the RC receiver and mix them with the presets stored for each mode. For example, Stabilize mode will take the inputs from the RC receiver and after executing those it will attempt to stabilize the aerial vehicle. The user could essentially take their hands off the controller and the plane will continue straight on until otherwise told.

In Autopilot mode, the autopilot is fully autonomous. The user can put the controller down and watch the aerial vehicle fly itself. The APM reads the mission stored on board and starts executing it. Usually the mission is a series of waypoints that can involve loops and conditional statements. This is when the most interaction happens between the ground station

and the autopilot. This is due to the fact that waypoints can be added during flight along with many other commands.

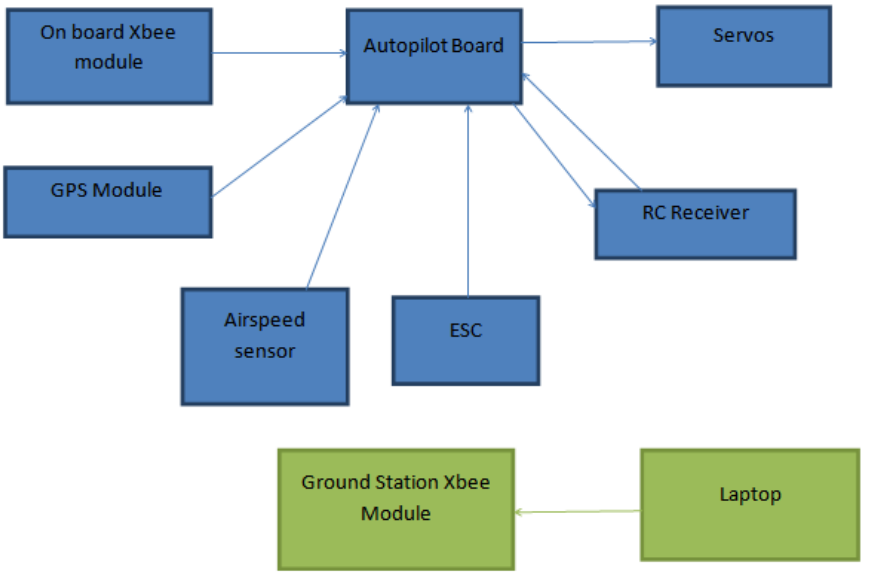

Figure 5.21 Autopilot Block Diagram

5.6 Video Feed System Design

The UAS wireless video system was designed in order to meet the required flight specifications for the AUSVI Student Competition. The flight mission required rapid image recognition of alphanumeric targets at an altitude of 100-750 ft MSL. The aircraft would be required to travel a maximum of 1.5 miles from ground station. The size of each target is relatively small, such that a powerful camera must be used in order to accurately see a target with a minimum size of 2 x 2 ft.

In order to maximize flight time and quickly identify targets our team decided a live video feed would be the best choice to acquire target information. In order to handle interference on the 1.2 GHz band an analog camera system was also chosen to send the video feed. The camera system is designed to mount underneath the bottom of the airframe and capture live video. The video is then streamed back to the ground station on Laptop 2, where the user can

write down the target characteristics or be processed through MATLAB using image recognition.

The figure below shows a block diagram of the Video Feed System.

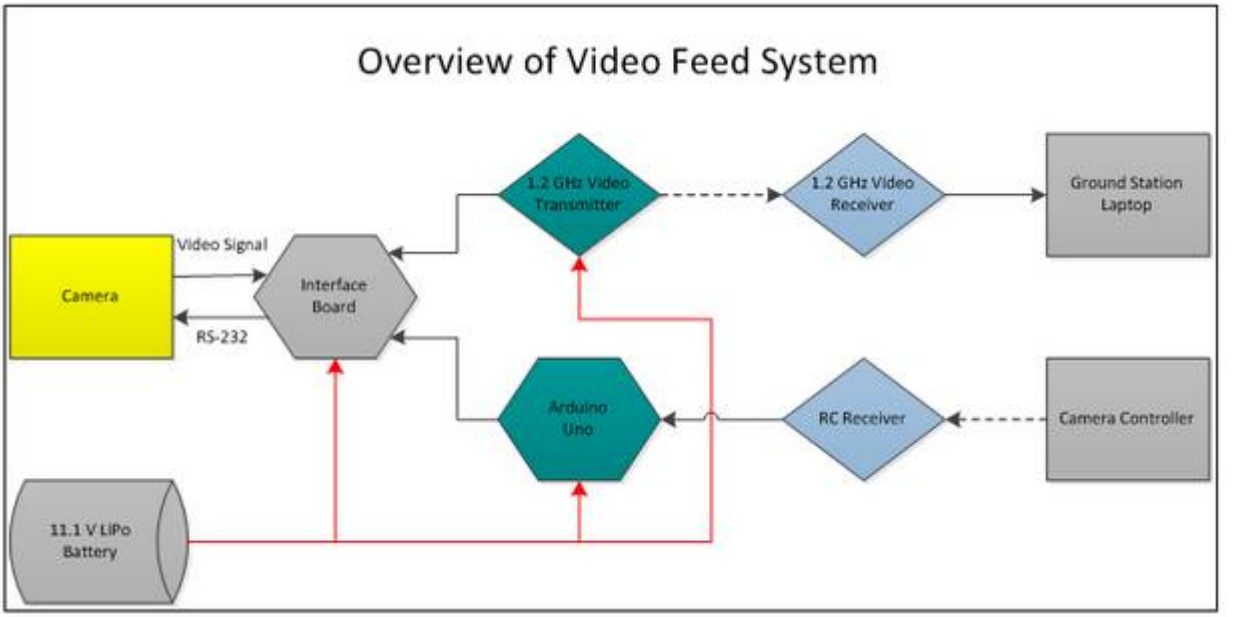

Figure 5.22: Video Feed System Block Diagram

This setup consists of the Sony Block Camera EX-980S, FCB-RS Interface Board, CN-1 and CN-3 Connector Harnesses, ThunderPower 11.1 V 1300 mAh LiPo battery. The camera is connected to an interface board through CN-3 harness which converts TTL to Serial commands for camera control. The CN-1 harness is connected to the camera and outputs the video signal through a RCA connector.

The camera used in the video feed design was the Sony Block Camera EX-980S. This camera is equipped with a incredibly high 26x telephoto zoom lens. It was chosen to provide a bird's eye view of the targets from high altitudes. The camera uses SMART (Sony Modular Automatic Lens Reset Technology) lens control and image stabilization servos contained within the camera housing. The camera can be controlled through the analog buttons on the rear surface

of the camera, or by the high-speed serial interface through TTL signal-level control (VISCA protocol). This camera is much larger than the Sony KX-181, but is still only 8.1 oz (0.507 lb) with a low power consumption of 1.6 W. The Sony Block Camera design is also surrounded in an aluminum casing, which makes this camera a robust platform for aerial surveillance.

Figure 5.23: Sony Block Camera FCB EX-980S

The Sony Block Camera is an industrial camera usually sold to manufactures not individuals. The camera was sent with a 9-pin ribbon cable connector and a 10-pin serial connector. It was decided that in order to properly connect the camera with the wireless transmitter and arduino an interface board was needed as a stepping stone to do serial conversions. The FCB-RS Interface Board was used in order to remotely communicate with the camera from the ground station, power the camera, and send video signals to the wireless transmitter.

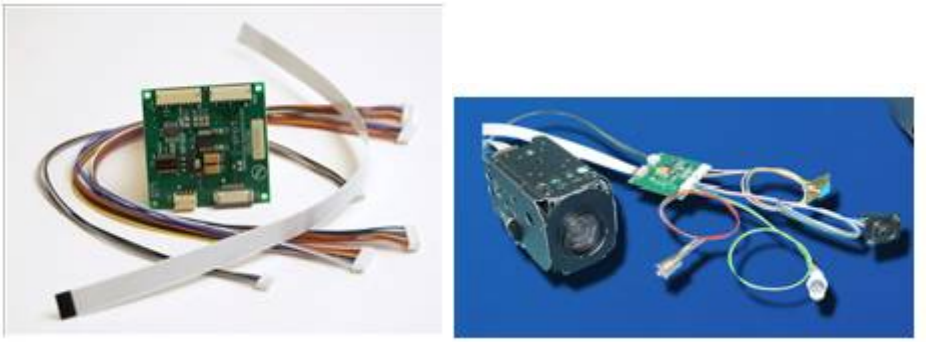

Figure 5.24: FCB-RS Interface Board (left) and Sony Block Camera connection types (right)

The Interface board outputs a high-resolution video as a composite video signal. The camera is controlled remotely by an RS-232 or TTL protocol, which uses the naive VISCA command structure.

The camera uses the VISCA (video system control architecture) protocol in order to control the various settings of the device. By sending commands by RS-232 or TTL the camera can zoom, focus, invert the image, display on screen text, and much more. In order to wirelessly control the camera from the ground serial commands would need to be sent every time the camera would pan/tilt or zoom in on a target. In order to do a Arduino Mega 2560 was used to receive PWM signals from an RC transmitter and output correlated serial commands. With a 16 MHz processor the ATmega board is extremely powerful and more than capable of quickly talking to the Sony Block Camera.

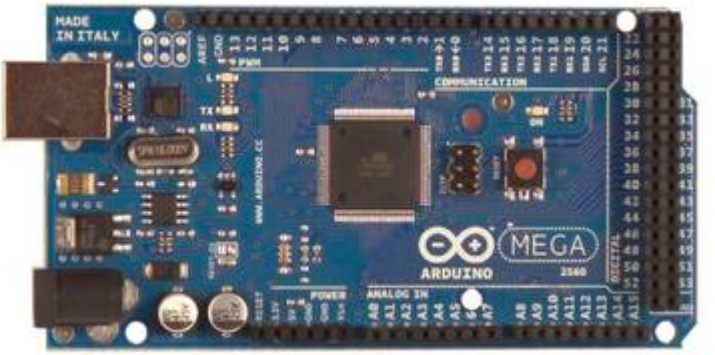

Figure 5.25: Arduino Mega 2560 - Front side

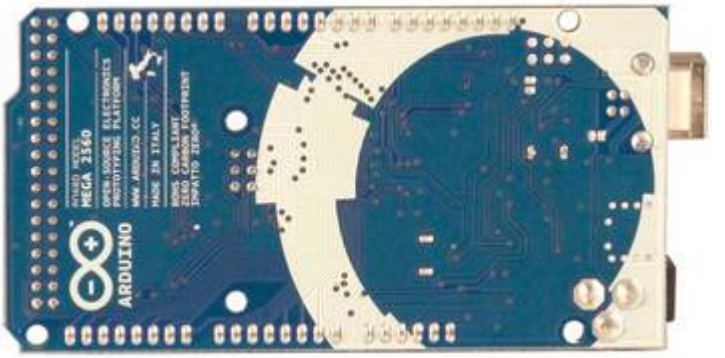

Figure 5.26 Arduino Mega 2560 - Back side

Using a 2.4 GHz RC receiver the PWM servo outputs are sent to the ATmega board through the bi-directional PWM inputs. On board the ATmega compares the signals duty cycle to check for a match. If a match is found on that channel the RS-232 command is fed to the camera allowing it to function properly.

Figure 5.27: Spektrum RC transmitter (left) and receiver (right)

5.7 Camera gimbal design

Figure 5.28 Pro-E design of gimbal system.

The basic function of the gimbal is to move the camera. This design is for the camera to rotate about two axes. The block on the left of the gimbal is where a low torque servo motor would be located. The rectangular space whole is the top of the design is where the high torque

servo will be located. In the figure below it show the dimensions of the gimbal. The dimensions are important because of the parameters. The camera only needs to rotate 60 deg up and down so the entire camera holder area doesn't need to clear the top of it enclosure.

5.8 Power Supply System Design

The power supply system components are the vital organs of the SUAS. The main goal of the power supply system is to keep all of the SUAS electronics running for the entire mission time. This includes ground pre-flight testing, takeoff, flight time and finally, landing. If the electronic systems fail at any time during the operation of the SUAS, the autopilot and all communications will be disabled, and the plane will most likely crash, causing critical damage to the SUAS.

The basic components of the final power supply system design are:

- Batteries
- Battery Eliminator Circuit (BEC)
- Electronic Speed Control (ESC)
- Autopilot Voltage Regulators (AVRs)

The ESC is considered part of the power supply system because it cuts power to the motor at critical voltage levels. The AVRs are also considered to be a power supply system component because they regulate the voltage required for the autopilot telemetry transmitter, as well as the GPS and airspeed sensor.

An important consideration of the power supply system concerns the utilization of lithium polymer (LiPo) batteries in the system. These batteries become damaged when over discharged. The ESC has a cutoff set at 3 V per cell, which will automatically cut power to the motor in event of battery over discharge. To prevent catastrophic failure of the SUAS, the batteries must be able to provide the current capacity required to power all the electronics for the entire mission timeframe. Based on the earlier final design, the batteries were sized to adequately cover the power consumptions from all the electronic components.

Batteries

The batteries were chosen based on the required current capacity and output voltage. Two battery packs were used, a large pack for the motor and a small pack for the camera and autopilot modules. The batteries are shown below in figures 5.29-5.30.

Figure 5.29: 8-cell 3850 mAh 29.6V Battery

Figure 5.30: 3-cell 1300 mAh 11.1V Battery

These particular batteries were chosen based on their low weight and high current capacity. By placing two of the 8-cell batteries in parallel, the required voltage for the motor is met, while the current capacity is doubled, to 7700 mAh. These parameters meet the final design requirements. By using these batteries, the SUAS is provided with adequate power to run all of the electronics for up to an hour.

Battery Eliminator Circuit

The BEC is basically a voltage regulator, but is engineered to work with extremely high voltages and will provide clean, regulated voltage in a programmable range of 5-10 V. The BEC draws power from the large battery pack and converts the 29.6V to a voltage output appropriate for the autopilot module, and the servos on the aircraft. By powering the autopilot board from the large battery pack, the nominal voltage of 8V can be supplied to the Autopilot module. The aircraft servos are then powered from the autopilot module. The BEC is shown in figure 5.31.

Figure 5.31: Castle creations BEC Pro

ESC Voltage Cutoff

As the large battery pack powers the motor, the voltage will stay steady at around 29.6 V. Over time, as the current is drawn from the batteries the individual battery cell voltage will begin to drop. LiPo batteries are designed so that the nominal voltage is outputted for as long as possible. To prevent damage to the expensive batteries, the ESC will cutoff power to the motor when the individual battery cells drop below 3 V. The BEC will also disable itself when the battery voltage reaches dangerous levels. To prevent catastrophic failure of the SUAS, the consumption of the entire electronics system was recorded over an hour, to insure the power supply system meets the mission requirements.

Autopilot Voltage Regulators

The ArduPilot Mega board contains several onboard voltage regulators which regulate the voltage from the BEC to appropriate levels for the GPS, airspeed sensor and any servos that are connected to the Autopilot. There is also an onboard voltage regulator dedicated for the autopilot telemetry transmitter.

Top level Power Supply System Detail

Arranging all these components, the top level design of the power supply system can be described. By utilizing battery plugs and receivers, the wiring can be plugged during operation and unplugged when not in use. By powering the autopilot board through the BEC, the electronics top level diagram changes from the original design, and is shown in figure 5.32.

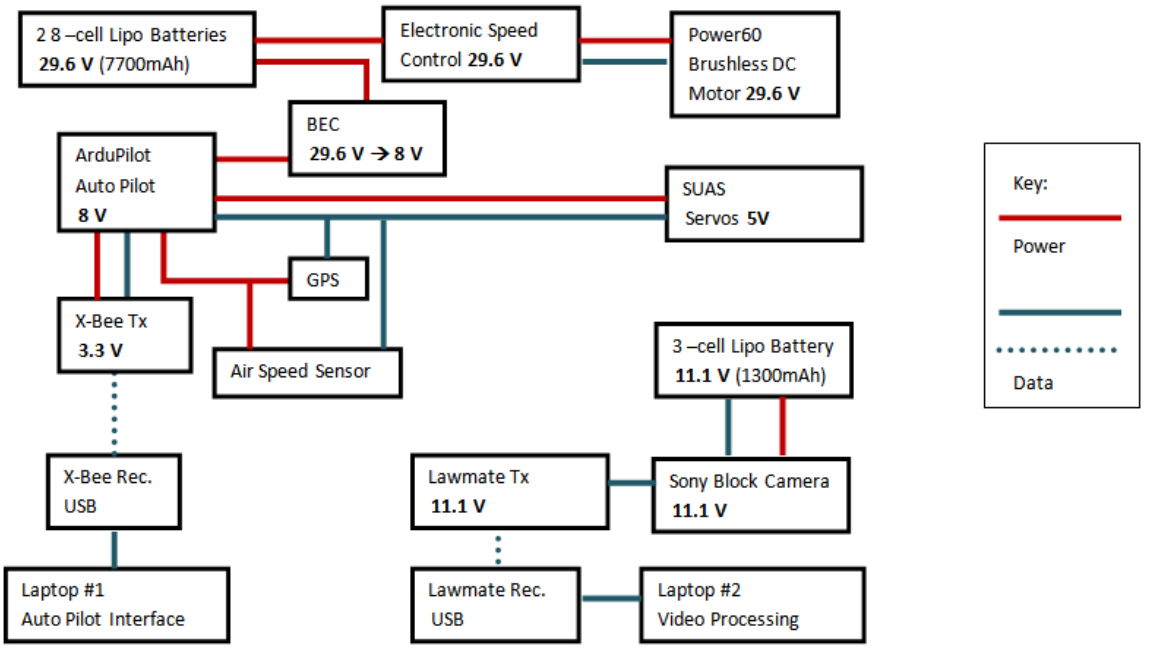

Figure 5.32: Final Electronics Top Level Diagram

6. Manufacturing Process

Spars:

Two 6” wide by 50” long strips of carbon fiber were cut and then prepped for coupling with resin. A smooth glass surface on a table was coated with PVA release film and surrounded by bagging tape. The glass surface was used to keep the strips of fiber completely flat during the bagging process. A layer of fiber was placed on the glass once the release film had dried and was then saturated with resin for both the layers. The second layer was then placed over the first and evenly smoothed out. A layer of peel ply was then placed over the fiber strips and the vacuum bag was applied. After the strips had cured they were cut into smaller ½” wide by 50” long strips using a water jet system.

Each strip was then applied to opposite sides of a 48” long square balsa wood core section of ½” width using CA glue. The rough surface produced by the peel ply was used as the bonding surface. These sections were then slipped into a 3k woven carbon fiber sleeve. The sleeve was then saturated in resin and the spar was vacuum bagged with a layer of peel ply around it.

Fuselage:

The fuselage of the plane was crafted by first producing a mold of the plane. This was achieved by making a female mold of a foam mockup of the fuselage. The foam mockup was constructed by gluing three sheets of 2” thick EPS foam, making the 6” width of the fuselage, larger than the entire section. The main fuselage body and nose section were handled with one section while the tail section was done separately. Pine wood cross sections of each part the plane dimensions were then cut. These cross sections were attached to the foam sections with pins and a simply constructed foam wire cutter was used to cut out the profile of the plane. Below is an image of the two sections after the cuts.

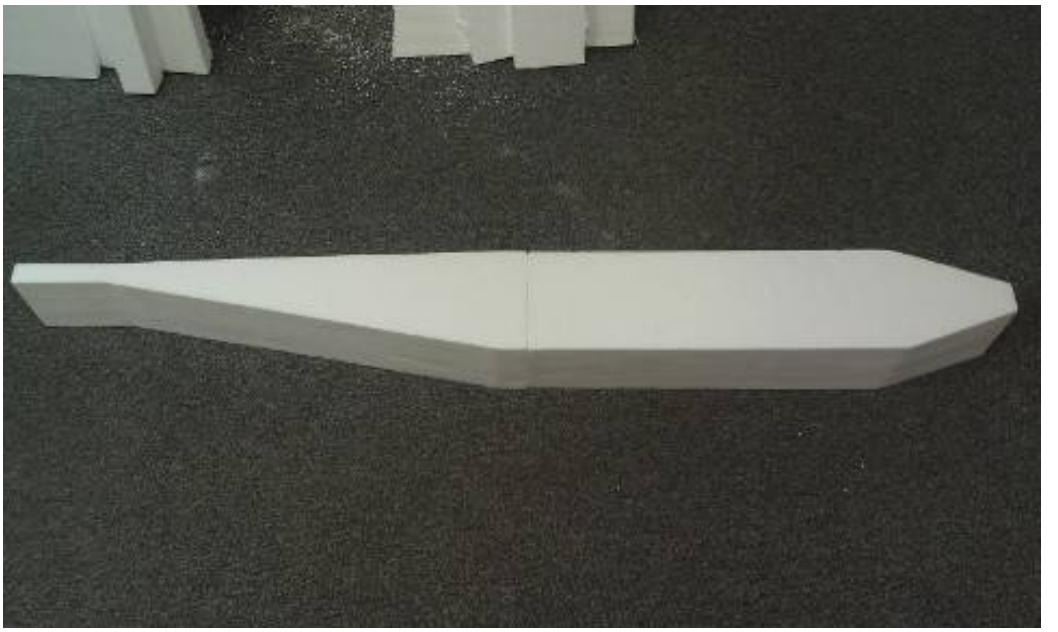

Figure 6.1: Foam profile of fuselage prior to sanding

The tail and body section were then glued together and sanded. The mockup was then cut vertically down the middle to assist in making the mold. Boxes were then constructed out of simple MDF sheet wood to house the foam mockups and create the molds around them. Stringers were nailed across the floor of the boxes to provide extra support under the weight of the mold. The two sections were then glued to the floor the boxes, ready to fill with plaster and fiber. Below is a picture of the completed boxes with foam mockups inside.

Figure 6.2: Boxes for construction of fuselage mold

To prepare the mold for removal from the box the insides of the walls and the foam mockup were coated with two layers of Johnson's paste wax and left to dry for a day. Construction of the mold then started by mixing a 5lb batch of gypsum molding plaster and applying it to the surface of the foam mockup. Another 5lb batch was layered over this and a sheet of loose weave fiberglass was fitted around the foam mockup. When laying in the fiber glass roughly half of the plaster batch was layed down first, then the sheet was worked evenly to the shape of the fuselage, and then the rest of the batch was applied. This was repeated for a total of seven layers. The molds were then left to dry for five days before being removed from the boxes. Below is a picture of the molds after removal from the boxes.

Figure 6.3: Plaster mold after removal from box

When the molds were removed from the box it was found that there were multiple spots where small holds had formed and the plaster had not worked into the fibers evenly. Small batches of plaster were mixed to patch the holes and uneven areas. The molds were then sanded down to a smooth finish.

The two molds were then prepared to be layed up. Two layers of Johnson's paste wax were applied over a two day period to the inside of the molding surface to fill any remaining small cracks and prevent the release film from soaking into the mold. The mold surfaces were then coated in PVA release film, completing preparation for the layup.

Strips of carbon fiber are then layed and fitted to the inside of the mold. Resin is painted into the fibers till they are properly saturated with enough for the layer of carbon fiber and fiber glass. Strips of Fiberglass are then layed and fitted to the carbon fiber. Cut sections of 1/8" balsa are then placed on all flat surfaces of the fuselage area, with only the rounded edges not being cover. Fiberglass is then layed and fitted to the balsa layer and saturated with enough resin for the two internal layers. The layer of carbon fiber strips are then fitted to the fiberglass layer. A sheet of perforated release film and then a sheet of breather/bleeder fabric are then applied to the inside of

the mold. The vacuum bag is then fitted around the entire mold, with vacuum tubing reaching inside of the mold area, and sealed. The parts were then left to cure.

After removal from the molds the two halves were super glued together and left under weights to ensure a good bond. Once joined cutouts were made on the bottom of the fuselage for the camera gimble system, near the tail section for the rear control surface servo rods, and one large cutout along the top of the fuselage for payload access. The holes for the wing connection rods were then drilled and the rods were placed and reinforced with CA.

Wings and Tail:

The wings were first prepped for the spar by cutting a channel out of the bottom surface of the wing. The spar was then placed inside the channel and a piece of foam was fitted and glued into the remaining space. Any excess foam sticking out of the profile was then sanded down. A channel was also cut and then covered for the path of the servo wires into the fuselage. The first 12” of the wing were then removed and the balsa sections supporting the joining tube were then applied. This section was then reattached to the rest of the wing. A loop of 150lb test fishing line was then wrapped around the length of the wing that could attach to screws in the fuselage, providing extra support for the wings and the option of dihedral.

The vacuum bagging process was started after the foam cores had been prepped. Two layers of carbon fiber were cut to slightly over the dimensions of the wing. One layer of fiber was layed on a table and saturated with enough resin for the two layers. The second layer of fiber was then layed onto the first and pressed down with a solid roller. This ensured a good bond between the two layers and removed any excess resin. The two layers were then wrapped around the wing profile. This was followed with a layer of perforated release film and breather/bleeder cloth around the entire wing before it was sealed inside of the vacuum bag. After the part had cured excess fibers were removed from the part and balsa cross sections were fitted to the root and tip chord. The control surfaces were then cut from the wings and a box was cut out of the underside for the placement of the servos.

The vertical and horizontal stabilizers were layed up in the same fashion as the wings but with only one layer of carbon fiber. The control surfaces were cut and the root and tip chord balsa

sections were also applied. The vertical stabilizer was prepped before the layup with a channel to house the pitot tubing.

7. Engineering Economics

7.1 Budget

Team #14 was sponsored by Florida Center for Advanced Aero-Propulsion. Our budget was based on the goal of designing an inexpensive UAS that could complete the key performance objectives defined earlier. Components of each subsystem were chosen based on performance and relative cost. The budget for our SUAS was initially capped at 3000$, however, because of parts required later in the project, FCAAP generously extended our spending limit to cover some minor additional expenses. Some unrecorded out of pocket spending was also done by team members on miscellaneous items. The budget breakdown by item, vendor and price is as follows:

Item	Vendor	units	Price ($)	Total Price ($)
Video Transmitter	ReadyMadeRC	1	89.9	89.9
Video Reciever	ReadyMadeRC	1	99.49	99.49
CCD Test Camera	ReadyMadeRC	1	69.99	69.99
Sony Block Camera	GoElectric	1	566.95	566.95
Block Camera Interface board	GoElectric	1	89.95	89.95
3oz 4hs Fiberglass Cloth (yd)	US Composites	10	6.5	65
Perforated Release Film	US Composites	12	5.6	67.2
Breather Absorber Cloth	US Composites	12	4	48
5.7oz Plain Weave Carbon Fiber	US Composites	7	33.5	234.5
Sealant Tape	US Composites	3	6.95	20.85
PVA #1 Mold Release (1 G)	US Composites	1	16.75	16.75
Nylon Bagging Film	US Composites	6	4.7	28.2
Epoxy Resin and Hardener kit	US Composites	1	72	72
Misc Materials	Varied	1	500	500
3oz 4HS Satin Weave E Glass	US Composites	10	6.65	66.5
Autopilot Telemetry	3D Robotics	1	142	142
Autopilot Board (Full)	3D Robotics	1	300	300
1300mAh 11.1V 3 Cell Lipo Battery	Thunderpower	1	39.99	39.99
Castle Link USB	Hobbytown USA	1	25	25
3850mAh 29.6V 8 Cell LiPo Battery	Thunderpower	2	216.95	433.9
60A Brushless ESC	Thunderpower	1	149.95	149.95
Li Poly Charger & Power Supply	Thunderpower	1	79.95	79.95
Wire and Battery Plugs	Hobbytown USA	1	10	10
Electronics			**Total =**	2097.07
Materials			**Total =**	1119
Grand Total			**Total =**	3216.07

Table 7.1: Team #14 SUAS Budget Breakdown

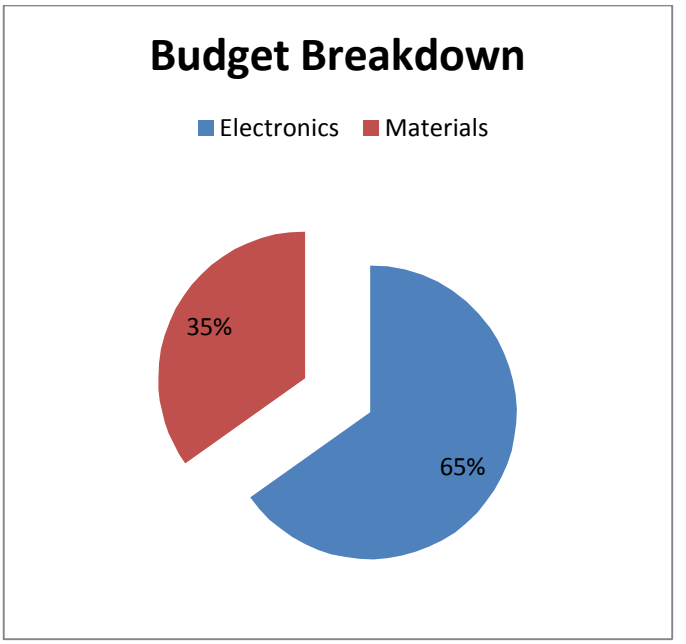

Graph 7.1: Budget Pie Chart

From the breakdown, it is obvious that the most expensive components of the SUAS were the electronic components. The electronics used in the engineering of the electronic subsystems accounts for almost half of the entire budget. The next most expensive category was the materials used to construct the SUAS aircraft. Miscellaneous expenses included materials and equipment for the Telemaster test aircraft, as well as electronic wiring and materials and aircraft construction items such as glue and tape.

7.2 Spending Justifications

The spending justifications for this project are broken down by subsystem. Each subsystem's purpose in the complete SUAS is described and the components in each subsystem listed.

7.2a Aircraft Subsystem

The SUAS aircraft subsystem is the physical aircraft that all the other subsystems are mounted onto. The aircraft subsystem is necessary to complete all of the primary performance objectives of the SUAS project. The components of the aircraft subsystem include:

- Fuselage

- Wings
- Horizontal Stabilizers
- Vertical Stabilizer
- Ailerons
- Rudder
- Elevator

The components in this subsystem were manufactured by the team, so are made of the materials described in the manufacturing section of this paper.

7.2b Autopilot Subsystem

The autopilot system fulfills the autonomy requirements of the performance objectives, including takeoff, landing, waypoint navigation and area search. The components of this system are as follows:

- ArduPilot Mega Board
- GPS sensor
- Airspeed Sensor
- USB Cable
- Xbee Telemetry Transmitter
- Xbee Telemetry Receiver

7.2c Propulsion System

The propulsion system provides the thrust needed for SUAS flight. Flight is necessary to complete all the performance objectives. The propulsion system is comprised of the following components:

- Power 60 Brushless DC motor
- CC Phoenix HV ESC
- Propeller
- Castle Link USB adaptor (Data Logging)

7.2d Power Supply System

The power supply system provides the electrical energy to the electronic subsystems in the aircraft. The electronics in the SUAS must operate in order to meet all performance objectives. Its components are:

- Big battery pack (2 8-cell 3850 mAh 29.6 V batteries)
- Small Battery pack (1 3-cell 1300 mAh 11.1 V battery)
- Battery plugs and wire
- Castle Creations Pro BEC
- Battery Charger

7.2e Video Feed System

To complete the image recognition and location performance objective, the video feed system is required on the SUAS. The video feed system components are:

- CCD camera (Testing)
- Sony Block Camera
- Lawmate Transmitter
- Lawmate Receiver
- Block Camera Interface Board

8. Project Prototype and Testing

8.1 Individual Component testing

8.1aTelemaster components

The Telemaster Senior aircraft was assembled to serve as a test rig for the electronic systems until the SUAS aircraft was completed. The components of the Telemaster included:

- Fuselage
- Wings with Aileron Control Surfaces
- Horizontal Stablilizer with Elevator Control Surface
- Vertical Stabilizer with Rudder Control Surface

The components of the plane were assembled with wood and super glues. Additional parts were required, such as servos and control arms to complete the aircraft. After the plane was completely assembled, the control surfaces were tested fpor correct deflection and the integrity of the aircraft was checked.

8.1b Cameras

The UAS Imagery System consists of two cameras built on an interchangeable system, one as a small lightweight test camera and the other as a competition target acquisition camera.

Sony KX-181

The first camera, Sony KX-181, is a pinhole lightweight camera. This device was not intended for competition use, it's purpose was to be a test platform for the wireless telemetry systems. The KX-181 small and compact design allowed it to be easily built into a mobile test rig. The Sony KX-181 is an analog camera with a horizontal resolution of 520 TV lines. The KX-181 was also used on the Telemaster Senior as a belly camera for in-flight tests.

Figure 8.1 Sony KX-181 Test Camera

Assembly

The Sony KX-181 was connected to power and the video transmitter through a RCA / 9V harness. The camera does record sound, but this was unnecessary so it was not connected. The camera output a composite video signal which was connected to the transmitter through a video (yellow) RCA connector. The power to the camera was provided by the ThunderPower 11.1 V LiPolymer battery. During assembly it was noticed that the camera

and transmitter RCA connectors were both female. This was fixed by purchasing a male-to-male connector that bridged the two signals. The transmitter and camera were wired in parallel providing equal voltage to both devices. Custom T-plug connectors were connected for quick and easy disconnects on battery. The only complication while assembling this component was the connector to the Sony KX-181 was not seated properly and needed to be fastened down using insulating epoxy resin.

Testing Phase

The Sony KX-181 was first bench tested using a small TV. The images were clear and reliable when the connector was re-seated on the rear of the camera. The next test was using a mobile shoebox that also tested the wireless capability of the telemetry system. The camera performed extremely well with many tests including campus walkabouts and a long distance test of 1.5 miles from the FSU Stadium Parking Garage to the top of the Tallahassee Capital Building. Although this test was designed as a stress test for the telemetry system it performed extremely well.

Figure 8.2: Telemetry Range Test

In the final testing phase of the Sony KX-181 it was mounted to the belly of the Senior Telemaster RC aircraft. The video feed was successful, but suffered several waves of interference. The Sony KX-181 camera was also a great test surface because it was rather inexpensive and expendable if the plane could not be recovered.

Sony Block Camera FCB EX-980S

Assembly

When first assembling the Interface Board there was no response from the Camera and or no video signal being transmitted to the TV. The connections were thoroughly tested and nodes

were probed to determine if voltage was being sent to the camera across the Interface's PCB. The multi-meter showed no voltage across the interface board, which was strange. Using a variable power supply a small amount of voltage was applied to the camera's ribbon cable to power the device. Since the ribbon cable connectors were so close to one another it was difficult to provide correct power application to the camera. Using this method there was no response from the camera. At this point it was concluded that the camera was defective. The distributor was contacted for a replacement camera was quickly sent.

Using this new camera and the same test methods the camera still was unable to produce any response. The company who produced the interface board was contacted for troubleshooting purposes, and while in contact with their electrical engineer it was discovered that the 9-pin wiring harness was wired backwards. Since the wires are color coded the wiring harness was providing power to the wrong nodes, thus explaining why there was no voltage being sent to the camera.

After switching the 9-pin harness around the correct connections were made, and the camera was powered up. In order to get an accurate current draw and precise voltage a variable power supply was used to test the Sony FCB camera. It was immediately noticeable that the camera was engaged because the lens focused in and out and the servos produced a clicking noise when powering up. The video signal was received on the TV as an composite video signal connected by an RCA video connector.

The Interface Board had several hanging wires that were shrink wrapped to streamline their design. The RCA connector was extended to reach the wireless transmitter mounted in the rear tail of the aircraft.

Testing Phase

The Block Camera was first tested on the bench in the lab to verify video signals were being received by the TV. The next test was to wirelessly transmit video, this was done in the lab at small distances.

The cameras zoom features were tested by targeting several objects at known distances. The camera focused on cars in the parking lot of the COE at 500 and 750 feet. The license plates

were accurately seen by the camera at these distances. The latest test of the FCB EX-980S was to secure it to the nose of the aircraft. This was done for two reasons, first because the test aircraft was too small to accommodate the camera from beneath the aircraft, and second because the test aircraft became more stable with weight in the front opposed to the mid-section.

8.1c Video telemetry

Assembly

The wireless video communication system was originally based on the 2.4 GHz band, but the manufacturer sent a 1.2 GHz which were not what the design called for. Fortunately the 1.2 GHz LawMate transmitter and receiver were capable of delivering long distance video, so the design was modified to use this frequency band. The wireless video system was first tested in the COE lab, and a small problem occurred when the lead from the wireless receiver became disconnected. The 4-pin connector was not secured very well due to a poor design. These nodes were very close to one another creating a difficult repair because it required soldering the tiny wires next to one another on the receiver. Once this was completed the wiring was sealed with an epoxy resin to prevent the connections from coming lose during flight.

Testing Phase

As seen in the camera section a shoebox was fitted as a mobile test rig for the video telemetry. Using this it was possible to determine safe distances to transmit video without large amounts of noise. During the preliminary test phases it was noticed that the wireless transmitter was extremely hot. With an operational voltage range of 10.5-13 V DC and a power output of 1000 mW, it was understandable that the device would become warm. But the raising temperature on the device directly decreased the wireless video performance. In the testing phases a 120 mm computer fan was added to the shoe box as a cooling mechanism. The device has a digital phase-lock-loop circuit that is designed to operate under high temperatures, but the manufacture did not indicate a maximum operational temperature. Hopefully this device would remain cool during flight due to the large amount of wind flow over the devices heat sink.

During flight tests the wireless transmitter successfully delivered a streaming video to the ground station laptop throughout the flight. Although, there was a noticeable amount of Gaussian

noise on the video. This interference could be due to many things. The noise appeared during flight tests only, and sporadically disturbed the signal.

It is very rare that wireless communication systems work perfectly. Changing locations and whether conditions can often reveal problems in the system. This section outlines many commonly experienced problems in wireless communications. In order to narrow down the possible causes of interferences the wireless system must be tested thoroughly .

a. Internal Source Noise

   Electronic components such as the autopilot, motor, or other wireless signals can generate signal noise that interferes with the video feed. Each of these interferences can easily cause the video signal to become completely unintelligible to the receiver. Even the slightest noise from the aircraft could limit the ground station from performing image processing by creating false data.

b. External Source Noise

   External sources are generally a contributing factor based upon the operating location of the aircraft and the broadcast frequency. Global System for Mobile Communications (GSM) operates between 900-1800 MHz. More specifically the wireless video feed could be damaged by WiFi, which operates on the 2.4 GHz band. Even the presence of high voltage power lines is a potential source for interference.

c. Narrow Band Interference

   This form of interference is directly caused when attempting to broadcast multiple devices on the same frequency. Narrowband interference causes a drastic reduction in the signal to noise ratio. Operating multiple devices on the 1.2 GHz band would be catastrophic, as seen by many RC enthusiasts. Although, by design the Autopilot and RC module are being operated at 900 MHz. It is possible that this may cause problems, but the autopilot most likely would not be transmitting data from the sensors if the manual over-ride was enabled.

d. Receiver Inundation

It is possible to dramatically lower the signal strength of the wireless communication links, in both the video and autopilot transmissions, by placing them near high power sources. Therefore, placing the transmitters near the motor could potentially power the signal reception.

e. Shadowing

Specific high density and/or conductivity materials are able to shield electromagnetic waves. Some of these materials are carbon fiber, copper, and aluminum. It is critical to mount the transmitter antennas outside the fuselage and away from these particularly harmful materials.

f. Multipathing

The loss of signal can be greatly influenced by creating multiple paths with the electromagnetic waves. This process, called Multipathing, commonly occurs when RC signals reflect off smooth and conductive surfaces creating multiple signal paths that effectively interferes with signal reception.

g. Summary

It is very important to understand the possible roots of problems when building wireless communication systems. Having multiple transmissions sent at different frequencies at variable locations based on ever changing weather patterns can be very unpredictable. The wireless communications must be tested on the ground several times before going airborne and will change based on the physical features of the aircraft as well.

8.1d Motor

The Power 60 brushless DC motor was initially tested using a Fluke multimeter and a clamp type motor stand. The motor was run with no prop on several different throttle levels using the Futaba transmitter and receiver. The current draw from the motor was recorded for three different throttle levels:

- ¼ Throttle: 1.01 A
- ½ Throttle: 1.46 A
- Full Throttle: 2.03 A

This was the unloaded current draw of the motor. The theoretical current draw of the motor during takeoff was then calculated. The power required for a quick takeoff was estimated to be 1000 W for a quick, short takeoff and 500 W for a slow, long takeoff. The takeoff will occur with either the throttle at full, for a quick takeoff, or the throttle at ½ for a slow takeoff. These estimations were based on a 15-20 Lb aircraft and the nominal battery voltage of 29.6V. For these two cases:

$$XhXX\ XXXXX\ XXXXXXX\ XXXXXXX = \frac{1000\ X\ XXXX}{29.6\ X} = 33.78\ X$$

$$XhXX\ XXXX\ \ XXXXXXX\ XXXXXXX = \frac{500\ X\ XXXX}{29.6\ X} = 16.89\ X$$

Based on these calculations and the unloaded current draw, the estimated current draw when taking off can be calculated with the power loss of the motor included.

$$XXXXXXX\ XXXX\ XXXXXXX\ XXXXXXX = 33.78\ X + 2.03X = 35.81\ X$$

$$XXXXXXXXX\ \ XXXXXXX\ XXXXXXX = 16.89\ X + 1.46X = 18.35X$$

The cruise current draw, which occurs at ¼ throttle can likewise be calculated with an estimated 150 watts required for a 15-20 Lb aircraft.

$$XhXX\ XXXXXX\ XXXXXXX = \frac{150\ X\ XXXX}{29.6\ X} = 5.06X$$

Which makes the actual cruise current with the motor power loss included:

$$XXXXXXXXXXX\ XXXXXXX = 5.06\ X + 1.01X = 6.07X$$

The total current consumption of the motor for the entire mission was then calculated as:

$$X_{XXX}(X) = X \quad X_{XXX} * X_{XXXXX} = (X_{XXXXXX} * X_{XXXXXX} + X_{XXXXXXX} * X_{XXXXXXX})$$

For a slow 3 minute takeoff, and 57 minute flight time, the total current consumption is then:

$$X_{XXX}(X) = 6.07X * 0.95h + 18.35X * 0.05h = 6.684\ Xh$$

For a fast 1 minute fast takeoff, and 59 minute flight time, the total current consumption is then:

$$X_{XXX}(X) = 6.07X * 0.98h + 35.81X * 0.02h = 6.665\ Xh$$

These calculations are well within the estimated current consumption used to design the power supply system.

8.1e Batteries

Because LiPo batteries are extremely sensitive to charging methods, an important theme during the testing of the batteries was correct charging and discharging methods. The large and small battery packs were charged half way initially, and were charged in the lab to their full capacity. To test the individual batteries, the batteries were charged fully, then discharged fully while the voltage was recorded. The batteries were discharged at 5 A, for testing, the large battery pack was separated and only one of the two 8-cell batteries were discharged. The results are shown below.

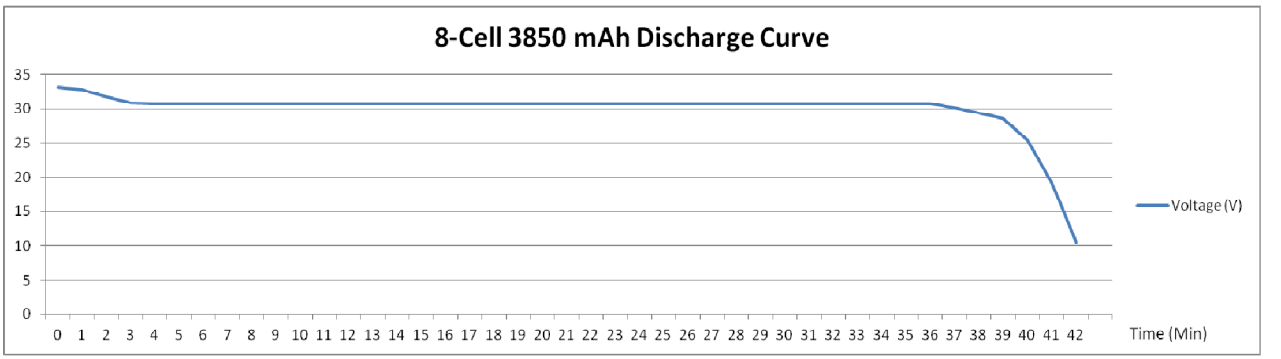

Graph 8.1: Big battery Discharge Curve at 5 A

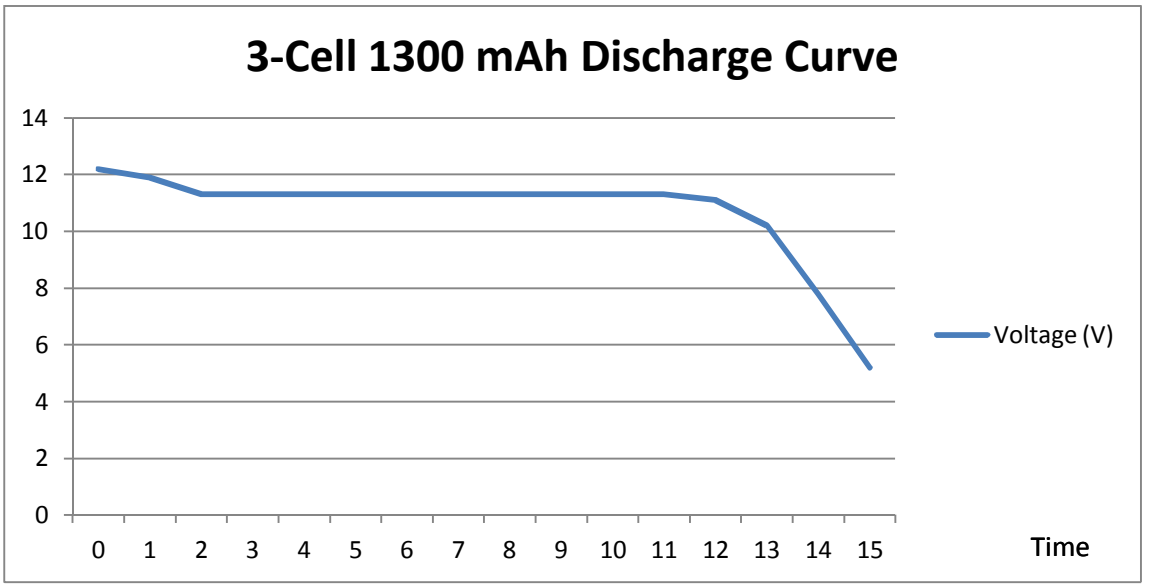

Graph 8.2: Small battery Discharge Curve at 5 A

The batteries were disconnected when their voltages reached a level where the rapidly dropping voltage may damage the battery cells. According to the discharge curves, the batteries follow the normal LiPo battery discharge curve, and are operational.

8.1f Autopilot board

As described before, the APM board consists of a 16MHz Atmega2560 processor, 256k flash program memory, 8k SRAM, 4k EEPROM, and many different types of ports for a variety of inputs. On the APM board is where the heart of the autopilot is. All types of data files loaded up to this board using a mini-usb cable. The main two files needed for flight are the hardware firmware and the mission plan. The hardware firmware is used to tell the autopilot what type of aerial vehicle is being flown (rotary or plane) and the mission plan just is the file containing the waypoints and other commands needed for the aerial vehicle to complete its mission.

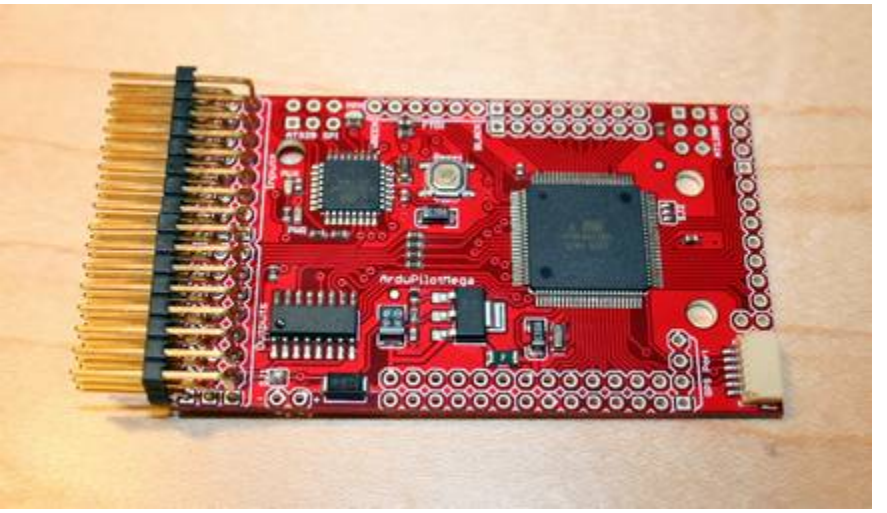

Figure 8.3: APM board

The board was constructed and tested by powering it through a variable power source. LED indicator lights on the board communicated correct construction of the board and proper component connections. The correct operation of the board was tested through the use oif the X-plane simulator.

8.1g Autopilot Telemetry

The autopilot telemetry handles the communication between the autopilot on the aerial vehicle and the ground station. This consists of two Xbee Pro 900MHz modules. These modules are commonly used for this type of application because there is not a need for high data

rates and they have a line of sight (LOS) range of more than five miles. The other components are the RP-SMA antenna and the two interface boards for the Xbee modules. The antenna is built for the 900MHz range and has a gain of 3.1dBi. The two interface boards are used to connect the Xbee Pro modules to the ground station and the autopilot.

The telemetry kit was tested by connecting the Autopilot to the software GUI wirelessly. The successful communication between the Autopilot and the laptop software acknowledged the proper construction of the telemetry circuits, and their wiring.

8.1h X-Plane Simulator

An important part of testing the autopilot system is using the X-Plane Simulator. Before testing the hardware in an actual aerial vehicle, it is important to first simulate your hardware. X-Plane 9 can be used to simulate the hardware in a simulation plane. The mission plan can be run through the simulator following the set up on www.diydrones.com. The simulator and the ground station communicate using udp ports through the computer. From there, the simulator can send the ground station GPS and airspeeds so the aerial vehicle can be seen through the ground station. Other hardware files can be uploaded to the APM board to test the telemetry system too.

Figure 8.4: X-Plane 9 Simulator interface

The X-plane Simulator was tested by downloading and installing the software, then running several test flights with a USB enabled controller. This controller is shown in figure 8.5.

Figure 8.5: USB Simulator controller

8.1i Autopilot GUI

Figure 8.6: Autopilot Ground station GUI.

The autopilot ground station graphical user interface (GUI) can be seen in Figure 3. There are three basic sections that can be seen in the graphic. The left side is showing the

orientation. This is measured using the 3-axis gyroscope on the APM board. The horizon is calibrated when the plane is first started. The top right of the interface is the "Tuning" measurements window. The user can specify which sensors are to be displayed in the window. In Figure 3, the yellow lines are the airspeed sensor being tested. The bottom right is the GPS coordinates being shown using Google Maps. The three lines help determine where the aerial vehicle is headed. The black line is the GPS direction of travel, the yellow line is the direct line to the target waypoint, and the red line is the current heading.

The Autopilot GUI was tested by connecting to the autopilot module. The test results were based on the reception of the GPS, gyro and airspeed sensors. By tilting the autopilot in 3 dimensions, the GUI response to the board movement was successful. The GPS signal was received and the GUI map displayed the test area properly. The airspeed sensor was tested by blowing into the nozzle, which caused the GUI to respond with a speed display.

8.2 Sub-system testing

8.2a Avionics Testing

Testing the avionics system was done through several steps. The first step was to connect the RC receiver to the control surface (CS) servos and power it through the BEC. After testing each CS servo for the correct operation, the Autopilot Module is attached. The second step was to test that all the Autopilot connections were soldered correctly. This is one of the most important things to do as if something was soldered wrong this could lead to a short and a useless board. The next step is to connect the autopilot system to the ground station via the mini-usb cable. With this, the user is able to connect to the autopilot system and test that the orientation and other sensors are working properly. Next, is to do a "hardware in the loop" simulation using the X-Plane 9 Simulator as described previously. The last step to testing is to take a plane out and fly it with the autopilot in it. It is crucial to follow all the preliminary steps before actually taking off and doing this last part of the test. www.diydrones.com has outlines several steps to take before each flight, and some additional steps for the first time flight. These steps are very important to follow.

8.2b Video feed System Testing

As a complete system the cameras and the video transmitter were mounted on the Telemaster test aircraft. The video receiver was plugged into a laptop on the ground, and video

was successfully fed to the lalptop and four flights were recorded. The first two flights were completed with the small test camera, and the last two flights were completed with the large test camera.

8.2c Propulsion System Testing

To test the entire propulsion system, the Power 60 brushless DC motor was mounted to the front of the Telemaster test aircraft. A 16X10 propeller was attached, and the ESC was mounted into the fuselage of the Telemaster and plugged into the motor. The big battery pack was then set into the front of the planes cockpit, and the battery leads were plugged into the ESC. The motor was then test run on the Telemaster on the ground with the Futaba receiver and transmitter. The Telemaster was driven around for approximately 20 min in the COE school parking lot. The motor and ESC were afterwards disconnected and checked for excessive heat. The operation of the propulsion system was a success, and operated nominally.

Figure 8.7: Telemaster Senior Test Aircraft on the Ground

A ground test of the Telemaster was not adequate to properly test the propulsion system, as a test flight would more accurately depict the conditions of the SUAS flight. The results of the Telemaster flight tests are discussed in the performance results section.

8.2d Power Supply system testing

The power supply system was tested by supplying the electronic components of the SUAS in the Telemaster test aircraft. When ground testing the aircraft, the small test camera was

attached to the bottom of the Telemaster, and the Lawmate transmitter was attached to its tail. The camera was run for the length of the ground trials, and the battery powered the camera and transmitter successfully. The BEC was also wired to the large battery pack, and powered the Futaba receiver and all the control surface servos. The autopilot was being debugged at this time, so was not included in the test rig. The testing setup is shown below in figure 8.8.

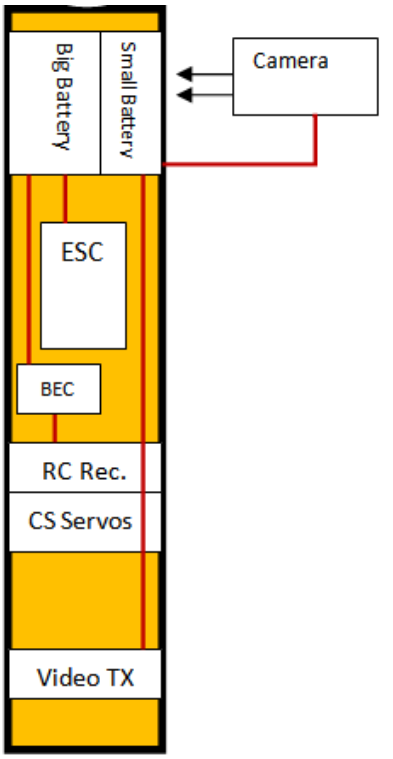

Figure 8.8: Power Supply System in Telemaster Senior

9. Performance Results

9.1 Telemaster Senior test flight results

Because the SUAS aircraft was not completed in time for extensive testing of the electronics subsystems, a Telemaster Senior test aircraft was constructed to serve as a test rig. This aircraft is available from Hobby Lobby international, and has the following characteristics:

- 94” Wingspan
- 64” Length
- 1330 square inch wing area
- “Dry” weight of 10lbs
- Constructed of balsa and hardwoods

Because the Telemaster senior is similar in characteristics and weight to the SUAS aircraft, it was chosen as an appropriate test platform for the SUAS electronics subsystems. The Telemaster Senior is shown in figures 9.1-9.10.

Figure 9.1: Telemaster being tweaked

Figure 9.2: Components installed in Telemaster

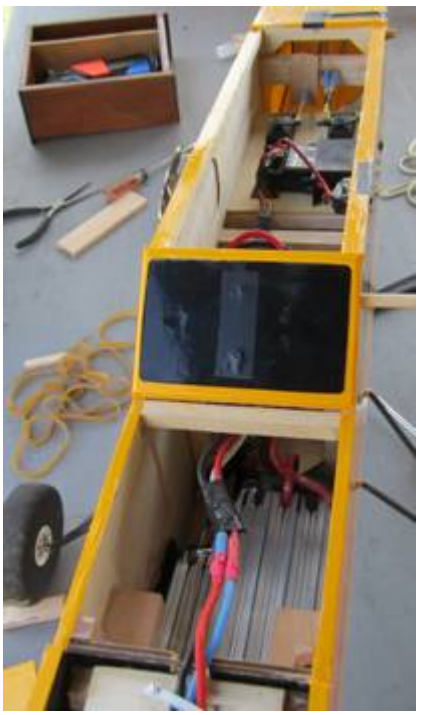

Figure 9.3: Batteries installed in Telemaster

Figure 9.4: Securing wings on Telemaster

Figure 9.5: Telemaster Senior Test Aircraft and Mr. Jim Ogorek

Figure 9.6: Telemaster Senior Test Aircraft Side View

Figure 9.7: Telemaster Senior Test Aircraft Back View

Figure 9.8: Telemaster taking off

Figure 9.9: Telemaster in flight (Back)

Figure 9.10: Telemaster in flight (Side)

The Telemaster was fitted with the following subsystems:

- Propulsion System
- Avionics System
- Power Supply System
- Video Feed System

The aircraft was then flown by our test pilot, Mr. Jim Ogorek, who graciously volunteered his time. The plane was flown at Seminole RC club's field on two separate occasions.

Test Flight #1 (March 15 2012)

The first test flight of the Telemaster was a quick flight used to trim the aircraft with the Futaba receiver trims. The first flight took place after several "field repairs" to tweak the plane for flight. After a quick takeoff, the plane was flown in several loops around the airfield and landed safely. The small test camera was attached to the underbelly of the plane, and video was successfully streamed to the laptop ground station.

Test Flight #2 (March 15 2012)

The second test flight was a repeat of the first test flight, with the additions of some easy maneuvers and higher flight. The flight ceiling during these flights was approximately 300ft.

Test Flight #3 (March 16 2012)

The third test flight was completed with the large camera attached to the "hood" of the Telemaster aircraft. Video from this camera was successfully transmitted back to the ground station laptop.

Test Flight #4 (March 16 2012)

The fourth and final test flight was a test of the test aircraft's aerobatic abilities. The test pilot flew several aerobatics, including a barrel roll. At some point during the flight, a rubber band securing the wings snapped, causing the wings to become detached from the fuselage. The test pilot attempted to land the plane, at which point the plane crashed into a tree. No electronics were damaged in this accident, and the plane received only minimal damage which was repaired the next weekend.

Videos of all of our test flights can be found on our website in the Media section.

http://eng.fsu.edu/me/senior_design/2012/team14/

Figure 9.11 Telemaster taxiing for Takeoff

9.1a Avionics

Because the Autopilot module was still being debugged at the time of the test flights, the avionics subsystem tested on the Telemaster was comprised of the four control surface servos, the Futaba RC transmitter, and the RC receiver. The four servos were plugged into the appropriate slots in the receiver, and the BEC was plugged into an auxiliary slot on the receiver. This allowed the receiver to be powered through the motor batteries.

Figure 9.12: Futaba RC Transmitter

Figure 9.13: Futaba RC Receiver

The control surface servos were trimmed during the first flight by our test pilot Mr. Jim Ogorek, using the trim tabs on the Futaba Transmitter. After trimming for level flight, the avionics system performed perfectly during all test flights. To test the limits of the CS servos, Mr. Ogorek performed some aerobatics during flight #4 and the CS servos responded well.

9.1b Propulsion

The testing of the propulsion system in the Telemaster aircraft was made easy by the CastleLink software and dynamic ESC logging. After all four test flights were complete; data from the ESC was downloaded and graphed using the software. This data includes battery voltage, motor power out, current consumption and several other less important parameters.

Flight #1 Results

Graph 9.1: Battery voltage and Motor consumption over time (Flight #1)

From graph 9.1, the current consumption describes the first flight of the Telemaster. The initial peak in current is the short takeoff, it is followed by the trimming period, where the control surface servos were trimmed for level flight. The current then drops, and the aircraft is flow in a slow loop and then landed.

Flight #2 Results

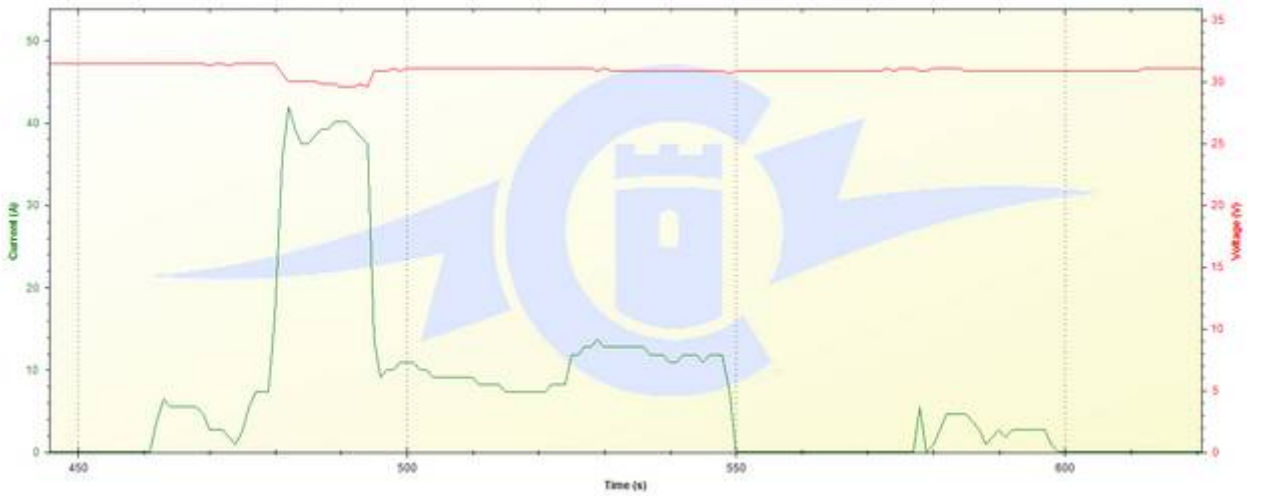

Graph 9.2: Battery voltage and Motor consumption over time (Flight #2)

For the second flight, another short, fast takeoff is performed followed by slow loops and an easy landing. Some current consumption also shows up at the tail end of the flight, as the aircraft is taxied back to the start.

Flight #3 Results

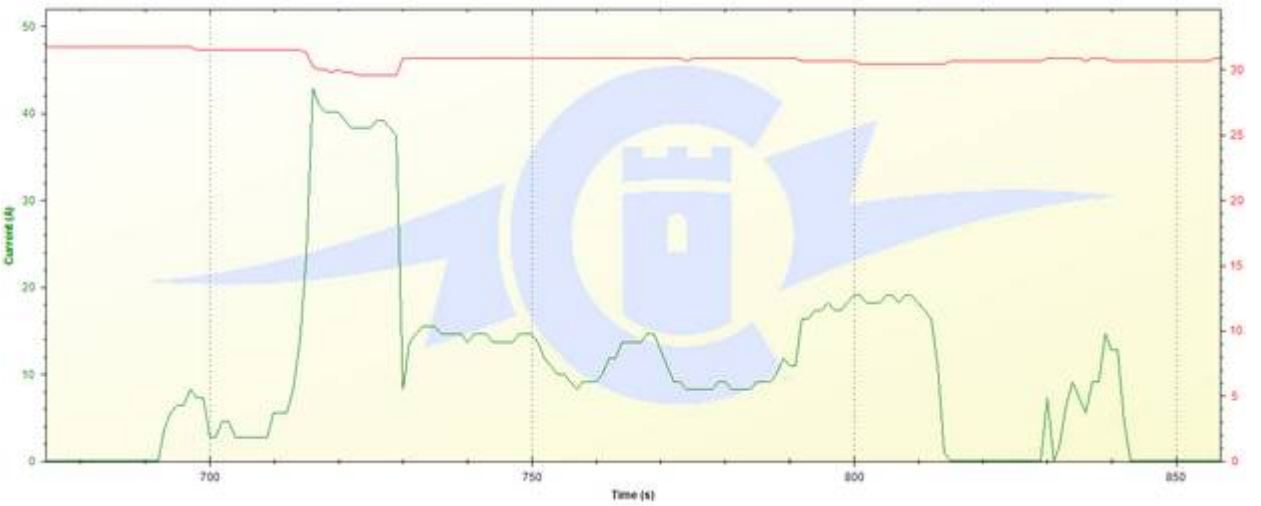

Graph 9.3: Battery voltage and Motor consumption over time (Flight #3)

Flight three is identical to flight #2, with the previously described current consumptions.

Flight #4 Results

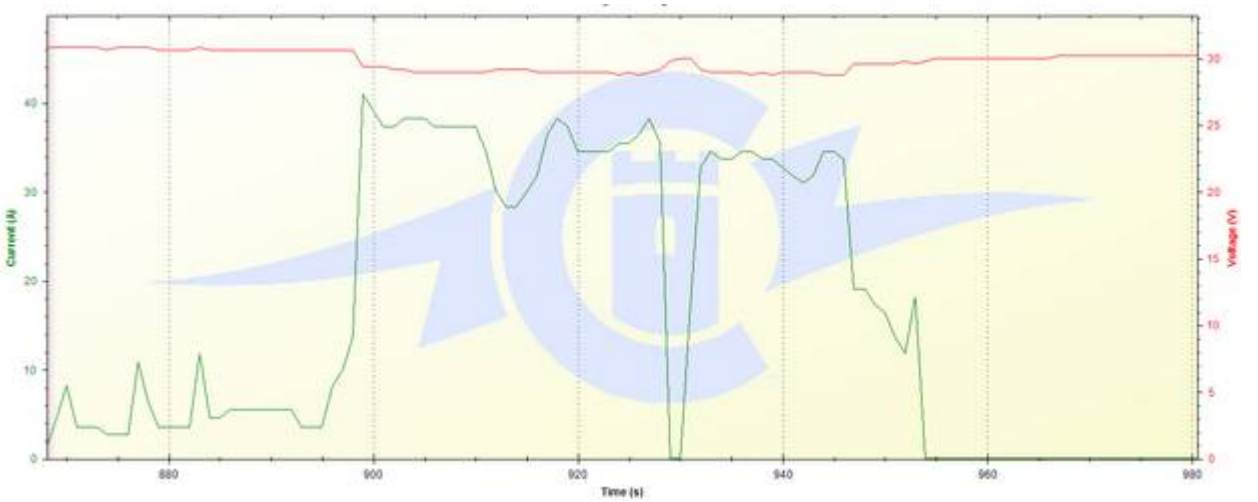

Graph 9.4: Battery voltage and Motor consumption over time (Flight #4)

Flight #4 is very different from the previous three flights. A fast, short takeoff is performed, followed by several aerobatics requiring max throttle. The sharp dip in the current is the lull after a loop was performed and the aircraft was recovering from being upside down.

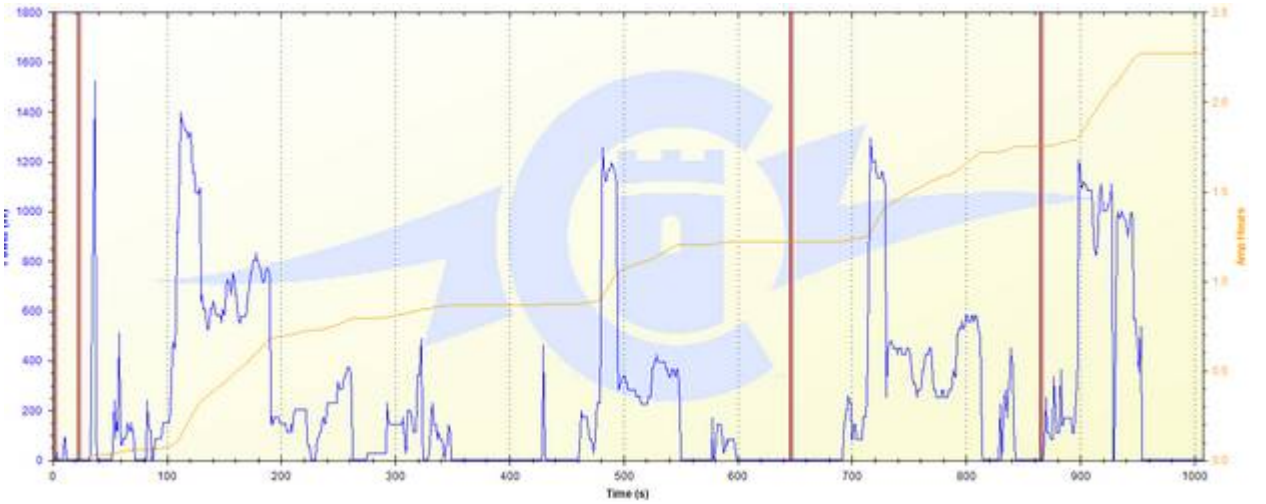

Graph 9.5: Power out and Amp Hours for all flights

Based on these graphs, the results of the propulsion system testing can be summarized as follows. The current consumption of the propulsion system during the four test flights was within the bounds calculated in the design. During the takeoff of the aircraft, the voltage drops to adjust for the maximum power output of the motor. Although the throttle was wide open during these takeoff, a slow, long takeoff will not require the current and voltage shown in these tests. The power output of the motor was shown to be close to what was estimated for this weight of aircraft. The test pilot also commented that the Power 60 motor used was overpowered for this particular plane, and that it would easily work for a much heavier plane. The Telemaster senior was weighed in at approximately 12.4 Lbs before the test flights. This suggests that the propulsion system should be able to handle the extra weight of the SUAS aircraft. It should be noted that these test flights were not representative of the mission parameters and mission time, and a much lower current consumption would be adequate for a slow takeoff and slow level flight.

9.1c Power Supply

The power supply system was responsible for supplying the propulsion system, avionics system and the video feed system during these four test flights. From graph 9.5, the motor batteries supplied nominal voltage for the 16 minutes of flight time. At the full throttle instances, large current pulls from the motor were outputted nominally. Approximately 2.3 Ah of current were used during the four test flights. Because the test flights were not representative of the mission flight the system was designed for, this current consumption will not be used to estimate total draw on the motor batteries for a 60 minute mission flight. However, the current consumptions are similar to the calculated values, it can be said that the power supply system will easily be able to handle the mission flight it was designed for.

Powering the other components, the BEC outputted the appropriate voltage for the Futaba receiver and the servos for all four flights. No excess heat was detected and the BEC operated nominally.

The camera battery powered both the small and large camera with the Lawmate video transmitter in operation. The video feed worked for all four flights, and the battery provided adequate current capacity for over an hour of testing.

9.1d Video Feed

During flight the Sony Block Camera provided excellent video footage. With autofocus enabled the image was not blurry, but did suffer a small amount of distortion. The interference seen by the laptop on the ground station was likely caused by the 1.2 GHz transmitter overheating or lack of shielding between the RC servo transmitter and the video transmitter.

Figure 9.14: Telemaster 3rd Flight - Above Seminole RC runway

The FCB EX-980S was tested twice in flight with approximately 10 minutes of total logged flight video. The aircraft performed several acrobatics during the last test flight. Unfortunately, during these maneuvers the wing became unsecured which disconnected the planes motor. While powerless in the attempt to land, the aircraft collided with a tree at a relatively low speed. The aircraft sustained the crash with minimal damage. It was a major concern that the camera would be damaged, but after inspection the camera was not affected by the crash. Further improvements may include an enclosure for the camera that protects the electrical circuitry from a crash or high-altitude moisture.

As part of the AUSVI Student Competition the designed aircraft will earn points based on the number of identifiable targets seen during the mission flight. The aircraft will be travelling at low speeds of approximately 44 mph, with a minimum altitude of 100 ft. and maximum of 750 ft. The video feed was designed to transmit live video data throughout the flight. Using this

method targets can be instantly identified and allow additional time to complete the flight mission.

Other than a few minor repairs the Sony KX-181 test camera worked flawlessly. The Sony Block Camera, used as a surveillance of ground based targets, had several problems. First the camera was dead on arrival and needed to be replaced, then the interface connector board was unresponsive due to the iShot board manufacturer sending harnesses that were wired incorrectly. Finally the serial communication was unresponsive, allowing no camera control through the RS-232 interface. The Sony Block Camera hardware proved to be robust after surviving a crash landing during the fourth flight test onboard the Telemaster RC plane. The video quality is excellent and zoom capability allows this device to capture far away images with good clarity. Currently the only problems to fix are the camera serial port control and reduce the amount of interference from the wireless video feed. The AUVSI competition requires aircrafts to navigate autonomously, but still prohibits manual control of a camera system.

If completed the camera system will be capable of panning and tilting over 60 degrees in 0.84 seconds. The Sony Block will use a highly telephoto lens to give the personnel on the ground an exceptionally clear image displaying shapes, colors, and alphanumerics. The user will simply adjust the sticks on the Spektrum wireless receiver to control the camera. The final design will be mounted underneath the new aircraft between the landing gear on a two axis pan/tilt gimbal.

Figure 9.15: Pan / Tilt Camera Gimbal Design Concept

Exploring several possibilities for interference can be beneficial in narrowing down the root cause of the problem, team members speculated that the high operating temperature of the device caused a decrease in signal quality. This problem could be improved by replacing the transmitter heat sink or upgrading the device. Another problem could be the length of the wire from the transmitter to the camera was creating a large amount of resistance, which could be fixed by shorting the twisted pair to a minimum length. The interference could also be due to a lack of shielding between the motor components, autopilot, and video telemetry. To correctly shield these devices a small piece of aluminum (100-300 μm) can be placed between each component. Another idea is to change the antenna structure on the aircraft to a Bluebeam Antenna, this type of wireless antenna uses reverse polarization to reject unwanted signals. The antenna configuration is arranged at 120 degree angles in a circular format. The antenna is an omnidirectional configuration with a gain between -8 to 19 dbi.

Figure 9.16: Bluebeam Cloverleaf Antennas

10. Safety, Health and Environmental Issues

10.1 Aircraft Safety

Every year there are hundreds of people injured by RC Aircrafts, their high speed velocities and unpredictability surprise beginners. Although common, many of these injuries can be prevented by following aircraft safety guidelines. In the sections below many safety precautions are outlined to ensure no injuries take place in operating these vehicles.

Figure 10.1: Lithium Polymer Battery Combustion

- **Prelaunch Checklist**

  Before flying make sure the assembly of the aircraft is flight worthy and in accordance to the airfield being used. It is common practice to have experienced users check the vehicle for any adjustments. Such as firmly attaching screws, covering holes in the aircraft, securing the propeller, anchoring all components in the fuselage. Try to use only parts contained in the original construction or purchase of the aircraft. Spare parts are great, but making sure they are compatible is greater!

  Check to see if the wings are angled properly to balance the aircrafts structure. Check to see if the aircraft is balanced correctly with the center of gravity, shifting the contents in the fuselage will result in improved stability and controllability of the aircraft. Communicate with other airmen at the field and do NOT fly multiple aircrafts on the same frequency. This will likely cause the controllers to interfere with one another and result in the loss of both aircrafts.

- **Preflight Tests and In-Flight Precautions**

  Check to see if the aircrafts propeller is fastened securely to the airplane. Next turn on the remote control power switch. Align the tail at 90 degrees to the fuselage and make sure the aircraft is balanced with the wings. With all participants clear of the aircrafts propeller, turn on the power switch to the airplane. Test the wireless controls of the aircraft to ensure the aircraft is responsive. With the aircraft secured users can test the speed, power, and propeller accuracy. It is extremely important to identify wind direction prior to taking off, hastiness may result in a short flight! Prior to taking off looking around to verify there are no hazards. There should be no people, telephone or power lines, cars, buildings, trees, etc. are within distance of the airplanes takeoff and flight. Planes should be flown in an area with ample space to quickly land in a hurry as well as a safe distance from the user or spectators. While in flight the aircraft should be carefully navigated, quickly adjusting the controls can easily cause the aircraft to lose control.

- **Landing**

  Allowing the aircraft to glide freely in approach for landing is a good technique that will slow the aircraft down for a gentle landing. Applying the throttle when the aircraft is approximately 4 feet from the ground will level the aircraft out to protect the nose. In the event that there are winds when approaching a landing the aircraft should attempt to land into the wind with level wings. Landing is arguably the most difficult part of flying, and should be done with a trainer aircraft.

- **Autonomous Aircrafts**

  Working on or being near an autonomous Aircraft is an extremely large risk. One must take several additional precautions in order to prevent injury or possible death. This aircraft is propelled by an extremely powerful brushless electric motor. While engaged this motor is a destructive force that can easily dismember anyone careless enough to stand near the blades. The aircraft is powered by several extremely powerful 65 C Lithium Polymer batteries. The chemistry of these batteries contain highly explosive and deadly volatile chemicals. It is crucial that operators monitor these devices very closely, as well as use safe charging methods and low voltage cutoffs. Batteries overcharged may

produce an explosion capable of claiming the lives off anyone in the nearby vicinity. Due to the autonomous nature of this aircraft it is recommended that by standards, personnel stay at least 100 ft from the aircraft at all times. Although it is not intended by design, an autonomous aircraft may fail and become dangerous resulting in possible catastrophic behavior. It should be noted that the operators perform a Prelaunch Checklist as well as testing all control surfaces before launch. During the landing approach pedestrians should stand clear of the aircraft to ensure a safe deceleration.

- **Additional Remarks**

  Training is helpful to learn the touch and feel of an aircraft; this can be done using a dual-controller system or a flight simulator. Using protective eye glasses is beneficial; many times parts of the aircraft may become loose during flight and turn into a projectile. Eye glasses also are required while working on the aircraft. Treat the propeller as if it is always connected when the battery enters the plane. Researching the aircrafts electronics is helpful to troubleshoot problems and reduce the chance of electrical shock. Understanding the dangers of Lithium Polymer batteries is very important. Users ignoring these risks should not use LiPo batteries, and taking them lightly puts the user and others in grave danger. Be responsible when using RC or autonomous aircrafts, they are travelling at high velocities and should not be flown around pets or people. Lastly, expect the unexpected! RC aircrafts may receive interference that causes the propeller to turn on without throttle. The batteries have a tendency to spontaneously combust and parts of the aircraft will likely be dislodged during flight. These endeavors are not for the wary! Responsible use and safe practice of these systems will result in an addicting fun filled flying experience!

10.2 Environmental hazards

The most important factor concerning the environmental impact of the SUAS project is the disposal of both construction materials and used Lithium Polymer batteries. Currently, a recycling infrastructure for LiPo batteries does not exist; because the chemicals making up the structure of the battery are harmful to the environment, these batteries must be disposed of through a hazardous waste facility.

The manufacturing of the SUAS aircraft produces waste that contains carbon fibers as well as some petroleum based chemical wastes. However, the most environmentally damaging waste is the several types of foam used. This foam takes an extremely long time to break down, and if not disposed of properly, will contaminate the ecosystem.

To insure that the environment is protected properly during the completion of the SUAS project, proper disposal guidelines were followed for all environmentally hazardous materials, and any recyclable materials, including cardboard boxes, were sorted and sent to a recycling facility.

10.3 Health issues

There are a variety of health issues stemming from the construction of the SUAS. These issues are mainly concerned with the manufacturing process and the hazards of the chemicals used in the construction of the SUAS aircraft and the Telemaster aircraft.

Some chemical hazards include:

- Epoxy
- Super Glue
- Hobby aircraft glue
- Resin and resin hardener

Caution must be used when applying these products to minimize skin contact and vapor inhalation. The by-products of the construction process must also be disposed of in the laboratory prescribed manner to prevent accidental spills or explosions.

11. Project Conclusion

11.1 Summary of results

The SUAS project was worked on by Team #14 members for nine months. During this time engineering principles learned by the students were utilized to design, construct and test the various subsystems of the SUAS. The product of this hard work at the time of the publishing of this paper are the near to complete SUAS aircraft, and the fully integrated and tested electronics systems.

In the months following the completion of the ME and ECE capstone course, senior design 1 and 2, work will continue on the SUAS. Although at this time the SUAS is not quite ready to compete in the 2012 AUVSI competition, work will continue as long as possible to either meet the competition performance objectives and safety requirements, or to complete the SUAS in such a fashion that next year's team can easily prepare it for next year.

The results of the 2011-2012 SUAS project are embodied in the fully tested Telemaster Test aircraft, and the constructed SUAS aircraft. The final step in this project, which has not yet been completed, is to integrate the ECE and ME sides of the project, namely the manufactured aircraft and the electronic subsystems.

11.2 Future developments

Some possible future developments in the 2011-2012 SUAS project are:

- Tweaking and testing of the SUAS aircraft
- AUVSI Safety requirements satisfaction
- Ground target position determination
- Autonomous takeoff and landing
- Conversion of 72 MHz RC to 2.4 GHz RC
- Autopilot GUI control of camera gimbal
- Autopilot GUI control of camera zoom
- Autonomous Image recognition using MATLAB

11.3 Lessons learned

One of the biggest challenges facing a team that is completing a task is the efficient and effective management of the most important resource: time. Although the SUAS project was completed over nine months, academic and other responsibilities always tend to distract the team from completing planned tasks. Beginning the project with clear cut goals and benchmarks is a necessary planning tool, but will not work unless characteristics of a large project are planned for in advance. Things we did not see coming, which delayed important steps in the SUAS project included:

- Part ordering delays
- Vendor errors (Sending wrong or defective parts)
- Laboratory safety procedures

- Manufacturing process delays
- Required additional parts (wires, plugs, materials)
- Required equipment

To summarize, if we had this project to do over from the start, special considerations would be made to determine what we were missing in our project planning. These missed details will delay the project significantly and can be identified through a thorough design process.

12. Acknowledgements

Team #14 would foremost like to thank the Florida Center for Advanced Aero-Propulsion for generously funding our SUAS project. We would also like to thank our advisors Dr. Rajan Kumar and Dr. Mike Frank, who repeatedly took time from their busy schedules to give us valuable assistance. We would also like to extend our utmost gratitude to Mr. Jim Orgorek and Seminole RC club, who helped us in the testing of our aircraft and provided invaluable advice and repair assistance. We could not have done it without all of you, and we thank you.

13. Student Biographies

Ryan Jantzen

Ryan Jantzen is a senior Mechanical Engineering student at Florida State University. Ryan was born in Panama City, FL and his current permanent address is in Niceville, FL. While at Florida State, Ryan has been involved with the American Institute of Aeronautics and Astronautics and the American Society of Mechanical Engineers. Ryan is also a member of Tau Beta Pi Engineering Honor Society as well as Pi Tau Sigma Mechanical Engineering Honors Society. Ryan currently works as a Teacher's Assistant for the Undergraduate Experimental Fluids lab and is also doing Computational Fluid Dynamics research under Dr. Kunihiko Taira. After graduation, Ryan will spend the summer at the Air Force Research Laboratory in Dayton, OH working as a researcher studying unsteady aerodynamics, specifically in the field of flapping wing vehicles for the development of future MAV platforms. Ryan will return to Florida State in the fall when he will begin his graduate education in pursuit of a Ph.D. in Mechanical Engineering studying Computational Fluid Dynamics.

Alek Hoffman

Alek Hoffman was born in Tallahassee, FL and grew up in Apalachicola, FL where he went to high school up until the 9th grade. In the 9th grade, Alek dropped out of high school and began home school. After working construction as a framing carpenter for three years, Alek applied and was accepted into Tallahassee Community College. After achieving his AA degree, Alek then transferred to Florida State University, and enrolled in the Naval Reserve Officer Training Corps. After seven years of hard work, Mr. Hoffman will receive a Bachelor's Degree in Electrical Engineering from Florida State University. Upon graduation, Alek will be commissioned as a United States Naval Officer and will attend flight school in Pensacola, Florida.

Brian Roney

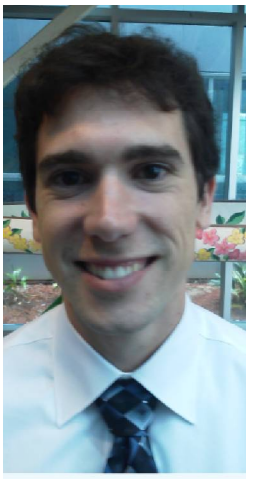

Brian Roney is a fifth year engineering student at the FAMU-FSU College of Engineering. His major is Computer Engineering. Outside of school, Brian has held internships with Elbit Systems of America and RCC Consultants. He is currently interning at RCC as a consultant for the Florida Department of Transportation. Brian also is the current vice president of Eta Kappa Nu, the Electrical and Computer Engineering honor society. In his spare time, he likes to play sports. Brian's favorite sports to play are soccer and football. Brian likes attending the football games at Florida State University. He also enjoys taking part in the intramural games at the university as well.

Walker Carr

Walker is a graduate of the mechanical engineering program at the FAMU-FSU College of Engineering specializing in the field of thermal fluid sciences. He has interests in the areas of high speed fluid flows and aerodynamics, combustion dynamics, and also alternative methods of power generation. He aspires to attend graduate school and enter the workforce in the area of power generation. It is undecided whether this work will be in alternative fields or traditional turbine power.

Eric Prast

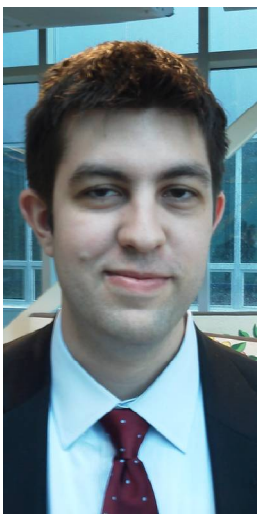

Eric Prast is a senior at Florida State University studying Electrical Engineering. He was born in Newport Beach, California but spent most of his life in St. Petersburg, FL. Eric always dreamed of following in the footsteps of his father, who also was an EE and electronic game design pioneer. Eric's primary interests in Electrical Engineering are intelligent systems, image recognition, robotics, and communications. He was interested in the AUVSI Unmanned Aerial System because it is a unique challenging experience that

incorporates a system level engineering approach to a seemly new and smart applicable technology.

Antwon Blackmon

Mr. Blackmon is Florida A&M University student. He was born and raised in Tallahassee, Florida. His interests include: materials engineering, bioengineering, robotics in the concentration of prosthetic limbs, testing engineering and analysis engineering with a concentration in aeronautics. He enjoys the challenge of figuring out the problems that other tends to give up on. His overall goal in life is to help people in the most efficient way possible.

14. Engineering Drawings

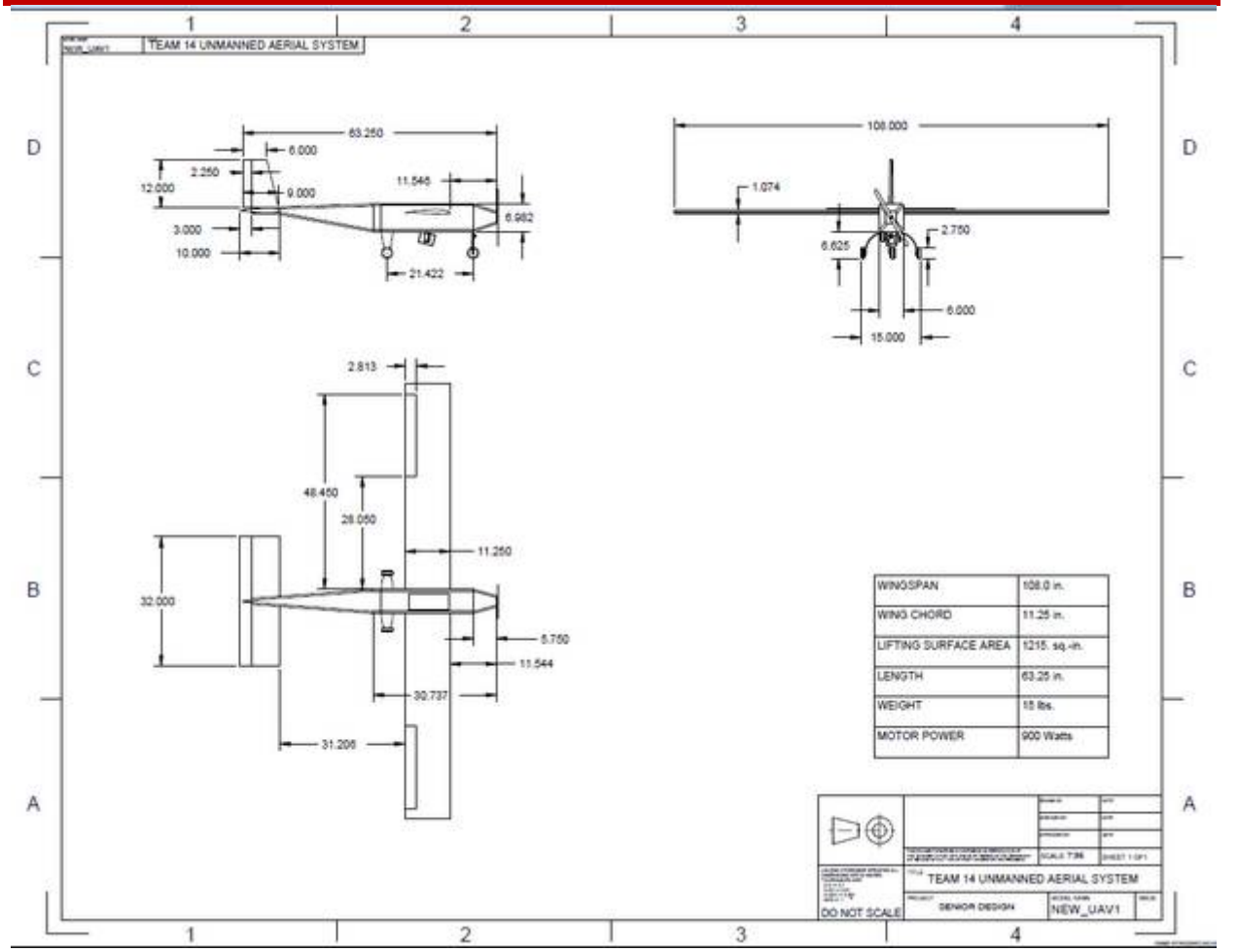

15. Appendix

A.1 Team # 14 Code of Conduct

Mission Statement:

The objective of this team is to work together to create a positive and professional learning environment. This will be established through trust, respect, integrity and communication. We will work in a timely manner but also carefully to ensure that the project is done properly.

Team Officer Positions:

Team Leader: Ryan Jantzen

The Team leader is responsible for setting reasonable goals and managing project completion. Assures that workload is distributed evenly between the team members. Schedules team meetings and informs team of meeting time and place. Team Leader resolves conflicts within the team and sets meeting agendas.

Secretary: Alek Hoffman

The Secretary maintains and submits minutes for each team meeting and publishes all important documents, websites, ect. to the group blog. Secretary maintains rules and regulations for the team and project and alerts team mates of upcoming academic assignments and milestones.

Treasurer: Antwon Blackmon

The Treasurer is responsible for the group's finances as well as keeping track of purchased parts and overall inventory. Treasurer asses required expenses and plans for appropriate funding.

Webmaster: Brian Roney

The Webmaster is responsible for maintaining the team's project website with up to date information and media. Webmaster will research and share important online information with his team mates.

ME Lead: Walker Carr

The Mechanical Engineering Lead is responsible for managing ME members of team and scheduling meetings with the ME advisor. ME Lead will manage overall ME project requirements with the team leader and will keep in constant contact with ECE lead to ensure project compatibility.

ECE Lead: Eric Prast

The Electrical/Computer Engineering Lead is responsible for managing ECE members of team and scheduling meetings with the ECE advisor. ECE Lead will manage overall ECE project requirements with the team leader and will keep in constant contact with ME lead to ensure project compatibility.

Communication:

The primary sources of communication between team members will be through emails, phone calls, and text messages. An account for Google Calendar was set up to track meeting times and schedule deadlines for deliverables.

Meetings:

Meetings have been established twice a week; Tuesdays at 6pm and Fridays at 2pm. All members are expected to attend both meetings and missing these meetings without a valid excuse will not be tolerated. If a team member must miss a scheduled meeting, they must notify the entire team of their absence at least 24 hours in advance. An Evernote Notebook account was created for the secretary to record meeting minutes and distribute them to all team members.

Conflict Resolution:

In the event that a conflict should occur the following steps should be taken:

- The individuals involved should try and come to some sort of an understanding either agree or agree to disagree.
- If the individuals involved cannot come to an agreement then the conflict some be discussed with the rest of the group.
- The conflict should be explained in a clear manor to the rest of the group then a vote should be taken.
- If the vote ends in a draw then the team leader should make a decision.
- If the team leader cannot come to a conclusion then the conflict should be resolved by some outside source such as the faculty advisor

Ethics:

The team will follow the Codes of Ethics and Standards established by the American Society of Mechanical Engineers.

As a team we have all read and understand the code of conduct described above and plan to abide by it.

Antwon Blackmon _____

Walker Carr _____

Alek Hoffman _____

Ryan Jantzen _____

Eric Prast _____

Brian Roney _____

A.2 Team #14 Gannt Chart

#	Activity	Begins	Ends	Start	Dur	Done
	Management					
1	Project Management	4-Jan-12	27-Apr-12	1	16	100%
2	Progress Report	4-Jan-12	19-Jan-12	1	2	100%
3	Mid-Point Review	19-Jan-12	16-Feb-12	3	5	100%
4	Final Project Review	16-Feb-12	5-Apr-12	8	8	100%
5	Final Report	16-Feb-12	5-Apr-12	8	8	100%
6	Operations Manual	16-Feb-12	5-Apr-12	8	8	100%
7	Open House	5-Apr-12	12-Apr-12	14	2	0%
8	Website	4-Jan-12	27-Apr-12	1	16	100%
	Initial Testing					
7	Propulsion System	4-Jan-12	17-Jan-12	1	3	100%
8	Power Supply System	4-Jan-12	17-Jan-12	1	3	100%
9	Imagery System	4-Jan-12	17-Jan-12	1	3	100%
10	Autopilot System	4-Jan-12	17-Jan-12	1	3	100%
11	Avionics	4-Jan-12	17-Jan-12	1	3	100%
13	Communications Testing	4-Jan-12	17-Jan-12	1	3	100%
	Interim Testing					
7	Propulsion System	17-Jan-12	14-Feb-12	4	4	100%
8	Power Supply System	17-Jan-12	14-Feb-12	4	4	100%
9	Imagery System	17-Jan-12	14-Feb-12	4	4	100%
10	Autopilot System	17-Jan-12	14-Feb-12	4	4	100%
13	Communications Testing	17-Jan-12	14-Feb-12	4	4	100%
	Aircraft Construction					
26	Fuselage Fabrication	17-Jan-12	14-Feb-12	4	1	100%
27	Shear Box Fabrication	17-Jan-12	14-Feb-12	4	1	100%
28	Tail Section Fabrication	17-Jan-12	14-Feb-12	4	1	100%
29	Wing Fabrication	31-Jan-12	7-Feb-12	5	1	0%
30	Aircraft Assembly	7-Feb-12	14-Feb-12	6	1	0%
	Prototype					
31	Complete Assembly	14-Feb-12	28-Feb-12	7	2	0%
32	System Integration	21-Feb-12	6-Mar-12	9	2	0%
33	Shakedown	6-Mar-12	20-Mar-12	11	2	0%
34	SUAS Tweak	20-Mar-12	3-Apr-12	11	2	0%
35	Mission Test	3-Apr-12	24-Apr-12	13	4	0%

A.3 SUAS Functional Diagram

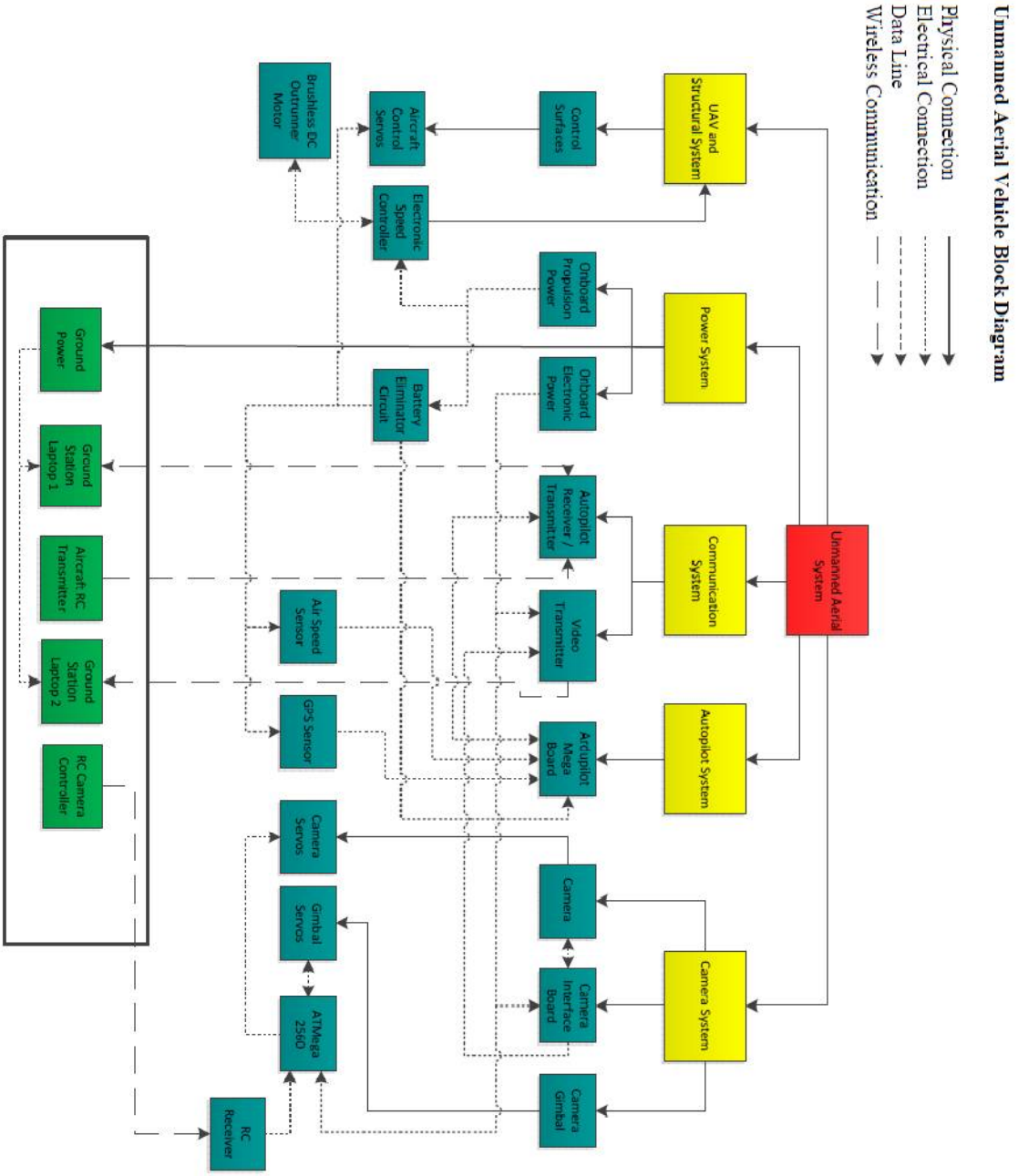

16. References

1. Anderson, Chris. *DIY Drones*. Web. 04 Dec. 2011. <http://diydrones.com/>.

2. "Eagle Tree –R/C RPV RC Unmanned Aerial Vehicle Telemetry" *Eagle Tree – R/C Telemetry OSD RC Pitot Prandtl Spektrum AR9000 JR R921*. Web. 04 Dec. 2011. <http://www.eagletreesystems.com/Standalone/standalone.htm>.

3. Faludi, Robert. "XBee-PRO® 900 RF Modules - Digi International." *Making Wireless M2M Easy - Digi International*. Digi Internation Inc. Web. 05 Dec. 2011. <http://www.digi.com/products/wireless-wired-embedded-solutions/zigbee-rf-modules/point-multipoint-rfmodules/xbee-pro-900>.

4. "Futaba 7CAP." *RC Universe Features Rc Cars, Rc Airplanes, Rc Helicopters, Rc Electric Planes, Rc Boats, Radio Control Jets, Rc Discussion Forums, Rc Classifieds and Auctions*. Web. 05 Dec. 2011. <http://www.rcuniverse.com/magazine/article_display.cfm?article_id=321>.

5. "Main Page - Paparazzi." *Paparazzi*. GNU Free Documentation. Web. 04 Dec. 2011. <http://paparazzi.enac.fr/wiki/Main_Page>.

6. "Lithium-ion polymer battery" *Wikipedia* Web. 04 Dec. 2011. <http://en.wikipedia.org/wiki/Lithium-ion_polymer_battery>.

7. "LiPo battery guide" *prototalk.net* Web. 04 Dec. 2011. <http://exoaviation.webs.com/pdf_files/Lipo%20Battery%20Guide.pdf>.

8. "LiPo safety warnings" *Thunderpower* Web. 04 Dec. 2011. <http://thunderpowerrc.com/PDF/THPSafetyWarnings.pdf>.

9. Raymer, Daniel P. *Aircraft Design: a Conceptual Approach*. Reston, VA: American Institute of Aeronautics and Astronautics, 2006. Print.

10. Lennon, Andy. *Basics of R/C Model Aircraft Design: Practical Techniques for Building Better Models*. Wilton, CT: Air Age, 1996. Print.

11. Simons, Martin. *Model Aircraft Aerodynamics*. Poole, Dorset [England: Special Interest Model, 2002. Print.

12. "XFLR5." *Http://sourceforge.net/*. Web. 8 Dec. 2011. <http://xflr5.sourceforge.net/>.

13. "NACA-4412" Airfoil Investigation Database. Web. 8 Dec. 2011. <http://www.worldofkrauss.com/foils/793>

14. "NACA-0012" Airfoil Investigation Database. Web. 8 Dec. 2011. < http://www.worldofkrauss.com/foils/1137>

15. Gray, P. (2001). *Lines of resolution*. Web. 01 Dec. 2011. <http://jkor.com/peter/tvlines.html>

16.Hickman, I. (1997). *Practical RF Handbook*. Butterworth-Heinemann. Text. 01 Dec. 2011.

17. McHugh, S. (ND). *Digital camera image noise.* Web. 01 Dec. 2011. <http://www.cambridgeincolour.com/tutorials/noise.htm>

18. Antenna Basics. *Welcome to the Antenna Theory Website.* Web. 01 Dec. 2011. <http://www.antenna-theory.com>

19. Space-Electronics (ND). *How to reduce jitter of airborne cameras*. Web. 01 Dec. 2011. <http://www.space-electronics.com/KnowHow/Reduce_camera_jitter.php>

20. Sputnik-Inc (2004). *Rf propagation basics*. Web. 01 Dec. 2011. <http:///www.sputnik.com/docs/rf_propagation_basics.pdf>

21. Zuech, N. (2007). *Analog vs digital cameras - what is being used in machine vision*. Web. 01 Dec. 2011. <http://www.machinevisiononline.org/public/articles/archivedetails.cfm?id=1528>

22. Schafer, Marlon K. *How to Pick the Right Antenna.* www.electro-comm.com, 2001. Web. 1 Dec. 2011. <http://www.odessaoffice.com/wireless/antenna/how_to_pick_the_right_antenna.htm>

22. FCB-IX Series Datasheet. Park Ridge, NJ: Sony Electronics Inc, 2005. PDF.

23. Olson, Jenna, Kelly Garcia, Mark Zanmiller, and Doug Miley. *CCT Product List*. Cloud Cap Technologies - Goodrich ISR Systems, 12 Jan. 2011. PDF.

24. Struzak, Ryszard. "Basic Antenna Theory." Lecture. *School on Wireless Networking*. ICTP-ITU-URSI School on Wireless Networking for Development The Abdus Salam International Centre for Theoretical Physics ICTP, 2007. Web. 1 Dec. 2011. <http://wirelessu.org/uploads/units/2008/08/12/39/5Anten_theor_basics.pdf>.